TECHNISCHE UNIVERSITÄT WIEN
Vienna University of Technology

DIPLOMARBEIT

Iron (II) SCO complexes based on alkyl imidazoles and pyrazoles

ausgeführt am

Institut für Angewandte Synthesechemie
der Technischen Universität Wien

unter der Anleitung von

Assistant Professor Priv. Doz. Dr. Peter Weinberger

durch

Willi Zeni, BSc

Mollardgasse 34/2/50-51
1060 Wien

Wien, am 05. Juli 2019 Willi Zeni

TABLE OF CONTENTS

LIST OF ABBREVIATIONS

1-Oct-Im	1-octyl-1H-imidazole
1-Oct-Pz	1-octyl-1H-pyrazole
1-Pr-Im	1-propyl-1H-imidazole
1-Pr-Pz	1-propyl-1H-pyrazole
ATR	Attenuated Total Reflectance
DFT	Density Functional Theory
Et_2O	Diethylether
HS	High Spin
Im-Bu-Im	1,4-di(1H-imidazol-1-yl)butane
Im-Et-Im	1,2-di(1H-imidazol-1-yl)ethane
Im-Pr-Im	1,3-di(1H-imidazol-1-yl)propane
Im-PX-Im	1,4-bis((1H-imidazol-1-yl)methyl)benzene
LS	Low Spin
MeCN	Acetonitrile
MeOH	Methanol
MIR	Mid-Range Infrared spectroscopy
NMR	Nuclear Mgnetic Resonance spectroscopy
Pz-Bu-Pz	1,4-di(1H-pyrazol-1-yl)butane
Pz-Et-Pz	1,2-di(1H-pyrazol-1-yl)ethane
Pz-Pr-Pz	1,3-di(1H-pyrazol-1-yl)propane
Pz-PX-Pz	1,4-bis((1H-pyrazol-1-yl)methyl)benzene
SCO	Spin Crossover
Sc-XRD	Single crystal X-Ray Diffraction
SMM	Single Molecule Magnet
THF	Tetrahydrofuran
VSM	Vibrating Sample Magnetometer
Δ_o	Ligand field splitting parameter

ABSTRACT

The discovery in 1931 of bi-stable compounds showing an electronic transition between high-spin (HS) and low-spin (LS) state upon external stimuli (e.g. temperature, pressure) opened a new field of research in inorganic chemistry and material science. The change in spin state implicates changes of the magnetic moment, dielectric constant, color, bond length etc. Spin crossover compounds represent thus a new class of molecular switches, meaning they could be used in memory and sensing devices.

During the 88 years since its discovery, the Spin Crossover (SCO) phenomenon has been deeply investigated and especially nowadays, in the Digital Age, efforts are made in order to make it accessible for technological application.

Major part of the SCO compounds is based on Fe(II) complexes with nitrogen ligands, often azoles. In the research group of Peter Weinberger, a lot of work in the SCO field has been done throughout the years, mostly focusing on tetrazoles as ligands.

The aim of this work was double: the broadening of the ligands library by synthesizing a new set of ligands and their complexation with Fe(II) species in order to obtain SCO compounds. The idea beneath the ligand design was decoupling electronic from steric influences on the SCO behavior, meaning instead of modifying the substituents on the tetrazole ring, moving to another ring system. For this reason comparable ligand systems, i.e. 5-membered azoles, have been prepared and their Fe(II) complexes compared.

The work has been successful since all the desired ligands and their complexes were synthesized and characterized.

ZUSAMMENFASSUNG

Die Entdeckung bistabiler Verbindungen, die einen elektronischen Übergang zwischen dem high-spin (HS) und low-spin (LS) Zustand durch äußere Einflüsse, wie Temperatur oder Druck aufweisen, eröffnete im Jahr 1931 ein neues Forschungsfeld in der Koordinationschemie und in den Materialwissenschaften. Die Änderung des Spinzustands bewirkt Änderungen von anderen Eigenschaften wie magnetisches Dipolmoment, dielektrische Konstante, Farbe, Bindungslänge usw. Spin crossover Verbindungen stellen eine neue Klasse von molekularen Schaltern dar; das bedeutet sie können als Speicher- oder Sensormaterialen angewendet werden.

Während den 88 Jahre seit der Erfindung, das Spin Crossover (SCO) Phänomen wurde intensiv erforscht, besonders heutzutage im Digitalzeitalter.

Der Großteil der SCO-Verbindungen basiert auf Fe(II) Komplexen mit Stickstoff Liganden, oft Azolen. In der Forschungsgruppe von Peter Weinberger wurde in den letzten Jahren viel im Forschungsfeld von Spin Crossover gemacht. Der Fokus lag auf unterschiedlich substituierten Tetrazolen als Liganden.

Diese Arbeit hat ein Doppelziel: die Verbreiterung der Liganden library durch die Synthese eines neuen Ligandensets und die Herstellung von SCO-Verbindungen durch Komplexierung mit Fe(II) Spezies. Die Idee hinter diesem Ligandendesign war die Entkopplung elektronischen von sterischen Einflüssen auf das SCO Verhalten, also anstelle einer Modifizierung von Substituenten am Tetrazolring andere Ringsysteme zu wählen. Aus diesem Grund wurden vergleichbare Ligandensysteme, d.h. 5-Ring-Azole, hergestellt und ihre jeweilige Fe(II) Komplexe verglichen.

Das Ziel wurde erreicht da alle erwünschten Liganden und Komplexe synthetisiert und charakterisiert wurden.

1 INTRODUCTION

1.1 THE SPIN CROSSOVER PHENOMENON – OVERVIEW

Spin Crossover is a phenomenon that occurs in some transition metal complexes in octahedral ligand field for the electronic configuration d^4-d^7. By applying external stimuli (variation of temperature, pressure, irradiation with light, magnetic field) to those systems the complex can switch between HS and LS state.[1] In the case of octahedral iron(II) complexes the LS state corresponds to the t_{2g}^6 electronic configuration, the HS to the t_{2g}^4 e_g^2 configuration.
According to ligand field theory, the change in the spin state is a transition from a LS ground state electronic configuration to a HS ground state electronic configuration of the metal's *d* atomic orbitals, or vice versa. The magnitude of the ligand field splitting energy (Δ_o) compared to the spin pairing energy of the complex determines whether the ground state has HS or LS configuration; therefore, the LS state is the ground state if Δ_o is bigger than the spin pairing energy, whereas the HS state is the ground state if the spin pairing energy is bigger than Δ_o.[2]
For spin crossover compounds Δ_o and the spin pairing energy are of almost the same magnitude, thus the small amount of energy gained or lost by the changes in temperature (the most common trigger) determines in which state the system is stabilized.

1.2 HISTORY OF SPIN CROSSOVER

The spin crossover phenomenon was first observed and described in 1931 by Cambi *et al.* for their tris(N,N-dialkyldithiocarbamatoiron(III) complexes.[3] During the following years the research on spin crossover materials focused mainly on iron(III) based compounds.[4]
In the early 1980's Haddad and coworkers found that the cooperativity between metal centers is a fundamental factor in determining the spin switching behavior.[5, 6]
In 1982 N1-substituted tetrazoles were introduced by Haasnoot as ligands for iron(II) spin crossover compounds.[7] Since N1-substituted tetrazoles only coordinate to the iron(II) center through the N4 position,[8] there is a wide range of possibilities to vary the electronic and structural properties with the introduction of different kinds of substituents.
Gütlich and coworkers started investigations focusing on $[Fe(1\text{-propyl-}1H\text{-tetrazole})_6]^{2+}$ complexes applying a wide range of different analytical techniques, to understand their structure and bonding properties.[9]
Many efforts were taken both in research as well as in theoretical modeling in order to predict the spin transition behavior of a given structure; nevertheless, due to the concomitant change of both electronics and sterics, it remains difficult.[10, 11]

1.3 CHOICE OF THE METAL CENTER

As one can probably imagine, the focus on iron(II) as metal of choice for SCO systems is not casual. For a possible applicability of SCO compounds, one would desire a difference in spin as big as possible. For this reason Fe(II), with electronic configuration d^6 represents the ideal choice: the LS state corresponds to a singlet state with S=0 whereas the HS state corresponds to a quintet state with S=2. The other electronic configurations allowing for SCO provide two paramagnetic states that differ only in the number of unpaired spins. It appears at this point clear that the d^6 configuration is the more convenient, having the biggest spin difference between the two states and because the LS configuration is diamagnetic, leading to a simple differentiation of the spin states in magnetic measurements.
Moreover, only metals of the first row are suitable for SCO compounds because their transitions occur in a reasonable temperature and pressure range. For element of the second and third row there is an increased stabilization for the LS state, thus preventing SCO. Furthermore, one will desire a metal precursor with a weak coordinating anion, and Fe(II) is compatible with such anions. Lastly, using Fe(II) gives the possibility for a variety of characterization techniques (Mößbauer, UV-VIS, MIR, FIR).
For all this reasons, Fe(II) was the metal of choice for this work.

1.4 CHOICE OF THE LIGAND SYSTEM

As mentioned before, a prerequisite for a system to be suitable for SCO is having Δ_o and spin pairing energy of the same magnitude. For Fe(II) compounds this prerequisite is fulfilled with homoleptic complexes having Fe-N bonds or heteroleptic systems featuring N, O or CN bonds. As previously stated, tetrazole have been widely investigated throughout the years. In this work it was decided to use other type of azoles and create a set of novel ligands, namely alkyl substituted imidazoles and pyrazoles. Azoles represent a good choice not only because they give homoleptic complexes by selectively coordinating on the N-atom, but also because they are easily accessible for functionalization.

1.5 AIM OF THE WORK

The work has two synthetic goals: the first one is the successful synthesis of a series of N1-alkylated imidazoles and pyrazoles, and the second one their complexation with Fe(II) species. Although a set of SCO compounds could be considered the main goal, that is not the case, since the here synthesized pyrazole and imidazole derivatives were up until now never used as ligands for this class of compounds, hence a systematic approach was taken to synthesize the complexes and define their magnetic behavior.

2 RESULTS AND DISCUSSION

2.1 SYNTHETIC PROTOCOL

An extensive literature search showed for every ligand at least four different synthetic protocols, all of them consisting in one-pot procedures. Furthermore, the literature-found species were always used as intermediate for more extensive organic systems. In this work a different, two-step procedure was adopted

2.2 ALKYL PYRAZOLES

The first step was the synthesis of potassium pyrazolate (**1**), which was the precursor for all the pyrazole-based ligands. Ligands were obtained by reaction of **1** with alkyl (di)bromides. All the alkylation reactions were carried out in anhydrous THF, heated to 90°C and left stirring for 18h. The same work-up procedure was adopted for all the ligands: filtration of the suspension to separate KBr, wash with anhydrous THF, evaporation of the solvent and isolation of the product. When needed, flash column chromatography was performed. All the ligands were characterized first via ^{1}H and ^{13}C NMR, and once the identity and the purity of the products were confirmed, MIR spectra were recorded as well.

2.2.1 Potassium Pyrazolate

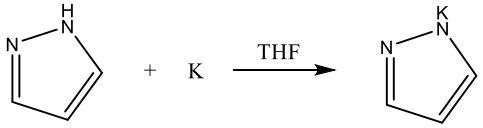

1

The compound was synthesized by reaction of 1-H-pyrazole with potassium in dry THF. As potassium was inserted, a white solid began to form. The mixture was left stirring, and after three hours there was no potassium left in the flask, meaning the reaction was complete. The mixture was suction-filtered to separate the solid product, which was finally dried in vacuum and isolated as a white solid.

2.2.2 1-propyl-1H-pyrazole

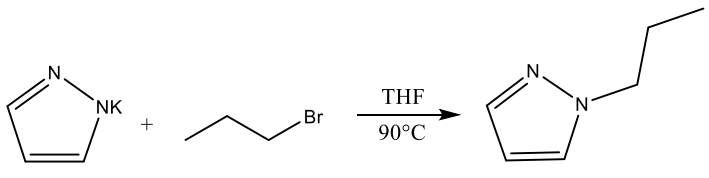

1 **2**

The product was obtained by reaction of **1** with 1-bromopropane in dry THF. After 18h, a suspension consisting of a white solid and a dark yellow liquid phase was formed. The work-up yielded a yellow oil. ^{1}H and ^{13}C NMR spectra showed presence of residual impurities, therefore, the raw mixture was purified via flash column chromatography (MeCN : CH_2Cl_2 = 3:2, R_f=0.5). The product was isolated as a yellow oil, whose purity was confirmed by ^{1}H and ^{13}C NMR spectra.

2.2.3 1-octyl-1H-pyrazole

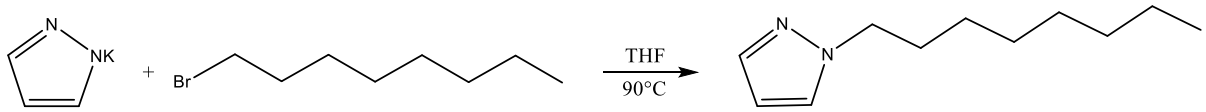

1 **3**

The product was obtained by reaction of **1** with 1-bromooctane in dry THF. After 18h, a suspension consisting of a brownish solid and a pale-yellow liquid phase was formed. The work-up yielded a colorless oil, whose purity was confirmed by ^{1}H and ^{13}C NMR spectra.

2.2.4 1,2-di (1H-pyrazol-1-yl) ethane

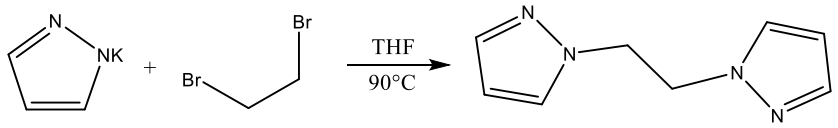

1 **4**

The product was obtained by reaction of **1** with 1,2-dibromoethane in dry THF. After 18h, a suspension consisting of a white solid and a yellow liquid phase was formed. The work-up yielded a yellow oil. ^{1}H and ^{13}C NMR spectra showed presence of residual impurities, therefore, the raw mixture was purified via flash column chromatography (MeCN : CH_2Cl_2 = 3:2, R_f=0.5). The product was isolated as a yellow paste, whose purity was confirmed by ^{1}H and ^{13}C NMR spectra.

2.2.5 1,3-di (1H-pyrazol-1-yl) propane

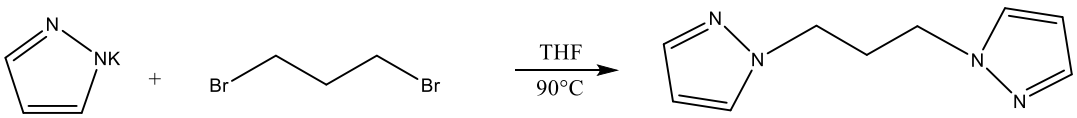

1 **5**

The product was obtained by reaction of **1** with 1,3-dibromopropane in dry THF. After 18h, a suspension consisting of a brownish solid and a yellow liquid phase was formed. The work-up yielded a yellow oil. Since ^{1}H and ^{13}C NMR spectra showed presence of residual impurities, flash column chromatography was performed (MeCN : CH_2Cl_2 = 3:2, R_f=0.5). The product was isolated as a yellow oil, whose purity was confirmed by ^{1}H and ^{13}C NMR spectra.

2.2.6 1,4-di (1H-pyrazol-1-yl) butane

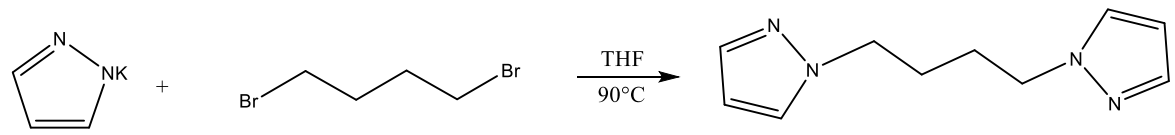

1 **6**

The product was obtained by reaction of **1** with 1,4-dibromobutane in dry THF. After 18h, a suspension consisting of a brownish solid and an orange liquid phase was formed. The work-up yielded an orange oil. Once again, ^{1}H and ^{13}C NMR spectra showed presence of residual impurities, and the raw mixture was purified via flash column chromatography (MeCN : CH_2Cl_2 = 3:2, R_f=0.5). The product was isolated as a yellow oil, whose purity was confirmed by ^{1}H and ^{13}C NMR spectra.

2.2.7 1,4-bis((1H-pyrazol-1-yl)methyl)benzene

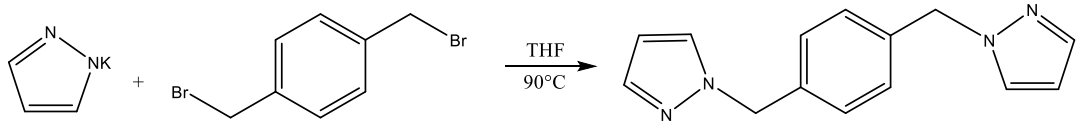

1 **7**

The product was obtained by reaction of **1** with 1,4-bis(bromomethyl)benzene. After 18h, a suspension consisting of a brownish solid and a pale-yellow liquid phase was formed. The work-up yielded a cream-white solid. ^{1}H and ^{13}C NMR spectra showed no presence of impurities, and the product was, therefore, isolated as such.

2.3 ALKYL IMIDAZOLES

The same synthetic procedure used for the pyrazole-based ligands was adopted, starting with the synthesis of the potassium salt as precursor. Ligands were obtained again by reaction of the precursor with alkyl (di)bromides. All the alkylation reactions were carried out in anhydrous THF, heated to 90°C and left stirring for 18h. The work-up procedure was identical as for the alkyl pyrazoles: filtration of the suspension to separate KBr, wash with anhydrous THF, evaporation of the solvent and isolation of the product. When needed, flash column

chromatography was performed. All the ligands were characterized first via ^{1}H and ^{13}C NMR, and once the identity and purity of the products were confirmed, MIR spectra were recorded as well.

2.3.1 Potassium imidazolate

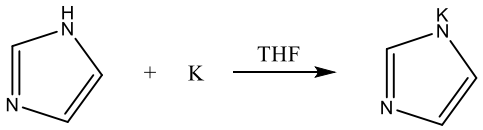

8

The compound was synthesized by reaction of 1H-imidazole with potassium in anhydrous THF. Immediately after the addition of potassium, a pale-yellow solid began to form. After two hours the reaction was complete, since no potassium was left in the reaction flask. The mixture was suction filtered to separate the product, which was then dried in vacuum and isolated as a yellow solid. It was finally characterized by MIR spectroscopy.

2.3.2 1-propyl-1H-imidazole

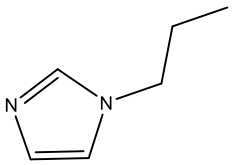

9

The product was commercially available (TCI) and used as such

2.3.3 1-octyl-1H-imidazole

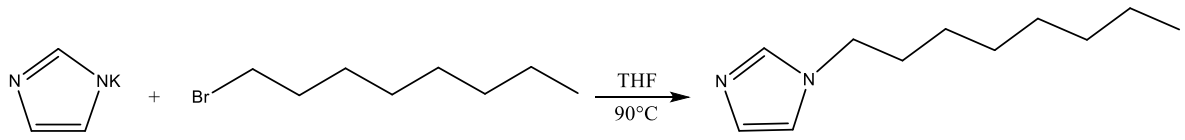

8 **10**

The product was obtained by reaction of **8** with 1-bromooctane in dry THF. After 18h, a suspension consisting of a brownish solid and a dark-orange liquid phase was formed. The work-up yielded a brown oil. ^{1}H and ^{13}C NMR spectra showed presence of residual impurities, therefore, the raw mixture was purified via flash column chromatography (MeCN : CH_2Cl_2 = 3:2, R_f=0.5). The product was isolated as a brown oil, whose purity was confirmed by ^{1}H and ^{13}C NMR spectra.

2.3.4 1,2-di (1H-imidazol-1-yl) ethane

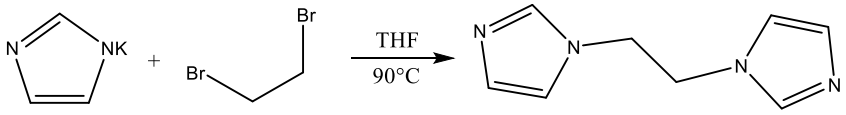

8 **11**

The product was obtained by reaction of **8** with 1,2-dibromoethane in dry THF. After 18h, a suspension consisting of a brownish solid and an orange liquid phase was formed. The work-up yielded a brown oil. ^{1}H and ^{13}C NMR spectra showed presence of residual impurities, therefore, the raw mixture was purified via flash column chromatography (MeCN : CH_2Cl_2 = 3:2, R_f=0.5). After purification, the 1H and 13C NMR spectra still showed the presence of by-products in minor quantity. It was decided to proceed and use the ligand as such.

2.3.5 1,2-di (1H-imidazol-1-yl) propane

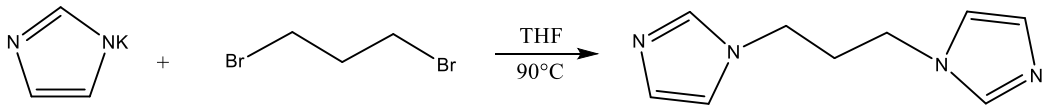

8 **12**

The product was obtained by reaction of **8** with 1,3-dibromopropane. After 18h, a suspension consisting of a brownish solid and a yellow liquid phase was formed. The work-up yielded a yellow oil. ^{1}H and ^{13}C NMR spectra showed presence of residual impurities, therefore, the raw mixture was purified via flash column chromatography (MeCN : CH_2Cl_2 = 3:2, R_f=0.5). The product was isolated as a yellow oil, whose purity was confirmed by ^{1}H and ^{13}C NMR spectra.

2.3.6 1,2-di (1H-imidazol-1-yl) butane

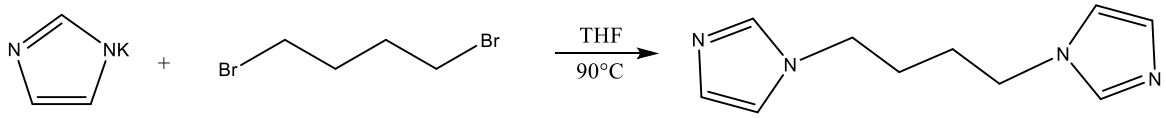

8 **13**

The product was obtained by reaction of **8** with 1,4-dibromobutane. After 18h, a suspension consisting of a brownish solid and a yellow liquid phase was formed. The work-up yielded a yellow oil. ^{1}H and ^{13}C NMR spectra showed presence of residual impurities, therefore, the raw mixture was purified via flash column chromatography (MeCN : CH_2Cl_2 = 3:2, R_f=0.5). The product was isolated as a yellow oil, whose purity was confirmed by ^{1}H and ^{13}C NMR spectra.

2.3.7 1,4-bis((1H-imidazol-1-yl)methyl)benzene

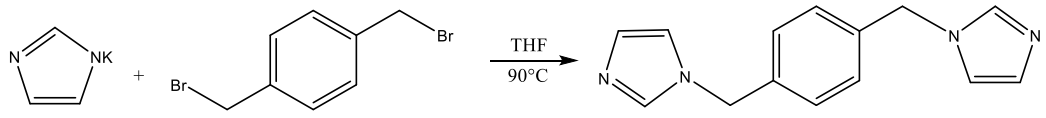

8 **14**

The product was obtained by reaction of **8** with 1,4-bis(bromomethyl)benzene. After 18h, a suspension consisting of a brownish solid and a pale-yellow liquid phase was formed. The work-up yielded a yellow solid. ^{1}H and ^{13}C NMR spectra showed no presence of impurities, and the product was therefore isolated as such.

2.4 COMPLEXATION OF THE LIGANDS

After the ligands were isolated, the next step was their complexation. Since the goal was to synthesize SCO compounds, the ligands were complexated with Fe(II) species, specifically, $Fe(BF_4)_2 \cdot 6H_2O$ and $Fe(ClO_4)_2 \cdot 6H_2O$. The choice of the precursors was based on the weak coordinating nature of the anions.
Since the synthesized ligands were until now never used as sole ligands with the purpose of building homoleptic metal complexes and/or SCO compounds, there was the necessity to prove their coordination mode and gather structural information about the resulting complexes. For this reason, in the early stages of the work, Ni(II) complexes were synthesized as well, using again the tetrafluoroborate (aqueous solution) and/or perchlorate hexahydrate salts as precursors. Due to the non-sensitivity of Ni(II) towards oxidation, its complexes were much easier to handle for crystallization attempts and for structural analysis.
The Fe(II) species were synthesized using the Schlenk technique, whereas the complexations of the Ni(II) ones were carried out in regular flasks. The reactions were heated to 45°C and left stirring overnight. Dry MeOH was the solvent of choice. Work-up consisted in solvent evaporation, precipitation in case an oil was remaining and wash of the complexes. Once the products were isolated, room-temperature MIR spectra were recorded.
A simple method was used to have a preliminary information about the SCO behavior of the complexes: reaction tubes/flasks were dived in liquid nitrogen, and the change in color was used as response.
For every complex species, crystallization attempts via solvent diffusion were carried out.

2.4.1 Complexation of 1-propyl-1H-pyrazole

Three complexes were synthesized using $Fe(BF_4)_2 \cdot 6(H_2O)$, $Ni(BF_4)_2$ and $Ni(ClO_4)_2 \cdot 6(H_2O)$ as precursors. The Fe(II) species presented itself as a red oil. Different precipitation attempts were

tried and finally by dissolving the product in ca. 2mL of CH_2Cl_2 and by addition of n-pentane a dark-red precipitate formed. The liquid phase was removed and the solid dried under vacuum. No thermal SCO was observed for this complex. As next step it was tried to obtain single crystals via diffusion in Et_2O and n-pentane, but none of the attempts was successful.
The Ni(II) species were isolated as blue (BF_4) and purple (ClO_4) solids. Crystals were obtained by dissolving the product in ca. 2 mL of MeOH and letting it evaporate, but they were too weak to give diffraction and, therefore, the structure could not be resolved.

2.4.2 Complexation of 1-octyl-1H-pyrazole

As for the previous ligand, three complexes were synthesized using $Fe(BF_4)_2 \cdot 6(H_2O)$, $Fe(ClO_4)_2 \cdot 6(H_2O)$, and $Ni(BF_4)_2$ as precursors.
The iron complexes were precipitated by dissolution in ca. 2 mL MeOH and addition of n-pentane; both were isolated as yellow solids. No thermal SCO was observed.
The Ni species was isolated as blue powder by simple solvent removal under vacuum.
For all the species it was tried to obtain single crystals via diffusion in Et_2O and n-pentane, and for the Ni(II) species by simple solvent evaporation as well; none of the attempts was successful.

2.4.3 Complexation of 1,2-di(1H-pyrazol-1yl)ethane

Three complexes were synthesized, using $Fe(BF_4)_2 \cdot 6(H_2O)$, $Fe(ClO_4)_2 \cdot 6(H_2O)$ and $Ni(BF_4)_2$ as precursors. After solvent evaporation the iron species were both isolated as pale-yellow solids, whereas the Ni species as a blue solid. The iron species didn't show thermal SCO. It was tried to obtain single crystals via diffusion in Et_2O and n-pentane, and for the Ni complex by simple evaporation of the solvent as well. None of the attempts was successful.

2.4.4 Complexation of 1,3-di(1H-pyrazol-1yl)propane

Two complexes were synthesized, using $Fe(BF_4)_2 \cdot 6(H_2O)$ and $Ni(BF_4)_2$ as precursors. After solvent evaporation the iron species was isolated as a yellow solid, whereas the Ni species as a blue solid. The iron species didn't show thermal SCO. It was tried to obtain single crystals for both species, by diffusion in Et_2O and n-pentane, and for the Ni complex by simple evaporation of the solvent as well. None of the attempts was successful.

2.4.5 Complexation of 1,4-di(1H-pyrazol-1-yl)butane

$Fe(BF_4)_2 \cdot 6(H_2O)$ and $Fe(ClO_4)_2 \cdot 6(H_2O)$ were used as precursors. After solvent evaporation the complexes were both isolated as cream-white solids. They didn't show thermal SCO. It was tried to obtain single crystals via diffusion in Et_2O and n-pentane, none of the attempts was successful.

2.4.6 Complexation of 1,4-bis((1H-pyrazol-1-yl)methyl)benzene

Two complexes were synthesized, using $Fe(BF_4)_2 \cdot 6(H_2O)$ and $Ni(BF_4)_2$ as precursors. After solvent evaporation the iron species was isolated as a white solid, whereas the Ni species as a blue solid. The iron species didn't show thermal SCO. For both complexes it was tried to obtain single crystals via diffusion in Et_2O and n- pentane, but none of the attempts was successful.

2.4.7 Complexation of 1-propyl-1H-imidazole

Two complexes were synthesized, using $Fe(BF_4)_2 \cdot 6(H_2O)$ and $Ni(BF_4)_2$ as precursors. After work up, a yellow solid was isolated for the iron species, a blue powder for the nickel species. The IR spectrum of the iron species showed an unusual band at 1736 cm^{-1}. Single crystals were obtained for the iron complex via diffusion in Et_2O and analyzed via XRD. The results were quite surprising: instead of the expected homoleptic complex, a cubic Fe-O cluster was obtained. Aside the obvious interest in studying the cluster itself to better define its properties, two questions arose at this point: how did the cluster form? Is it possible to drive the reaction towards the formation of the cluster or rather the homoleptic complex? The first thing to determine was the source of oxygen. There are two possibilities: the oxygen can come from the solvate water molecules of the salt or from the solvent. Two other variables could have influenced the reaction outcome: temperature and the reaction time. Pondering all those variables, three other syntheses were performed, involving a change in the aforementioned parameters: a) same reagents and solvent but reaction time reduced from 18 h to 2 h; b) anhydrous $Fe(BF_4)_2$ instead of the hexahydrate salt (reaction performed in the glove box), reaction time 18h; c) anhydrous $Fe(BF_4)_2$ and dry MeCN instead of MeOH as solvent (reaction performed in the glove box), reaction time 18h.
All the reactions led to the formation of the homoleptic complex. Although further investigation is needed, two hypotheses can be made with the information collected: a) the oxygen source seems to be the solvate water of the salt, and b) the homoleptic complex is formed first, thus being the kinetic product, whereas the cluster, observed when the reaction proceeds for longer time, is the thermodynamic product.
Regarding the SCO behavior of the homoleptic complex, no thermal SCO was observed. Crystals were isolated via diffusion in Et_2O for both the Fe(II) and Ni(II) homoleptic complexes and analyzed via XRD. The analysis confirmed the homoleptic complexes were obtained.
Other than the complex itself, the cluster was further investigated as well. This topic will be treated in detail in chapter 2.3.13

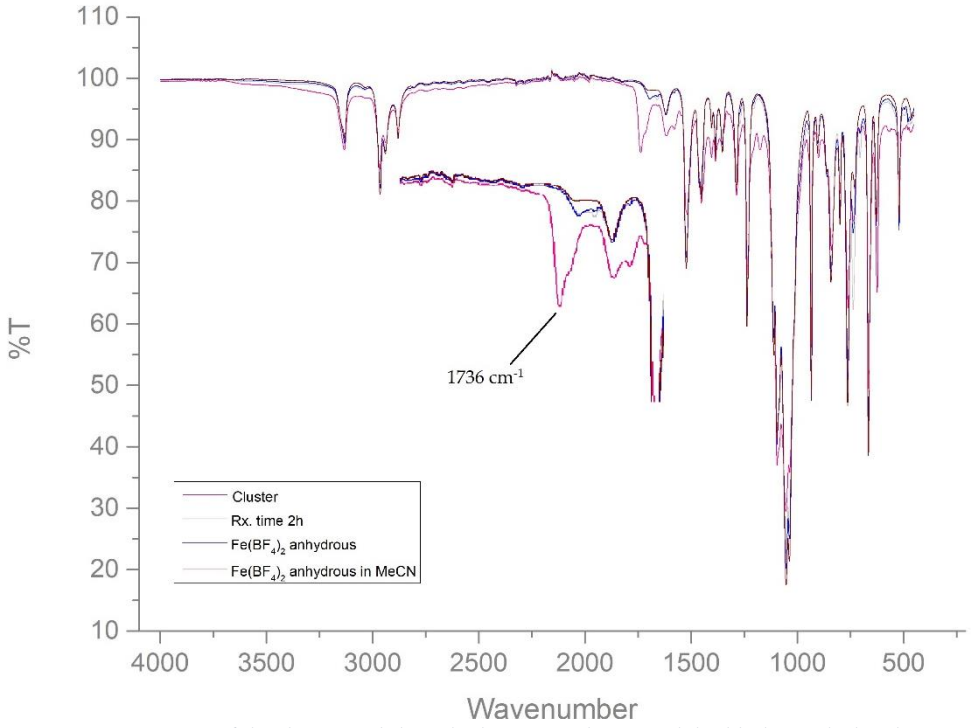

Figure 1:MIR spectra of the cluster and the anhydrous complexes, with highlight on the band at 1736 cm^{-1}

2.4.8 Complexation of 1-octyl-1H-imidazole

Two complexes were synthesized, using $Fe(BF_4)_2 \cdot 6(H_2O)$ and $Ni(BF_4)_2$ as precursors. After solvent evaporation a pale yellow oil was obtained for the Fe(II) complex and a blue oil for the Ni(II) complex. All the species were precipitated with Et_2O and isolated as cream-white (Fe) and blue (Ni) solids, respectively. The iron species didn't show thermal SCO. Crystallization via diffusion in Et_2O and n-pentane was tried, and for the Ni(II) species by slow evaporation of the solvent as well, but no crystals were isolated.

2.4.9 Complexation of 1,2 di (1H-imidazol-1-yl)ethane

Three complexes were synthesized, using $Fe(BF_4)_2 \cdot 6(H_2O)$, $Fe(ClO_4)_2 \cdot 6(H_2O)$ and $Ni(BF_4)_2$ as precursors. After solvent evaporation the iron species were both isolated as a yellow solid, whereas the Ni species as a blue solid. The iron species didn't show thermal SCO. Crystallization via diffusion in Et_2O and n-pentane was tried, and for the Ni complex by simple evaporation of the solvent as well, but none of the attempts was successful.

2.4.10 Complexation of 1,3 di (1H-imidazol-1-yl)propane

Two complexes were synthesized, using $Fe(BF_4)_2 \cdot 6(H_2O)$ and $Fe(ClO_4)_2 \cdot 6(H_2O)$ as precursors. After solvent evaporation the iron species were isolated as yellow solids, the Ni species as a blue solid. The iron species didn't show thermal SCO. It was tried to obtain single crystals for

both species, by diffusion in Et_2O and n-pentane, and for the Ni complex by simple evaporation of the solvent as well. None of the attempts was successful.

2.4.11 Complexation of 1,4 di (1H-imidazol-1-yl)butane

$Fe(BF_4)_2 \cdot 6(H_2O)$ and $Fe(ClO_4)_2 \cdot 6(H_2O)$ and were used as precursors. After solvent evaporation the complexes were isolated as cream-white solids. They didn't show thermal SCO. It was tried to obtain single crystals for both species by diffusion in Et_2O and n-pentane, but none of the attempts was successful.

2.4.12 Complexation of 1,4-bis((1H-imidazol-1-yl)methyl)benzene

Two complexes were synthesized, using $Fe(BF_4)_2 \cdot 6(H_2O)$ and $Ni(BF_4)_2$ as precursors. After solvent evaporation the iron species were isolated as yellow solids, the Ni species as a blue solid. The iron species didn't show thermal SCO. It was tried to obtain single crystals for both species, by diffusion in Et_2O and n-pentane, and for the Ni complex by simple evaporation of the solvent as well. None of the attempts was successful.

2.4.13 Fe-O cluster

As reported in chapter 2.3.7, single crystals were produced and analyzed.

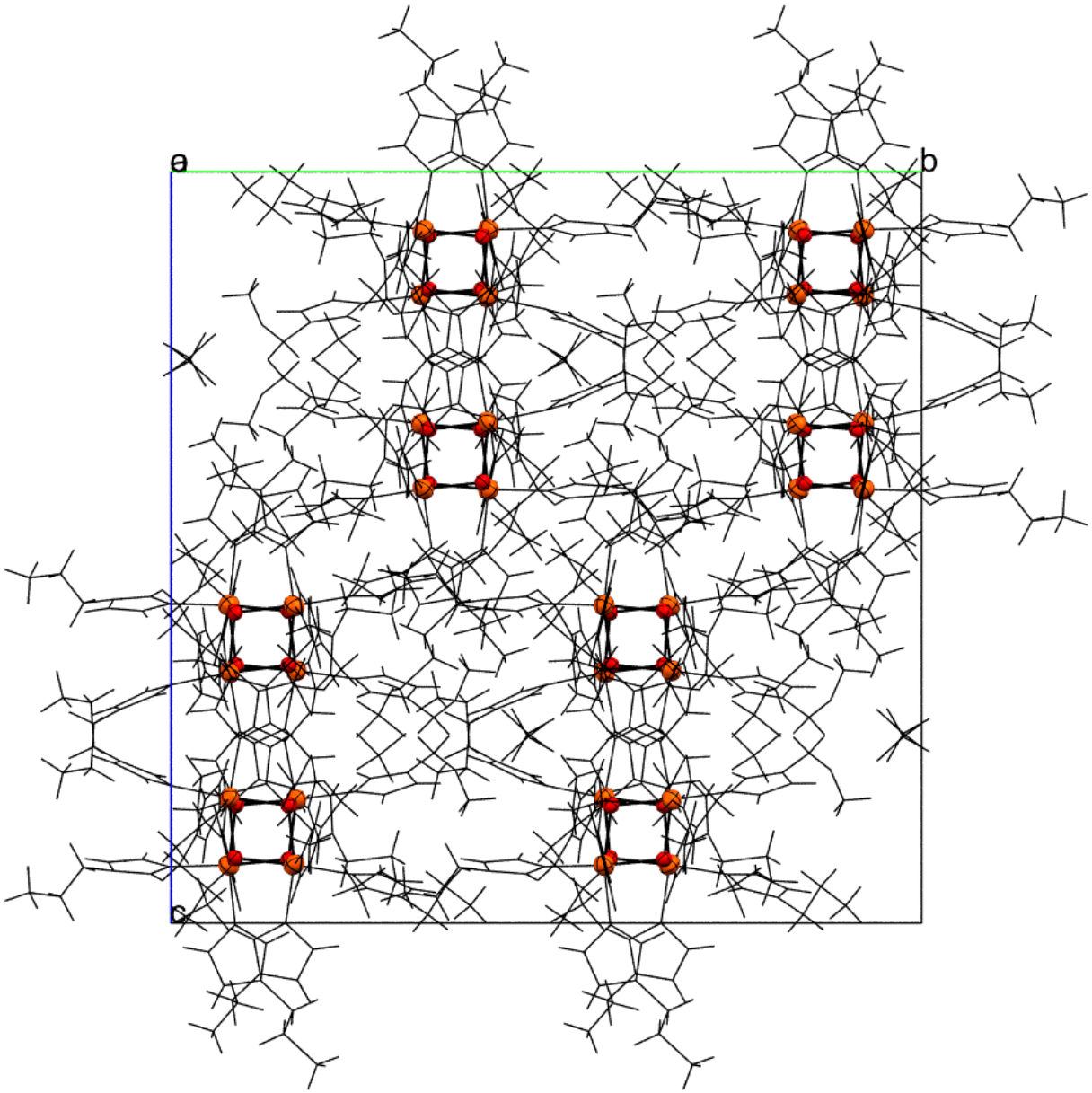

Figure 2: Crystal packing of the Fe-O cluster

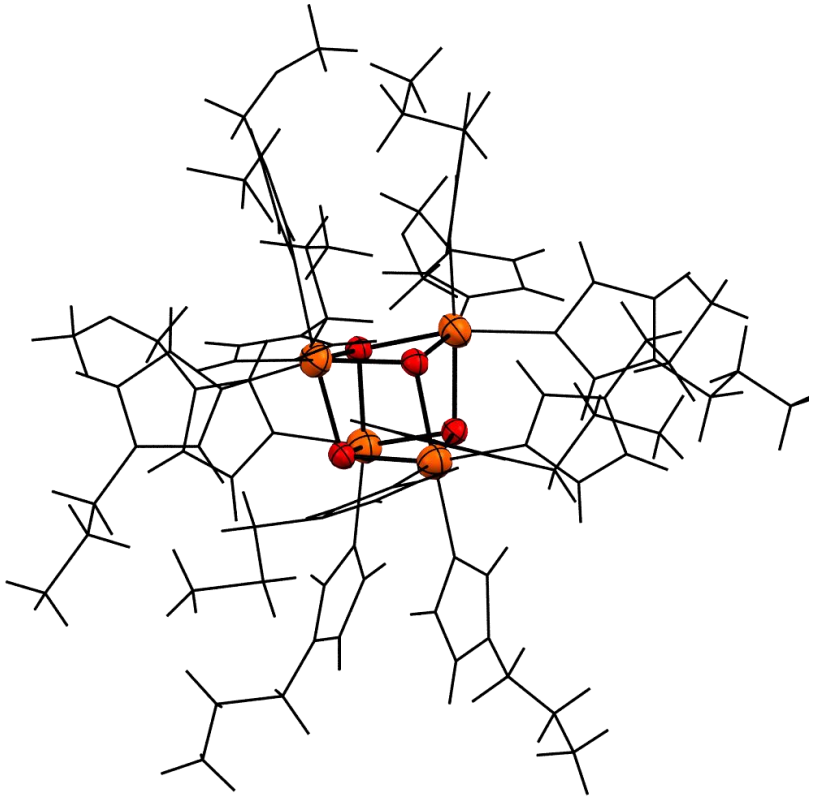

Figure 3: Molecular structure of the Fe-O cluster

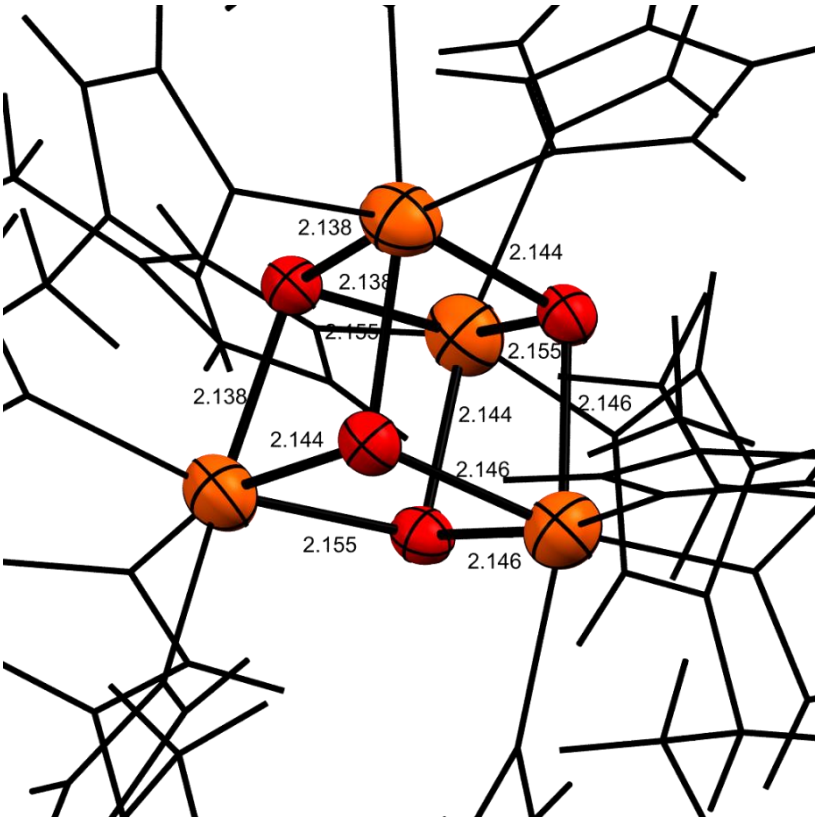

Figure 4: Detail on the cubic central unit of the Fe-O cluster

As can be seen in figure 4, the resolved structure showed an interesting detail: the cluster has three iron atoms that are identical (all of them make three bonds of different lengths, and the lengths are identical for all three atoms), whereas the fourth iron atom makes three identical long bonds, meaning that the latter is somehow different than the others.
Cyclic voltammetry was used to have confirmation about that, and the plot shows just one peak, indicating that one iron atom can selectively undergo a redox process.

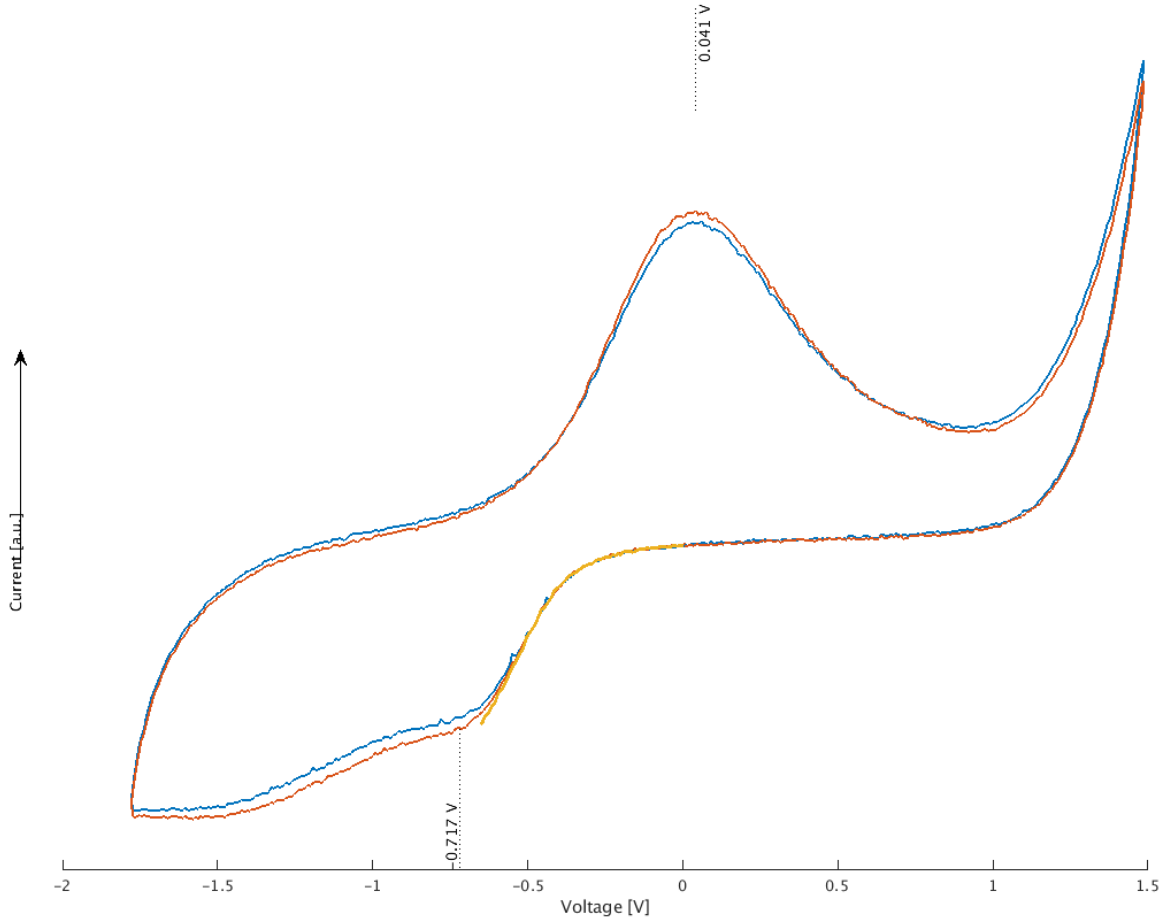

Figure 5: Cyclic voltammetry plot of the Fe-O cluster

Furthermore, the cluster represents a so called "frustrated spin system", compounds were the more convenient electron spin arrangement would be antiferromagnetic, but it is physically impossible to reach this state due to the number of neighboring iron atoms: as a result, the spins tilt on the axis, therefore the term frustrated. This class of compounds have the requirements to be Single Molecule Magnets (SMM). In order to collect information about the possible SMM behavior, magnetic measurement of the powder (magnetic moment vs. field) were made. The results are shown in figure 6.

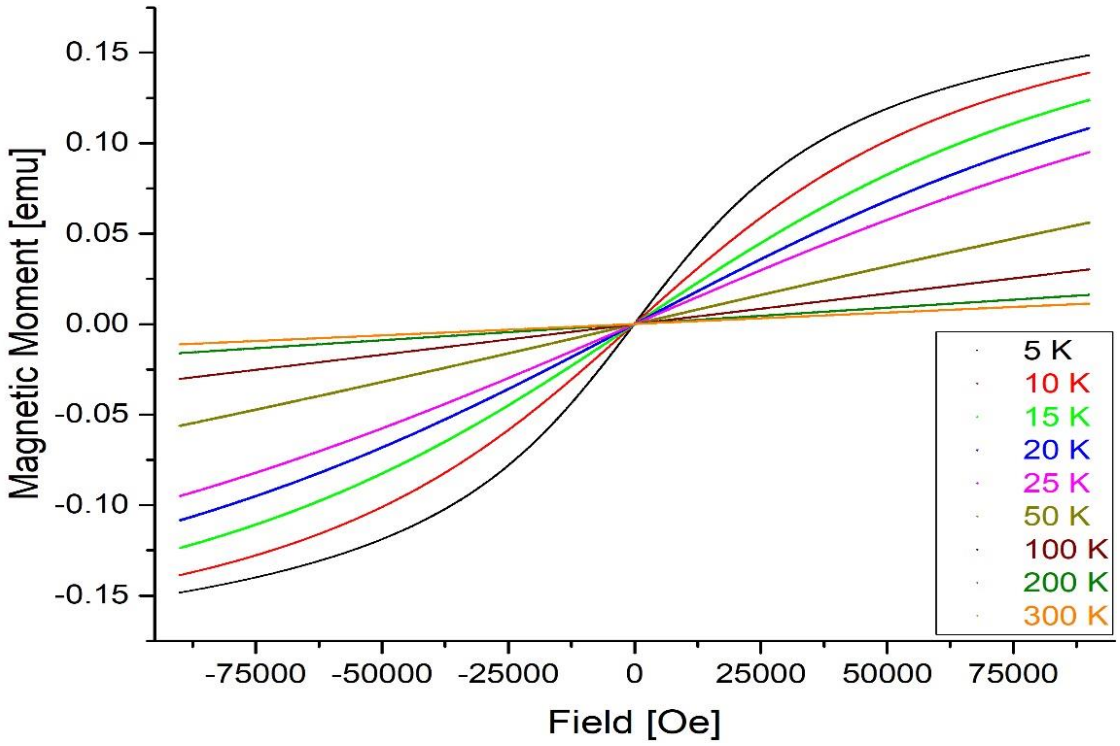

Figure 6: AC susceptibility measurement of the Fe-O cluster (powder)

In first approximation, the SMM behavior can not be excluded. The "S" shape of the plots is just due to Brownian random motions, who tend to average the magnetic moment. For a more detailed analysis about the SMM behavior single crystals were necessary. We were able to re-obtain them and proceeded with the magnetic characterization. The preliminary AC susceptibility measurements suggest a SMM behavior.

2.4.14 Theoretical calculations and synthesis of heteroleptic complexes

Since the first synthesized complexes did not show thermal SCO it was decided to run DFT calculations, to compare a tetrazole-based system known to be SCO active with the corresponding pyrazole- and imidazole-based systems. Propyl derivatives of 1-H-pyrazole, -imidazole and -tetrazole were chosen as model for the calculations. The results of the calculation are reported in figure 7, 8 and 9.

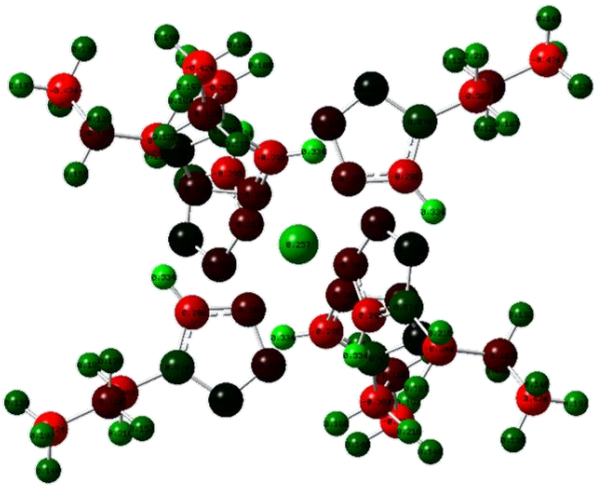

Figure 7: Calculated structure of $[Fe(1\text{-}Pr\text{-}tz)_6]^{2+}$

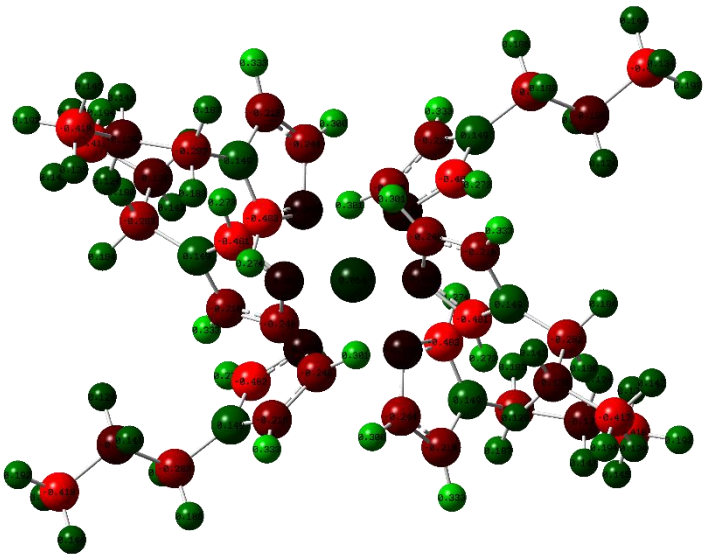

Figure 8: Calculated structure of $[Fe(1\text{-}Pr\text{-}Im)_6]^{2+}$

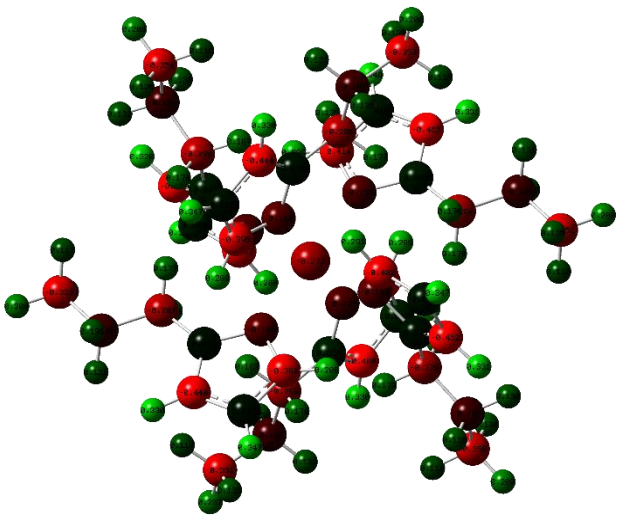

Figure 9: Calculated structure of $[Fe(1\text{-}Pr\text{-}Pz)_6]^{2+}$

As it can be seen, there is a dramatic change in the electronic density on the Fe(II) atom when shifting from a tetrazole-based complex (0.257) to an imidazole- (0.064) and, especially, pyrazole-based (-0.124) complex. Nevertheless, imidazole-based SCO compounds are reported in literature and for that reason it was decided to proceed with the complexation of the whole imidazole series.
At this point was decided to synthesize heteroleptic complexes, using 1-propyl-1H-tetrazole - $[Fe(1Pr\text{-}Tz)_6](BF_4)_2$ is literature-known and SCO active - and 1-propyl-1H-imidazole as ligands. The idea was to create a more tetrazole-like system but still with imidazole in it, thus reducing the gap in electron density between a purely tetrazole-based and a purely imidazole-based system. Five syntheses were performed, using the ligands in different ratioes (5:1, 4:2, 3:3, 2:4, 1:5), and mixing them with $Fe(BF_4)_2 \cdot 6H_2O$ in MeOH. Unfortunately, none of the syntheses was successful, since each of them only yielded a homoleptic complex, having the ligand present in higher amount as sole coordinating species. It was then tried to perform the reaction in a weak-coordinating solvent, specifically MeCN, inserting first the ligand present in minor quantity, stirring for 1h and then inserting the second ligand. This method led to the same result as the first. Regarding the synthesis with the ligands present in the same ratioes, no homoleptic complex was expected, since both ligands were present in equal amount. In fact, no product at all could be isolated from the reaction: short after the insertion of the reagents the mixture became a black mud. IR spectra was recorded, but no recognizable peaks were present. The syntheses were repeated but led to the same result as in the first try.

2.4.15 Final résumé and conclusion

As reported in the introduction, there were two goals of this work: a) successful synthesis of imidazole and pyrazole alkyl derivatives and their complexation and b) obtaining complexes that give SCO.
From the synthetic point of view no major problem were encountered, for both ligands and complexes. All the syntheses proceeded smoothly and except for a small number of compounds (**5**, **11**) the yields were satisfactory. That can in part be attributed to the chosen synthetic pathways: all of the literature-known syntheses for the ligands consist of one-pot reactions, but for this work a two-step pathway was chosen instead (synthesis of the precursor by deprotonation with potassium and the alkylation) in order to have fewer by-products and hence less challenging work-up procedures.
Regarding the magnetic behavior it appears clear that the scope of the work must be expanded, and the design of new ligand systems is needed. None of the synthesized complexes showed thermal SCO, meaning the electronics and/or the steric of the ligands must be changed, by introducing different substituents. The complexation results of the pyrazolo-derivatives are in line with the expectations as the coordinating N is right next to the N1-substituted nitrogen atom. This would enforce a drastic change upon coordination in comparison to the tetrazole complexes. Due to steric reason the complexation should be severely hampered, which was experimentally proved. In a first approach one would think the solution to this problem is to run calculations before proceeding with the synthesis; as mentioned in the introduction this approach has already been tried and proven ineffective. Since the SCO phenomenon does not

only involve the electronics of the systems but the sterics as well, it's not that simple to engineer the ligand system and/or predict if a certain ligand will give SCO active compounds or not.
It must also be said that this was somehow uncharted territory: the reported alkyl derivatives of pyrazole and imidazole were till now never used as ligands for SCO compounds. Since, as mentioned before, it is almost impossible to predict if a certain ligand will yield SCO compounds, the only way was to take a systematic approach, synthesizing and complexating all the ligands and finally defining their magnetic behaviour.
The isolation of single crystals was the other major problem encountered in this work. In order to overcome this problem, the steric of the system needs to be changed. There are two main changes one can make: the substituents on the azole ring and the counter anion (e.g. tosylate could be good option due to π-π stacking, which could give a better packing of the molecules). Lastly, the Fe-O cluster needs to be further investigated, on the one hand regarding the synthetic aspect to confirm our hypothesis about it being the thermodynamic product and the homoleptic complex the kinetic one, on the other hand is necessary to define the single crystal magnetic behavior in order to determine whether it is a SMM or not.

3 EXPERIMENTAL

3.1 GENERAL METHODS

All operations involving Fe(II) species were carried out under inert atmosphere (Argon 5.0) and neat conditions. The glassware was oven dried at 125°C for at least 2 hours before use. All the solvents were distilled and dried before use and stored over molecular sieves 3Å in William flasks under argon. For particularly delicate operations a glove box was used.

3.1.1 Operations involving $Fe(ClO_4)_2 \cdot 6(H_2O)$

All the procedures involving $Fe(ClO_4)_2 \cdot 6(H_2O)$ have an additional preliminary step: due to its partial oxidation, before being inserted in the reaction vessel the salt was put in a vial together with a small amount of ascorbic acid, and under inert atmosphere ca. 2mL of solvent were added. The yellow solution was mixed until it became colorless, meaning Fe(III) was re-reduced back to Fe(II). The solution was finally taken up with a syringe and inserted in the reaction vessel after filtration with a syringe filter, in order to remove residual ascorbic acid.

3.2 IR SPECTROSCOPY

Mid-range IR spectra were recorded in ATR technique within the range of 4000 - 450 cm^{-1} using a Perkin-Elmer Spectrum Two FTIR spectrometer with an UATR accessory attached. The background was measured with opened anvil versus ambient air.

3.3 NMR SPECTROSCOPY

All spectra were recorded in dry, deuterated solvents.
^{1}H and $^{13}C\{1H\}$ NMR spectra were recorded on a Bruker AVANCE-250 spectrometer and on a Bruker 200 FS FT-NMR. All NMR chemical shifts are reported in *ppm;* ^{1}H and ^{13}C shifts are established based on the residual solvent resonance.

3.4 CHARACTERIZATION OF THE MAGNETIC MOMENT

The magnetic moment of the Fe(II)-complexes was measured using a Physical Property Measurement System (PPMS®) by *Quantum Design.* The experimental setup consisted of a vibrating sample magnetometer attachment (VSM), bearing a brass-sample holder with a PMMA powder container. The moment was determined in an external field of 1T in the range of 120K to 375K.

3.5 SINGLE CRYSTAL X-RAY DIFFRACTION (SC-XRD)

The single crystal X-ray diffraction measurements were carried out in collaboration with Berthold Stöger at the X-Ray Center at Vienna University of Technology and with Gerald Giester at the Institute of Mineralogy at Vienna University. Single crystals were attached to a glass fiber by using perfluorinated oil and were mounted on a Bruker KAPPA APEX II diffractometer equipped with a CCD detector. Data were collected at 100 K and 200 K in a dry stream of nitrogen with Mo-Kα radiation (λ = 0.71073 Å). Redundant data sets up to $2\theta = 55°$ were collected. Data were reduced to intensity values by using SAINT-Plus[12], and an absorption correction was applied by using the multi-scan method implemented by SADABS.[12] The structures at 100 K were solved by using charge-flipping implemented by SUPERFLIP.[13] Initial models of the complexes at 200 K were derived from models based on 100 K data. The structures were refined against F values with JANA2006.[14] For the iron(II) complexes, protons were placed at calculated positions and refined as riding on the parent C atoms. All non-H atoms were refined with anisotropic displacement parameters.

3.6 CYCLIC VOLTAMMETRY

Cyclic voltammetry measurements were performed on an Agilent 33120A Waveform Generator combined with an Agilent 34970A Data Acquisition Unit. Data were acquired with a sweep-range -1.7 to +1.5 Volt and a sweep rate of 50mV/s. A calomel electrode was used as reference, a platinum electrode as working electrode. Tetrabutylammonium tetrafluoroborate was used as conducting salt, dry MeCN as solvent. No internal standard was used.

3.7 SYNTHESIS OF THE LIGANDS

3.7.1 Synthesis of potassium pyrazolate

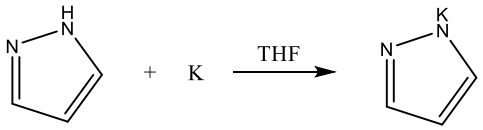

1

A 250mL single neck round bottomed flask was charged with 12.00g of 1H-pyrazole (0.176mol, 1.1eq.) and 60mL of dry THF. Under inert atmosphere 6.25g of potassium (0.16mol, 1eq.) were added in the flask in small pieces. The flask was equipped with a reflux condenser and cooled with an ice bath. Right after the addition of potassium, a white solid began to form. After 2 hours all the potassium was consumed. The suspension was filtered, the flask and the solid were washed three times each with dry THF. The product was finally dried under vacuum and isolated as a white solid (12g, 70.54% yield). IR spectrum was recorded. A second synthesis with identical protocol was performed (13.82 g, 81%yield).

3.7.2 Synthesis of 1-propyl-1H-pyrazole

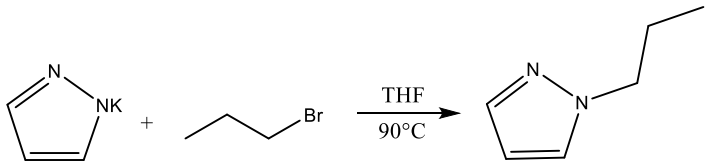

1 **2**

A vial was charged with 0.77g of **1** (7.25mmol, 1eq.) and sealed. Under inert atmosphere 1.88g of 1-bromopropane (8.70mmol, 1.2eq.) and 20mL dry THF were inserted. The reaction was heated to 90°C and left stirring for 18h. A white precipitate was formed. The mixture was filtered and both the vial and the solid were washed three times each with dry THF. The liquid phase was collected, the solvent evaporated and a yellow oil was isolated. ^{1}H and ^{13}C NMR spectra showed presence of residual impurities. The product was purified via flash column chromatography (MeCN : CH_2Cl_2 = 3:2, R_f=0.5) and isolated as a yellow oil (0.2g, 25% yield). Due to the insufficient amount of product, a second synthesis was performed, using the same protocol (including purification via flash column chromatography) but using 5g (47.09mmol, 1eq.) of **1** and 6.95g (56.51mmol, 1.2eq.) of 1-bromopropane. The product was isolated as a yellow oil (4.51g, 87.1% yield)

^{1}H NMR (400 MHz, $CDCl_3$) δ 7.42 (d, *J* = 1.5 Hz, 1H), 7.29 (d, *J* = 2.1 Hz, 1H), 6.15 (t, *J* = 2.1 Hz, 1H), 4.01 (t, 2H), 1.81 (m, 2H), 0.83 (t, *J* = 7.4 Hz, 3H).

^{13}C NMR (101 MHz, $CDCl_3$) δ 139.03, 128.85, 105.09, 53.74, 23.78, 11.13.

3.7.3 Synthesis of 1-octyl-1H-pyrazole

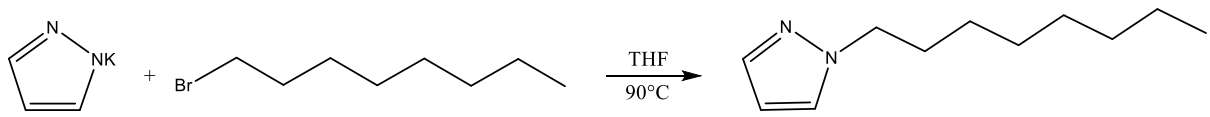

1 **3**

A vial was charged with 1.50g of **1** (14.13mmol, 1eq.) and sealed. Under inert atmosphere 3.27g of 1-bromooctane (2.95mL, 16.95mmol, 1.2eq.) and 20mL dry THF were added. The reaction was heated to 90°C and left stirring for 18h. A brownish precipitate was formed. The mixture was filtered and both the vial and the solid were washed three times each with dry THF. The liquid phase was collected and the solvent evaporated. The resulting oil was finally dried under vacuum and after NMR analysis confirmed its purity, **3** was isolated as a colorless oil (2.2 g, 88%yield)

^{1}H NMR (400 MHz, $CDCl_3$) δ 7.42 (dd, *J* = 4.6, 1.4 Hz, 1H), 7.29 (dd, *J* = 4.6, 1.9 Hz, 1H), 6.25 – 6.01 (m, 1H), 4.04 (td, *J* = 7.2, 4.9 Hz, 2H), 1.79 (s, 3H), 1.23 (s, 14H), 0.92 – 0.62 (m, 4H).

^{13}C NMR (101 MHz, $CDCl_3$) δ 139.21, 130.83, 106.95, 52.66, 31.65, 29.01, 27.55, 26.97, 22.94, 14.02.

3.7.4 Synthesis of 1,2-di(1H-pyrazol-1-yl)ethane

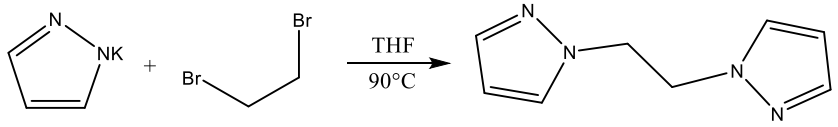

1 **4**

A vial was charged with 2.00g of **1** (18.84mmol, 1eq.) and sealed. Under inert atmosphere 1.70g of 1,2-dibromoethane (0.78mL, 9.04mmol, 0.48eq.) and 20mL dry THF were added. The reaction was heated to 90°C and left stirring for 18h. A white precipitate was formed. The mixture was filtered and both the vial and the solid were washed three times each with dry THF. The liquid phase was collected, the solvent evaporated, and a yellow oil was isolated. ^{1}H and ^{13}C NMR spectra showed the presence of residual impurities. The product was purified via flash column chromatography (MeCN : CH_2Cl_2 = 3:2, R_f=0.5) and isolated as yellow paste (1.08g, 35% yield).

^{1}H NMR (400 MHz, $CDCl_3$) δ 7.55 (dd, *J* = 7.5, 1.4 Hz, 2H), 7.40 (dd, *J* = 7.5, 1.6 Hz, 2H), 6.22 (t, *J* = 7.5 Hz, 2H), 4.41 (s, 4H).

^{13}C NMR (101 MHz, $CDCl_3$) δ 139.21, 130.83, 106.95, 45.95.

3.7.5 Synthesis of 1,3-di(1H-pyrazol-1-yl)propane

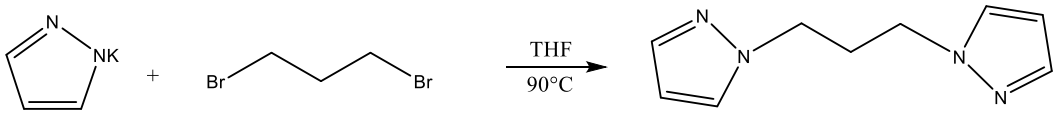

1 **5**

A vial was charged with 2.00g of **1** (18.84mmol, 1eq.) and sealed. Under inert atmosphere 1.83g of 1,3-dibromopropane (0.92mL, 9.04mmol, 0.48eq.) and 20mL dry THF were added. The reaction was heated to 90°C and left stirring for 18h. A brownish precipitate was formed. The mixture was filtered and both the vial and the solid were washed 3 times each with dry THF. The liquid phase was collected, the solvent evaporated and a yellow oil was isolated. ^{1}H and ^{13}C NMR spectra showed the presence of residual impurities. The product was purified via flash column chromatography (MeCN : CH_2Cl_2 = 3:2, R_f=0.5) and isolated as a yellow oil (1.63g, 78% yield)

^{1}H NMR (400 MHz, $CDCl_3$) δ 7.44 (d, *J* = 1.3 Hz, 2H), 7.29 (d, *J* = 2.0 Hz, 2H), 6.15 (d, *J* = 1.9 Hz, 2H), 3.99 (t, *J* = 6.5 Hz, 4H), 2.32 (p, *J* = 6.5 Hz, 2H).

^{13}C NMR (101 MHz, $CDCl_3$) δ 139.53, 129.61, 105.42, 48.55, 30.88.

3.7.6 Synthesis of 1,4-di(1H-pyrazol-1-yl)butane

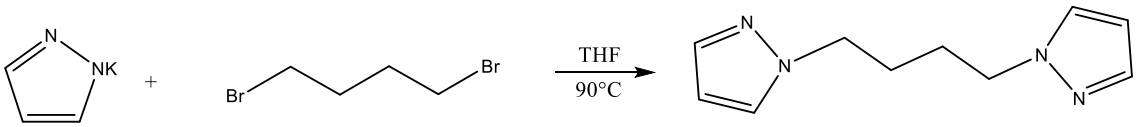

1 **6**

A vial was charged with 2.00g of **1** (18.84mmol, 1eq.) and sealed. Under inert atmosphere 1.95g of 1,4-dibromobutane (1.07mL, 9.04mmol, 0.48eq.) and 20mL dry THF were added. The reaction was heated at 90°C and left stirring for 18h. A brownish precipitate was formed. The mixture was filtered and both the vial and the solid were washed 3 times each with dry THF. The liquid phase was collected, the solvent evaporated and an orange oil was isolated. ^{1}H and ^{13}C NMR spectra showed the presence of residual impurities. The product was purified via flash column chromatography (MeCN : CH_2Cl_2 = 3:2, R_f=0.5) and isolated as a yellow oil (1.74g, 49% yield)

^{1}H NMR (400 MHz, $CDCl_3$) δ 7.49 (d, *J* = 1.5 Hz, 2H), 7.33 (d, *J* = 2.2 Hz, 2H), 6.22 (t, *J* = 2.1 Hz, 2H), 4.09 (m, 4H), 1.82 (m, 4H).

^{13}C NMR (101 MHz, $CDCl_3$) δ 139.26, 129.06, 105.40, 51.35, 27.46.

3.7.7 Synthesis of 1,4-bis((1H-pyrazol-1-yl)methyl)benzene

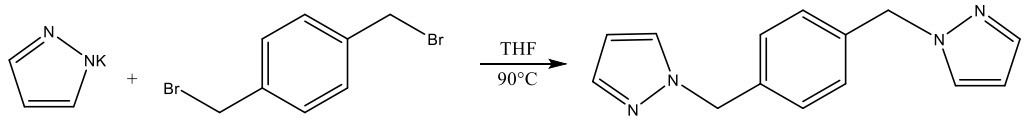

1 **7**

A vial was charged with 1.5g of **1** (14.13mmol, 1eq.) and sealed. Under inert atmosphere 1.79g of 1,4-dibromomethylbenzene (6.78mmol, 0.48 eq.) and 20mL dry THF were added. The reaction was heated at 90°C and left stirring for 18h. A white precipitate was formed. The mixture was filtered and both the vial and the solid were washed 3 times each with dry THF. The liquid phase was collected, the solvent evaporated and the product isolated as a cream-white solid, whose purity was confirmed by ^{1}H and ^{13}C NMR spectra (1.75g, 52% yield).

^{1}H NMR (400 MHz, $CDCl_3$) δ 7.48 (s, 2H), 7.31 (s, 2H), 7.12 (s, 4H), 6.22 (s, 2H), 5.25 (s, 4H).

^{13}C NMR (101 MHz, $CDCl_3$) δ 139.43, 136.45, 129.43, 128.13, 106.13, 77.35, 77.03

3.7.8 Synthesis of potassium imidazolate

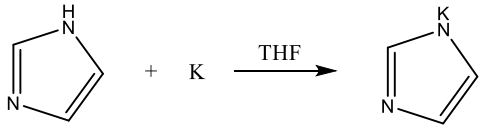

8

A 250 mL single neck round bottomed flask was charged with 12.00g of 1H-imidazole (17.63mmol, 1.1eq.) and 60mL of dry THF. Under inert atmosphere 6.25g of potassium (15.98mmol, 1eq.) were added in the flask in small pieces. The flask was equipped with a reflux condenser and cooled with an ice bath. Right after the addition of potassium, a white solid began to form. After 2 hours no residual potassium was left in the flask. The suspension was filtered, the flask and the solid were washed three times each with dry THF. The product was finally dried under vacuum and isolated as a yellow solid (16,3 g, 96 % yield).

3.7.9 Synthesis of 1-octyl-1H-imidazole

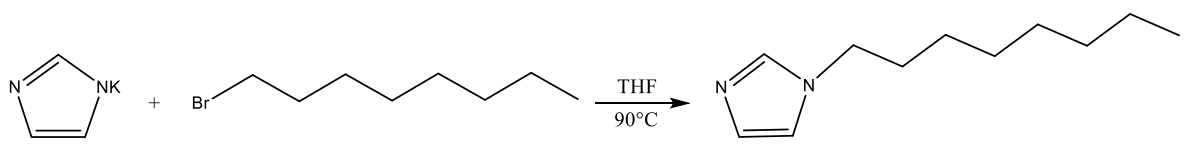

8 **10**

A vial was charged with 1.50g of **8** (14.13mmol, 1eq.) and sealed. Under inert atmosphere 3.27g of 1-bromooctane (2.95mL, 16.95mmol, 1.2eq.) and 20mL dry THF were added. The reaction was heated to 90°C and left stirring for 18h. A brownish precipitate was formed. The mixture

was filtered and both the vial and the solid were washed 3 times each with dry THF. The liquid phase was collected and after solvent evaporation a brown oil was isolated. ^{1}H and ^{13}C NMR spectra showed the presence of residual impurities, therefore, the product was purified via flash column chromatography (MeCN : CH_2Cl_2 = 3:2, R_f=0.5) and isolated as brown oil (2.31g, 90% yield)

^{1}H NMR (400 MHz, $CDCl_3$) δ 7.27 (s, 2H), 7.05 (d, *J* = 7.5 Hz, 2H), 6.96 (d, *J* = 7.5 Hz, 2H), 3.85 (dd, *J* = 14.8, 7.6 Hz, 4H), 1.78 (p, *J* = 7.9 Hz, 4H), 1.50 – 1.19 (m, 10H), 0.99 (t, *J* = 6.4 Hz, 6H).

^{13}C NMR (101 MHz $CDCl_3$) δ 139.62, 127.18, 122.83, 47.99, 31.65, 29.01, 27.47, 27.36, 22.94, 14.02.

3.7.10 Synthesis of 1,2-di(1H-imidazol-1yl)ethane

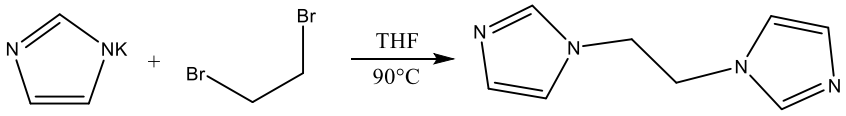

8 **11**

A vial was charged with 2g of **8** (18.84mmol, 1eq.) and sealed. Under inert atmosphere 1.70g of 1,2-dibromoethane (0.78mL, 9.04mmol, 0.48eq.) and 20mL dry THF were added. The reaction was heated to 90°C and left stirring for 18h. A brownish precipitate was formed. The mixture was filtered and both the vial and the solid were washed 3 times each with dry THF. The liquid phase was collected, the solvent evaporated, and a brown oil was isolated. ^{1}H and ^{13}C NMR spectra showed the presence of residual impurities, therefore, the product was purified via flash column chromatography (MeCN : CH_2Cl_2 = 3:2, R_f=0.5) and isolated as an orange oil (1.20g, 40% yield)

^{1}H NMR (400 MHz, $CDCl_3$) δ 7.66 (s, 2H), 7.19 (d, *J* = 12.7 Hz, 2H), 6.96 (d, *J* = 15.5 Hz, 2H), 4.22 (s, 4H).

^{13}C NMR (101 MHz, $CDCl_3$) δ 137.09, 135.00, 130.14, 47.91.

3.7.11 Synthesis of 1,3-di(1H-imidazol-1yl)propane

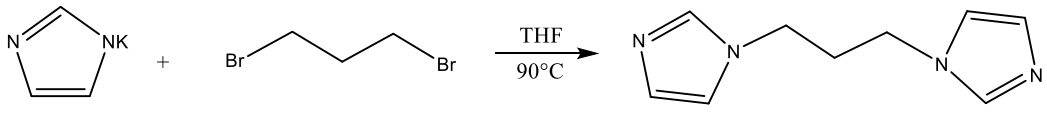

8 **12**

A vial was charged with 2.00g of **8** (18.84mmol, 1eq.) and sealed. Under inert atmosphere 1.83g of 1,3-dibromopropane (0.92mL, 9.04mmol, 0.48eq.) and 20mL dry THF were added. The reaction was heated to 90°C and left stirring for 18h. A brownish precipitate was formed. The mixture was filtered and both the vial and the solid were washed 3 times each with dry THF. The liquid phase was collected, the solvent evaporated, and a yellow oil was isolated. ^{1}H and ^{13}C NMR spectra showed the presence of residual impurities. The product was purified via

flash column chromatography (MeCN : CH_2Cl_2 = 3:2, R_f=0.5) and isolated as a yellow oil (1.50g, 45% yield)

^{1}H NMR (400 MHz, $CDCl_3$) δ 7.40 (s, 2H), 7.02 (s, 2H), 6.86 (s, 2H), 3.87 (t, *J* = 6.9 Hz, 4H), 2.23 (p, *J* = 6.8 Hz, 2H).

^{13}C NMR (101 MHz, $CDCl_3$) δ 136.98, 129.76, 118.71, 43.47, 31.81.

3.7.12 Synthesis of 1,4-di(1H-imidazol-1yl)butane

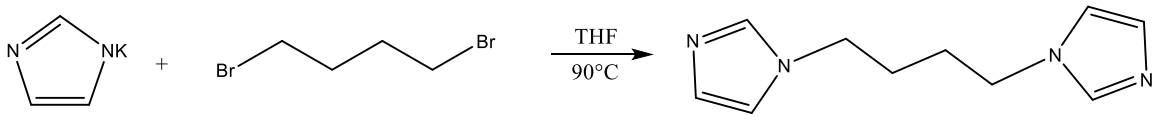

8 **13**

A vial was charged with 2g of **8** (18.84mmol, 1eq.) and sealed. Under inert atmosphere 1.95g of 1,4-dibromobutane (1.07mL, 9.04mmol, 0.48eq.) and 20mL dry THF were added. The reaction was heated at 90°C and left stirring for 18h. A brownish precipitate was formed. The mixture was filtered and both the vial and the solid were washed 3 times each with dry THF. The liquid phase was collected, the solvent evaporated, and a yellow oil was isolated. ^{1}H and ^{13}C NMR spectra showed the presence of residual impurities. The product was purified via flash column chromatography (MeCN : CH_2Cl_2 = 3:2, R_f=0.5) and isolated as a yellow oil (1.60g, 44.5% yield)

^{1}H NMR (400 MHz, $CDCl_3$) δ 7.28 (s, 2H), 7.05 (d, *J* = 7.5 Hz, 2H), 6.97 (d, *J* = 7.5 Hz, 2H), 3.91 (d, *J* = 36.6 Hz, 4H), 1.80 (t, *J* = 2.7 Hz, 4H).

^{13}C NMR (101 MHz, $CDCl_3$) δ 139.62, 127.18, 122.83, 47.98, 25.51.

3.7.13 Synthesis of 1,4-bis((1H-imidazol-1yl)methyl)benzene

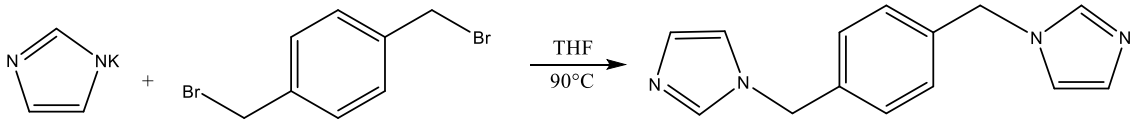

8 **14**

A vial was charged with 3g of **8** (28.25mmol, 1eq.) and sealed. Under inert atmosphere 3.58g of 1,4-dibromomethylbenzene (13.56mmol, 0.48eq.) and 20mL dry THF were added. The reaction was heated at 90°C and left stirring for 18h. A brownish precipitate was formed. The mixture was filtered and both the vial and the solid were washed 3 times each with dry THF.

The liquid phase was collected, the solvent evaporated and the product isolated as a pale yellow solid (2.98g, 90% yield), whose purity was confirmed by ^{1}H and ^{13}C NMR spectra.

^{1}H NMR (400 MHz, $CDCl_3$) δ 7.34 (s, 2H), 7.15 (s, 4H), 7.13 (d, *J* = 7.5 Hz, 2H), 7.06 (d, *J* = 7.5 Hz, 2H), 4.92 (d, *J* = 5.7 Hz, 4H).

^{13}C NMR (101 MHz, $CDCl_3$) δ 138.31, 134.42, 129.79, 128.56, 126.18, 49.10.

3.8 SYNTHESIS OF THE COMPLEXES

3.8.1 Synthesis of $[Fe(1\text{-}Pr\text{-}Pz)_6](BF_4)_2$

A Schlenk tube was charged with 0.509g of $Fe(BF_4)_2 \cdot 6H_2O$ (1.5mmol, 1eq.). Under inert atmosphere 1g (9mmol, 6eq.) of **2** was added along with 10mL of dry MeOH. The reaction was heated to 45°C and left stirring for 18 hours. After solvent evaporation a dark red oil remained in the tube. Precipitation of the product was tried, first by dissolving the product in ca. 1mL of MeOH and then adding Et_2O, but no precipitation was observed. Finally, after various attempts using different solvents and precipitating agents, by dissolving the product in ca 1mL CH_2Cl_2 and adding n-pentane, a dark-red precipitate formed. After removing the liquid phase, the wet solid was dried under vacuum and the product was isolated as a dark red powder (0.90g, 67% yield).

3.8.2 Synthesis of $[Ni(1\text{-}Pr\text{-}Pz)_6](BF_4)_2$

A single neck round-bottom flask was charged with 0.5g (4.5mmol, 6eq.) of **2**, 0.174g (0.75mmol, 1eq) of $Ni(BF_4)_2$ (0.348g of a 50%wt aqueous solution) and 10mL MeOH. The reaction was heated to 45°C and left stirring for 18h. The solvent was evaporated under vacuum and the product isolated as a blue powder (0.47g, 68%yield).

3.8.3 Synthesis of $[Ni(1\text{-}Pr\text{-}Pz)_6](ClO_4)_2$

A single neck round-bottom flask was charged with 0.5g (4.5 mmol, 6eq.) of **2**, 0.274g (0.75mmol, 1eq) of $Ni(ClO_4)_2 \cdot 6H_2O$ and 10mL MeOH. The reaction was heated to 45°C and left stirring for 18h. The solvent was evaporated under vacuum and the product isolated as a purple powder (0.50g, 72% yield).

3.8.4 Synthesis of $[Fe(1\text{-}Oct\text{-}Pz)_6](BF_4)_2$

A Schlenk tube was charged with 0.156g (0.46mmol, 1eq.) of $Fe(BF_4)_2 \cdot 6H_2O$. Under inert atmosphere 0.5g (2.8mmol, 6eq.) of **3** were added along with 10mL of dry MeOH. The reaction

was heated to 45°C and left stirring for 18 hours. After solvent evaporation a tangerine oil remained in the tube. Precipitation of the product was achieved by dissolving it in ca. 1mL CH_2Cl_2 and adding ca. 5mL of n-pentane, resulting in the formation of a yellow precipitate. After removal of the liquid phase, the wet solid was dried under vacuum and the product was isolated as a yellow powder (0.42g, 70% yield).

3.8.5 Synthesis of $[Fe(1\text{-}Oct\text{-}Pz)_6](ClO_4)_2$

A Schlenk tube was charged with 0.167g (0.46mmol 1 eq.) of $Fe(ClO_4)_2 \cdot 6H_2O$. Under inert atmosphere 0.5g of **3** were added (2.8mmol, 6eq.) along with 10mL of dry MeOH. The reaction was heated to 45°C and left stirring for 18 hours. After solvent evaporation a yellow oil remained in the tube. Precipitation of the product was achieved by dissolving it in ca. 1 mL CH_2Cl_2 and adding ca. 5 mL of n-pentane, a dark-orange precipitate formed. After removing the liquid phase, the wet solid was dried under vacuum and the product was isolated as a yellow powder (0.4g, 65% yield).

3.8.6 Synthesis of $[Ni(1\text{-}Oct\text{-}Pz)_6](BF_4)_2$

A single neck round-bottom flask was charged with 0.5g (2.8mmol, 6eq.) of **3**, 0.106g (0.46mmol, 1eq) of $Ni(BF_4)_2$ (0.212g of a 50%wt aqueous solution) and 10mL MeOH. The reaction was heated to 45°C and left stirring for 18h. The solvent was evaporated under vacuum and the product isolated as a blue powder (0.38g, 62%yield).

3.8.7 Synthesis of $[Fe(Pz\text{-}Et\text{-}Pz)_3](BF_4)_2$

A Schlenk tube was charged with 0.156g (0.37mmol, 1eq.) of $Fe(BF_4)_2 \cdot 6H_2O$. Under inert atmosphere 0.36g (2.22mmol, 6eq.) of **4** were added along with 10mL of dry MeOH. The reaction was heated to 45°C and left stirring for 18 hours. After solvent evaporation an orange oil remained in the tube. Precipitation of the product was achieved by dissolving it in ca. 1mL MeOH and adding ca. 5mL of Et_2O, resulting in the formation of a yellow precipitate. After removal of the liquid phase, the wet solid was dried under vacuum and the product was isolated as a pale-yellow powder (0.15g, 56% yield).

3.8.8 Synthesis of $[Fe(Pz\text{-}Et\text{-}Pz)_3](ClO_4)_2$

A Schlenk tube was charged with 0.134g (0.37mmol 1 eq.) of $Fe(ClO_4)_2 \cdot 6H_2O$. Under inert atmosphere 0.36g (2.22mmol, 6eq.) of **4** were added along with 10mL of dry MeOH. The reaction was heated to 45°C and left stirring for 18 hours. After solvent evaporation a yellow oil remained in the tube. Precipitation of the product was achieved by dissolving it in ca. 1 mL MeOH and adding ca. 5 mL of Et_2O, a yellow precipitate formed. After removing the liquid

phase, the wet solid was dried under vacuum and the product was isolated as a pale-yellow powder (0.10g, 36% yield).

3.8.9 Synthesis of $[Ni(Pz\text{-}Et\text{-}Pz)_3](BF_4)_2$

A single neck round-bottom flask was charged with 0.36g (2.22mmol, 6eq.) of **4**, 0.086g (0.37mmol, 1eq) of $Ni(BF_4)_2$ (0.172g of a 50%wt aqueous solution) and 10mL of MeOH. The reaction was heated to 45°C and left stirring for 18h. The solvent was evaporated under vacuum and the product isolated as a blue powder (0.2g, 73% yield).

3.8.10 Synthesis of $[Fe(Pz\text{-}Pr\text{-}Pz)_3](BF_4)_2$

A Schlenk tube was charged with 0.128g (0.38mmol, 1eq.) of $Fe(BF_4)_2 \cdot 6H_2O$. Under inert atmosphere 0.402g (2.27mmol, 6eq.) of **5** were added along with 10mL of dry MeOH. The reaction was heated to 45°C and left stirring for 18 hours. After solvent evaporation an orange oil remained in the tube. Precipitation of the product was achieved by dissolving it in ca. 1mL MeOH and adding ca. 5mL of Et_2O, resulting in the formation of a yellow precipitate. After removal of the liquid phase, the wet solid was dried under vacuum and the product was isolated as a yellow powder (0.18g, 62% yield).

3.8.11 Synthesis of $[Ni(Pz\text{-}Pr\text{-}Pz)_3](BF_4)_2$

A single neck round-bottom flask was charged with 0.403g (2.27mmol, 6eq.) of **5**, 0.088g (0.38mmol, 1eq) of $Ni(BF_4)_2$ (0.176g of a 50%wt aqueous solution) and 10mL MeOH. The reaction was heated to 45°C and left stirring for 18h. The solvent was evaporated under vacuum and the product isolated as a blue powder (0.14g, 47% yield).

3.8.12 Synthesis of $[Fe(Pz\text{-}Bu\text{-}Pz)_3](BF_4)_2$

A Schlenk tube was charged with 0.148g (0.44mmol, 1eq.) of $Fe(BF_4)_2 \cdot 6H_2O$. Under inert atmosphere 0.501g (2.63mmol, 6eq.) of **6** were added along with 10mL of dry MeOH. The reaction was heated to 45°C and left stirring for 18 hours. After solvent evaporation an orange oil remained in the tube. Precipitation of the product was achieved by dissolving it in ca. 1mL MeOH and adding ca. 5mL of Et_2O, resulting in the formation of a yellow precipitate. After removal of the liquid phase, the wet solid was dried under vacuum and the product was isolated as a cream-white powder (0.20g, 57% yield).

3.8.13 Synthesis of $[Fe(Pz\text{-}Bu\text{-}Pz)_3](ClO_4)_2$

A Schlenk tube was charged with 0.160g (0.44mmol 1 eq.) of $Fe(ClO_4)_2 \cdot 6H_2O$. Under inert atmosphere 0.503g (2.63mmol, 6eq.) of **6** were added along with 10mL of dry MeOH. The reaction was heated to 45°C and left stirring for 18 hours. After solvent evaporation a yellow oil remained in the tube. Precipitation of the product was achieved by dissolving it in ca. 1 mL MeOH and adding ca. 5 mL of Et_2O, a yellow precipitate formed. After removing the liquid phase, the wet solid was dried under vacuum and the product was isolated as a cream-white powder (0.24g, 66% yield).

3.8.14 Synthesis of $[Fe(Pz\text{-}PX\text{-}Pz)_3](BF_4)_2$

A Schlenk tube was charged with 0.118g (0.35mmol, 1eq.) of $Fe(BF_4)_2 \cdot 6H_2O$. Under inert atmosphere 0.501g (2.10mmol, 6eq.) of **7** were added along with 10mL of dry MeOH. The reaction was heated to 45°C and left stirring for 18 hours. After solvent evaporation a yellow solid remained in the tube. The solid was washed with dry CH_2Cl_2, and dried under vacuum to yield the product as a white powder (0.28g, 84%yield)

3.8.15 Synthesis of $[Ni(Pz\text{-}PX\text{-}Pz)_3](BF_4)_2$

A single neck round-bottom flask was charged with 0.502g (2.10mmol, 6eq.) of **7**, 0.081g (0.35mmol, 1eq) of $Ni(BF_4)_2$ (0.162g of a 50%wt aqueous solution) and 10mL MeOH. The reaction was heated to 45°C and left stirring for 18h. The solvent was evaporated under vacuum and the product isolated as a blue powder (0.25g, 73% yield).

3.8.16 Synthesis of $[Fe(1\text{-}Pr\text{-}Im)_6](BF_4)_2$

A Schlenk tube was charged with 0.509g of $Fe(BF_4)_2 \cdot 6H_2O$ (1.5mmol, 1eq.). Under inert atmosphere 1g (9mmol, 6eq.) of **9** was added along with 10mL of dry MeOH. The reaction was heated to 45°C and left stirring for 18 hours. After solvent evaporation a yellow solid remained in the tube. The solid was washed with dry CH_2Cl_2 and dried under vacuum to yield the product as a yellow powder (yield). This turned out to be the Fe-O cluster, so three synthesis were performed using a)the same protocol but reducing the reaction time to two hours, b)using anhydrous $Fe(BF_4)_2$ instead of the hexahydrate salt and c) using anhydrous $Fe(BF_4)_2$ and MeCN as solvent instead of MeOH. All three syntheses yielded the monomolecular species, which was isolated as a cream-white solid (a)0.80g, 60% yield, b)1.00g, 75% yield, c)0.95g, 71% yield).

3.8.17 Synthesis of $[Ni(1\text{-}Pr\text{-}Im)_6](BF_4)_2$

A single neck round-bottom flask was charged with 0.5g (4.5mmol, 6eq.) of **9**, 0.174g (0.75mmol, 1eq) of $Ni(BF_4)_2$ (0.348g of a 50%wt aqueous solution) and 10mL MeOH. The reaction was heated to 45°C and left stirring for 18h. The solvent was evaporated under vacuum and the product isolated as a blue powder (0.50g, 73% yield).

3.8.18 Synthesis of $[Fe(1\text{-}Oct\text{-}Im)_6](BF_4)_2$

A Schlenk tube was charged with 0.156g (0.46mmol, 1eq.) of $Fe(BF_4)_2 \cdot 6H_2O$. Under inert atmosphere 0.5g (2.8mmol, 6eq.) of **10** were added along with 10mL of dry MeOH. The reaction was heated to 45°C and left stirring for 18 hours. After solvent evaporation a pale-yellow oil remained in the tube. Precipitation of the product was achieved by dissolving the product in ca 1mL CH_2Cl_2 and adding ca. 5mL of n-pentane, resulting in the formation of a yellow precipitate. After removal of the liquid phase, the wet solid was dried under vacuum and the product was isolated as a cream-white powder (0.35g, 58% yield).

3.8.19 Synthesis of $[Ni(1\text{-}Oct\text{-}Im)_6](BF_4)_2$

A single neck round-bottom flask was charged with 0.5g (2.8mmol, 6eq.) of **10**, 0.106g (0.46mmol, 1eq) of $Ni(BF_4)_2$ (0.212g of a 50%wt aqueous solution) and 10mL MeOH. The reaction was heated to 45°C and left stirring for 18h. The solvent was evaporated under vacuum and the product isolated as a blue powder (0.50g, 81% yield).

3.8.20 Synthesis of $[Fe(Im\text{-}Et\text{-}Im)_3](BF_4)_2$

A Schlenk tube was charged with 0.156g (0.37mmol, 1eq.) of $Fe(BF_4)_2 \cdot 6H_2O$. Under inert atmosphere 0.36g (2.22mmol, 6eq.) of **11** were added along with 10mL of dry MeOH. The reaction was heated to 45°C and left stirring for 18 hours. After solvent evaporation an orange oil remained in the tube. Precipitation of the product was achieved by dissolving the product in ca. 1mL MeOH and adding ca. 5mL of Et_2O, resulting in the formation of a yellow precipitate. After removal of the liquid phase, the wet solid was dried under vacuum and the product was isolated as a yellow powder (0.16g, 60% yield).

3.8.21 Synthesis of $[Fe(Im\text{-}Et\text{-}Im)_3](ClO_4)_2$

A Schlenk tube was charged with 0.134g (0.37mmol 1 eq.) of $Fe(ClO_4)_2 \cdot 6H_2O$. Under inert atmosphere 0.36g (2.22mmol, 6eq.) of **11** were added along with 10mL of dry MeOH. The reaction was heated to 45°C and left stirring for 18 hours. After solvent evaporation a yellow oil remained in the tube. Precipitation of the product was achieved by dissolving the product in ca. 1 mL MeOH and adding ca. 5 mL of Et_2O, a yellow precipitate formed. After removing

the liquid phase, the wet solid was dried under vacuum and the product was isolated as a yellow powder (0.18g, 66% yield).

3.8.22 Synthesis of $[Fe(Im\text{-}Pr\text{-}Im)_3](BF_4)_2$

A Schlenk tube was charged with 0.128g (0.38mmol, 1eq.) of $Fe(BF_4)_2 \cdot 6H_2O$. Under inert atmosphere 0.402g (2.27mmol, 6eq.) of **12** were added along with 10mL of dry MeOH. The reaction was heated to 45°C and left stirring for 18 hours. After solvent evaporation an orange oil remained in the tube. Precipitation of the product was achieved by dissolving the product in ca. 1mL MeOH and adding ca. 5mL of Et_2O, resulting in the formation of a yellow precipitate. After removal of the liquid phase, the wet solid was dried under vacuum and the product was isolated as a yellow powder (0.19g, 66% yield).

3.8.23 Synthesis of $[Fe(Im\text{-}Pr\text{-}Im)_3](ClO_4)_2$

A Schlenk tube was charged with 0.138g (0.38mmol 1 eq.) of $Fe(ClO_4)_2 \cdot 6H_2O$. Under inert atmosphere 0.401g (2.27mmol, 6eq.) of **12** were added along with 10mL of dry MeOH. The reaction was heated to 45°C and left stirring for 18 hours. After solvent evaporation a yellow oil remained in the tube. Precipitation of the product was achieved by dissolving the product in ca. 1 mL MeOH and adding ca. 5 mL of Et_2O, a yellow precipitate formed. After removing the liquid phase, the wet solid was dried under vacuum and the product was isolated as a yellow powder (0.2g, 67% yield).

3.8.24 Synthesis of $[Fe(Im\text{-}Bu\text{-}Im)_3](BF_4)_2$

A Schlenk tube was charged with 0.148g (0.44mmol, 1eq.) of $Fe(BF_4)_2 \cdot 6H_2O$. Under inert atmosphere 0.501g (2.63mmol, 6eq.) of **13** were added along with 10mL of dry MeOH. The reaction was heated to 45°C and left stirring for 18 hours. After solvent evaporation an orange oil remained in the tube. Precipitation of the product was achieved by dissolving the product in ca. 1mL MeOH and adding ca. 5mL of Et_2O, resulting in the formation of a yellow precipitate. After removal of the liquid phase, the wet solid was dried under vacuum and the product was isolated as a cream-white powder (0.23g, 65% yield).

3.8.25 Synthesis of $[Fe(Im\text{-}Bu\text{-}Im)_3](ClO_4)_2$

A Schlenk tube was charged with 0.160g (0.44mmol 1 eq.) of $Fe(ClO_4)_2 \cdot 6H_2O$. Under inert atmosphere 0.503g (2.63mmol, 6eq.) of **13** were added along with 10mL of dry MeOH. The reaction was heated to 45°C and left stirring for 18 hours. After solvent evaporation a yellow oil remained in the tube. Precipitation of the product was achieved by dissolving the product in ca. 1 mL MeOH and adding ca. 5 mL of Et_2O, a yellow precipitate formed. After removing

the liquid phase, the wet solid was dried under vacuum and the product was isolated as a cream-white powder (0.25g, 69% yield).

3.8.26 Synthesis of $[Fe(Im\text{-}PX\text{-}Im)_3](BF_4)_2$

A Schlenk tube was charged with 0.118g (0.35mmol, 1eq.) of $Fe(BF_4)_2 \cdot 6H_2O$. Under inert atmosphere 0.501g (2.10mmol, 6eq.) of **14** were added along with 10mL of dry MeOH. The reaction was heated to 45°C and left stirring for 18 hours. After solvent evaporation a yellow solid remained in the tube. The solid was washed with dry CH_2Cl_2, and dried under vacuum to yield the product as a yellow powder (0.25g, 75% yield)

3.8.27 Synthesis of $[Ni(Im\text{-}PX\text{-}Im)_3](BF_4)_2$

A single neck round-bottom flask was charged with 0.502g (2.10mmol, 6eq.) of **14**, 0.081g (0.35mmol, 1eq.) of $Ni(BF_4)_2$ (0.162g of a 50%wt aqueous solution) and 10mL MeOH. The reaction was heated to 45°C and left stirring for 18h. The solvent was evaporated under vacuum and the product isolated as a blue powder (0.28g, 82% yield).

ACKNOWLEDGEMENTS

The present work in its final form would have not been accomplished without the help and support of different people. Therefore, I would like to thank:

- My supervisor Assistant Professor Priv. Doz. Dr. Peter Weinberger, for giving me the opportunity to work in his group in the first place, for the numerous advices and for the freedom he gave me during my work

- My colleague Dr. Danny Müller, for constantly following my work in the lab with remarkable patience and sharing his vast knowledge on the SCO topic and his impressive synthetic skills

- My other colleagues Dr. Christian Knoll, Marco Seifried, Georg Gravogl and Frieda Kapsamer, for the long coffee breaks who helped reduce the work-induced stress

- My family, for constantly supporting me over the years

- The FWF, project P 31 076 for their financial support

4 APPENDIX

4.1 NMR SPECTRA OF DISCUSSED SUBSTANCES

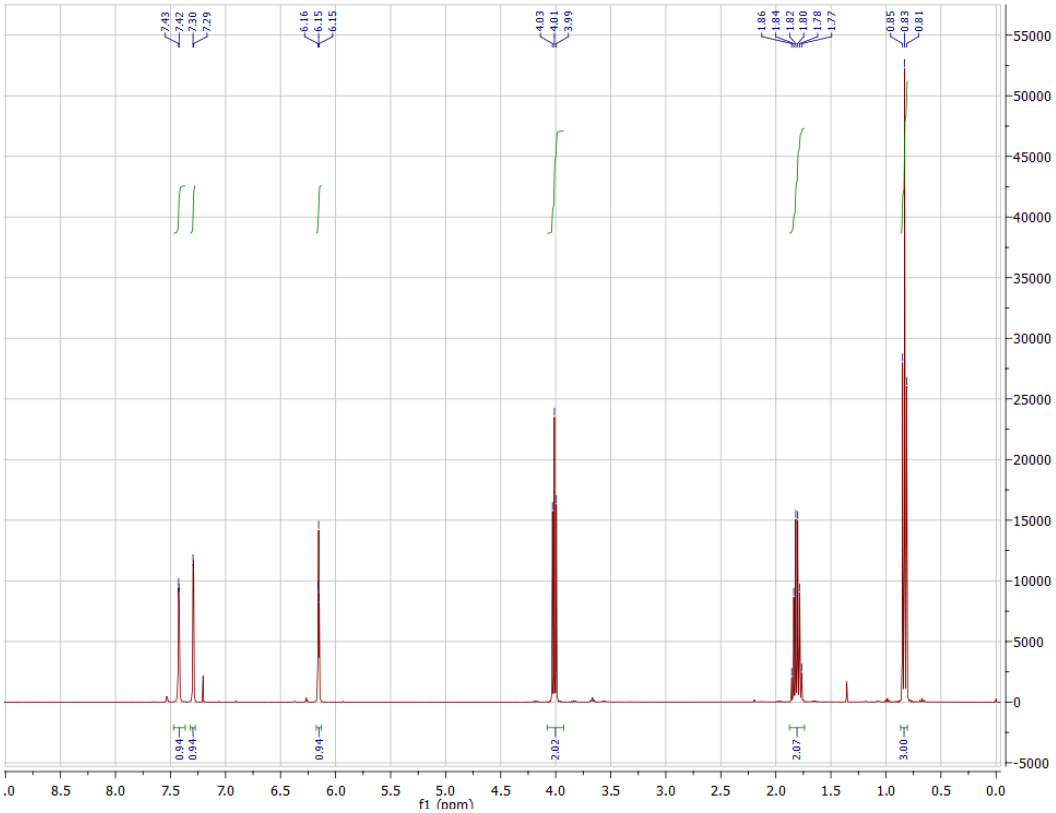

Figure 10: 1H NMR spectrum of 2

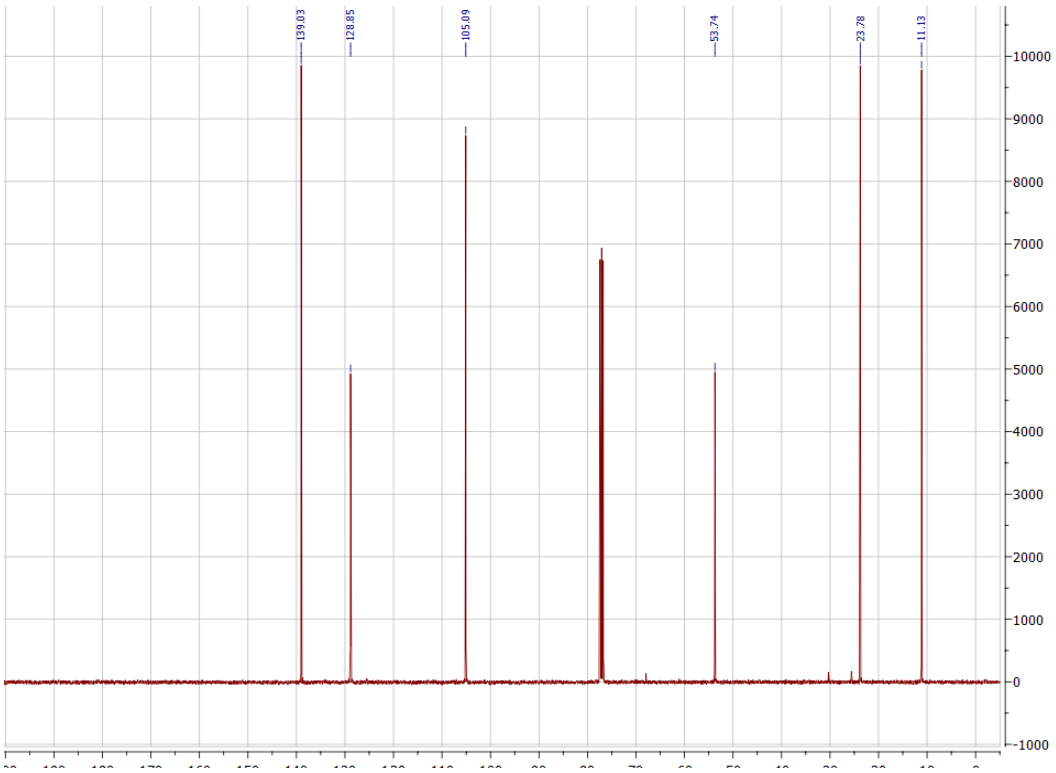

Figure 11: 13C NMR spectrum of 2

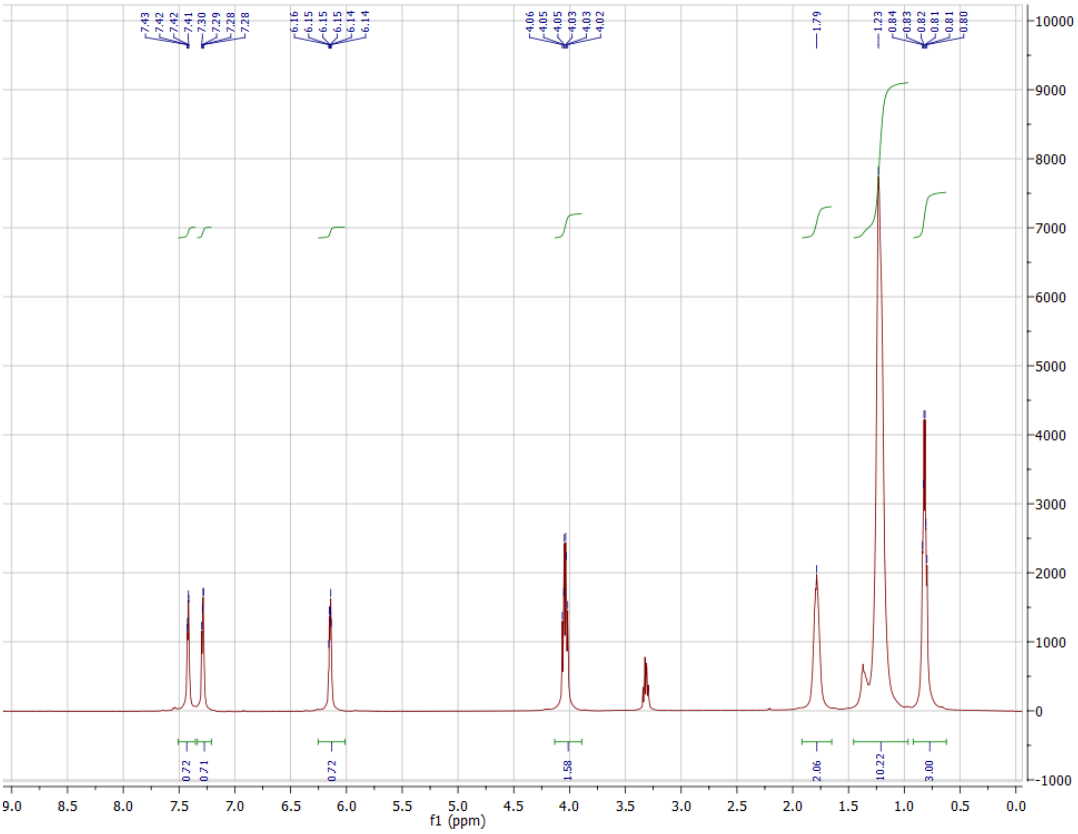

Figure 12: 1H NMR spectrum of 3

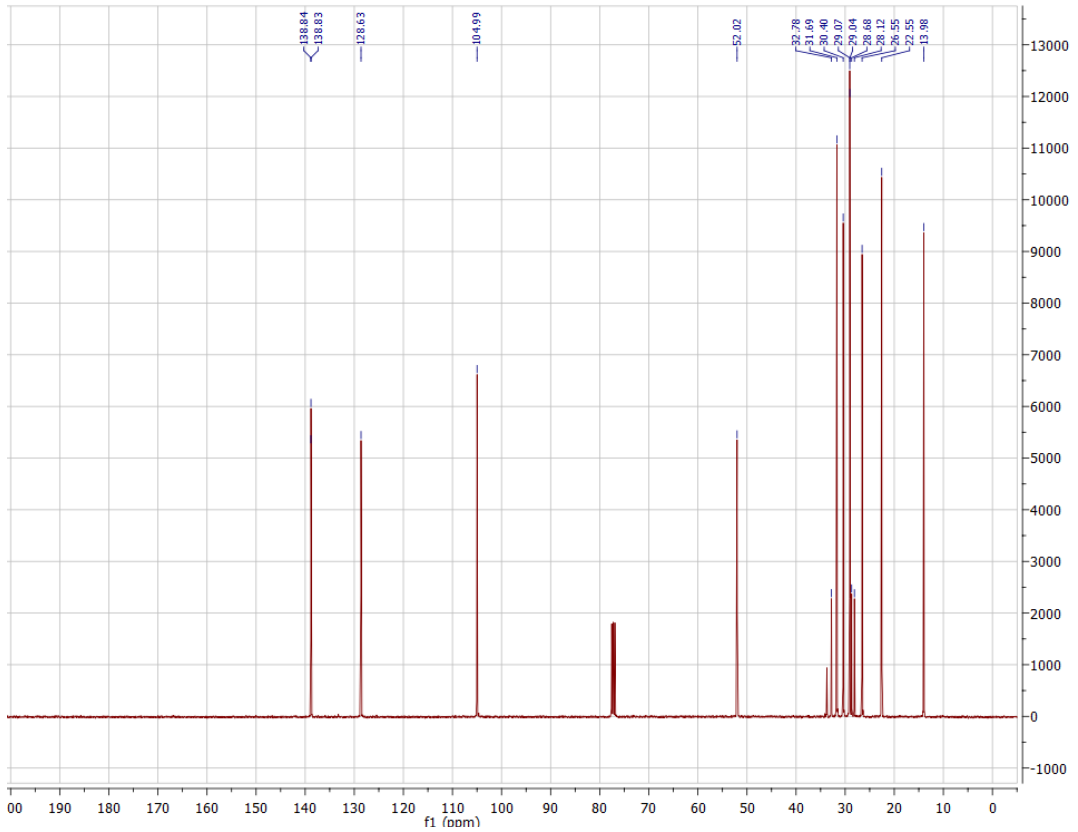

Figure 13: 13C NMR spectrum of 3

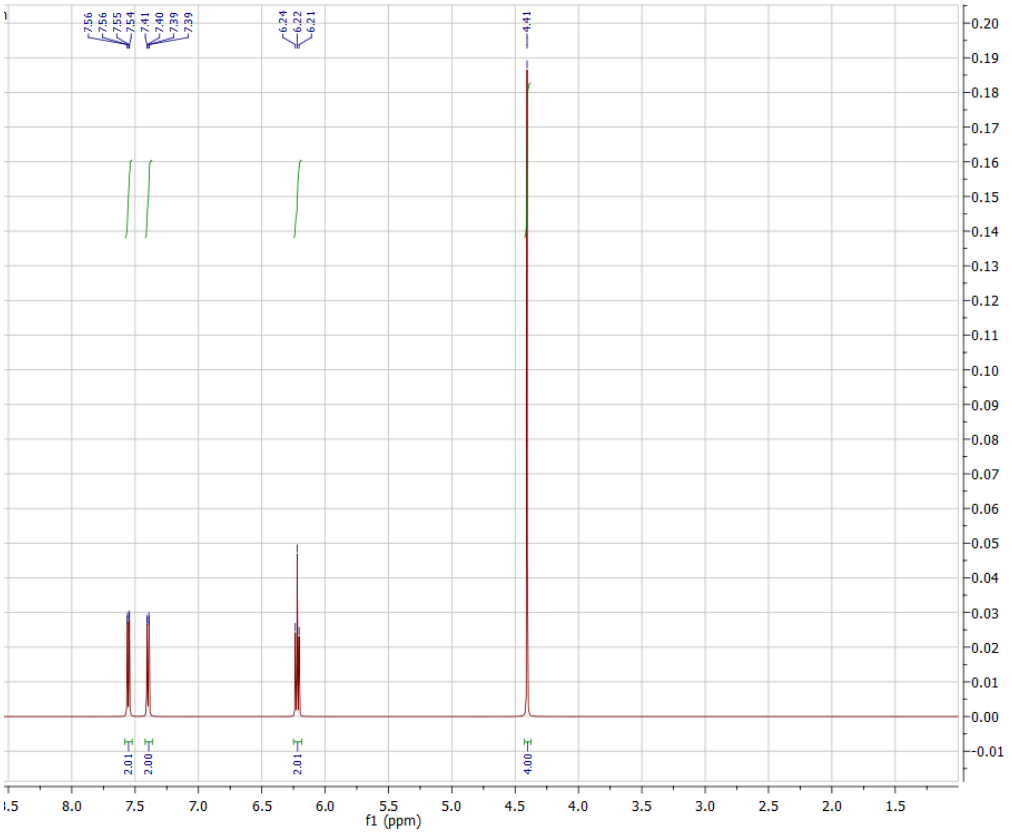

Figure 12: 1H NMR spectrum of 4

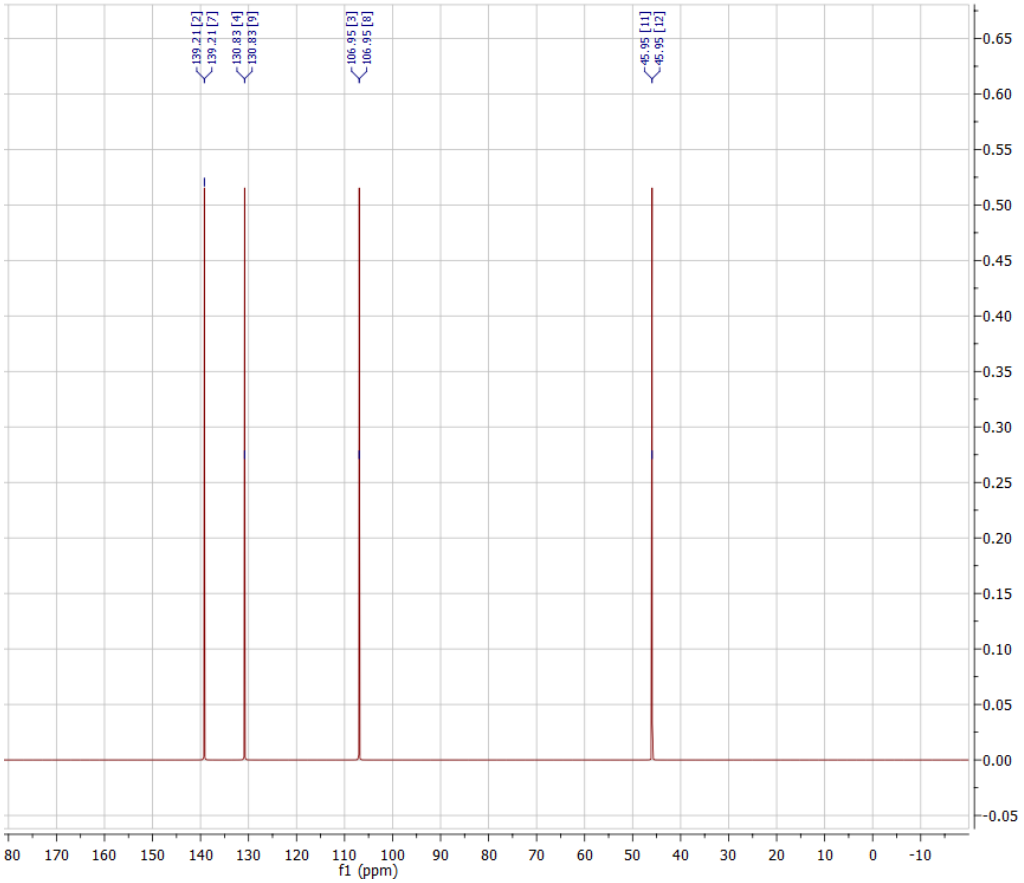

Figure 13: 13C NMR spectrum of 4

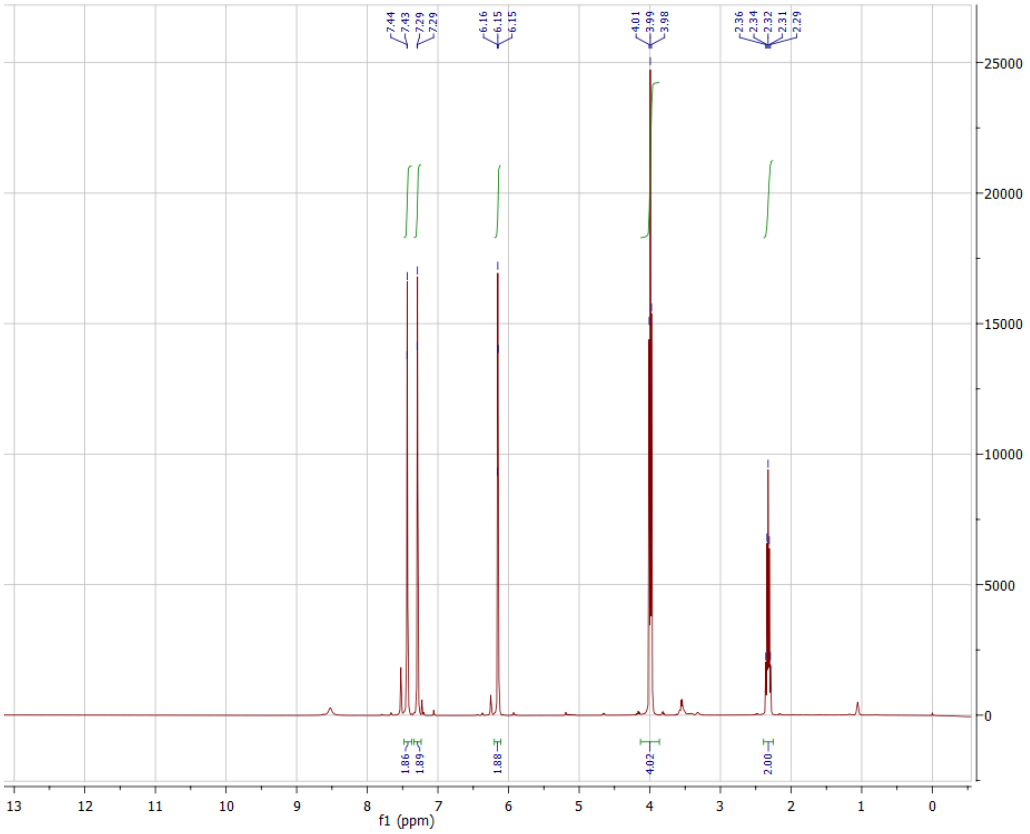

Figure 14: 1H NMR spectrum of 5

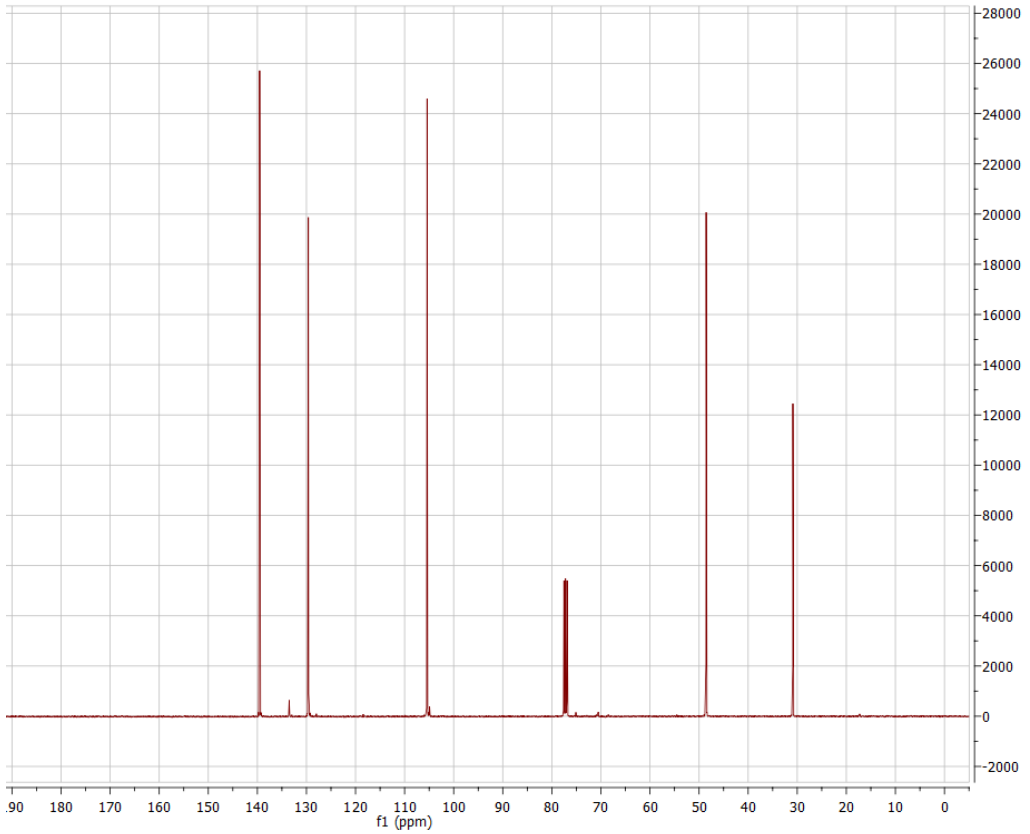

Figure 15: 13C NMR spectrum of 5

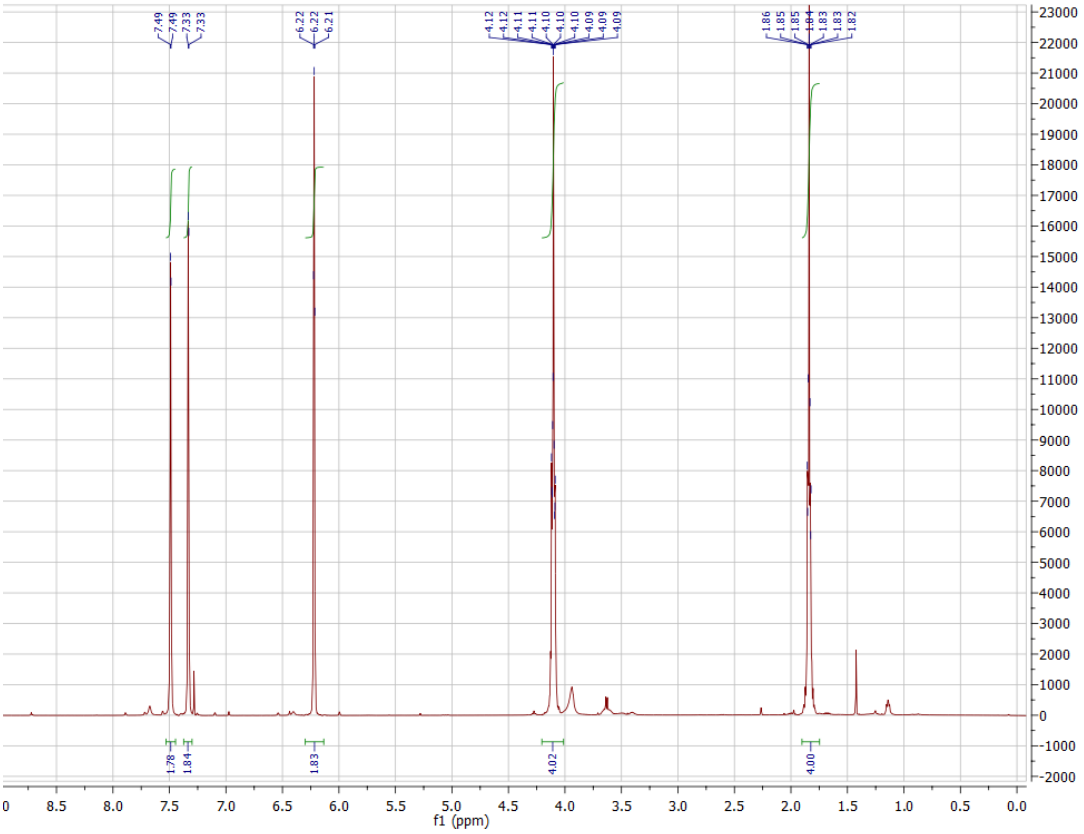

Figure 18: 1H NMR spectrum of 6

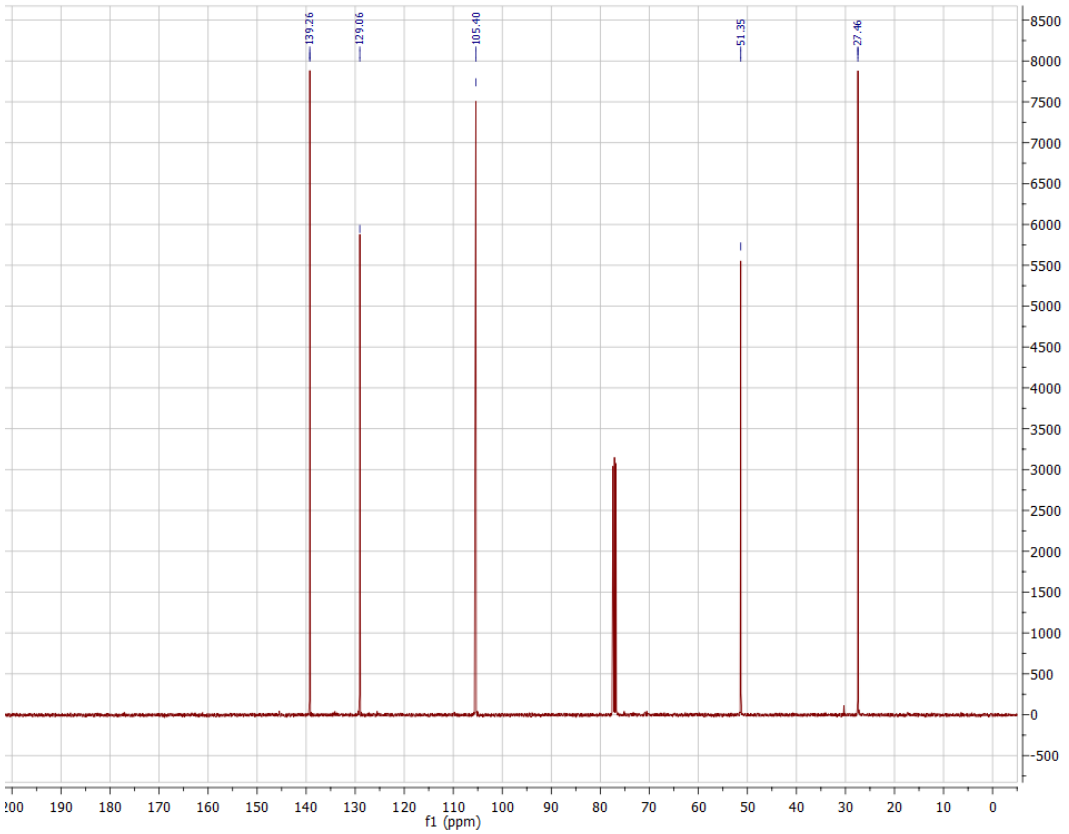

Figure 19: 13C NMR spectrum of 6

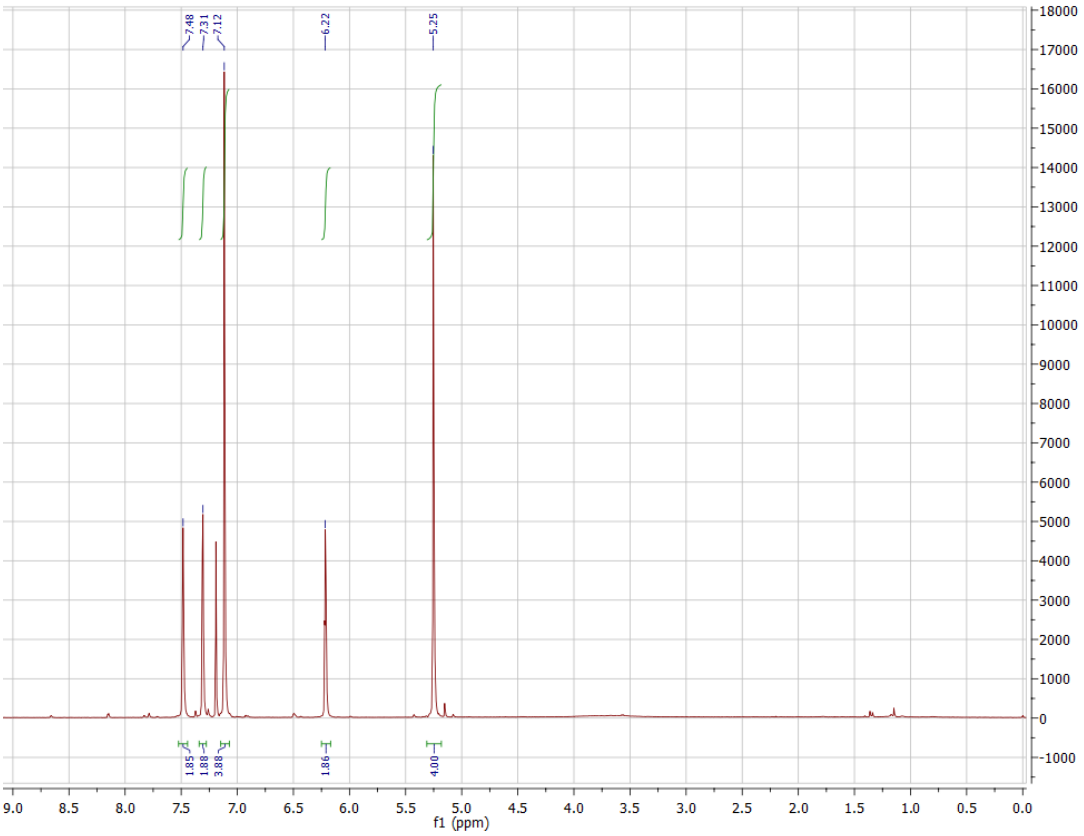

Figure 20: 1H NMR spectrum of 7

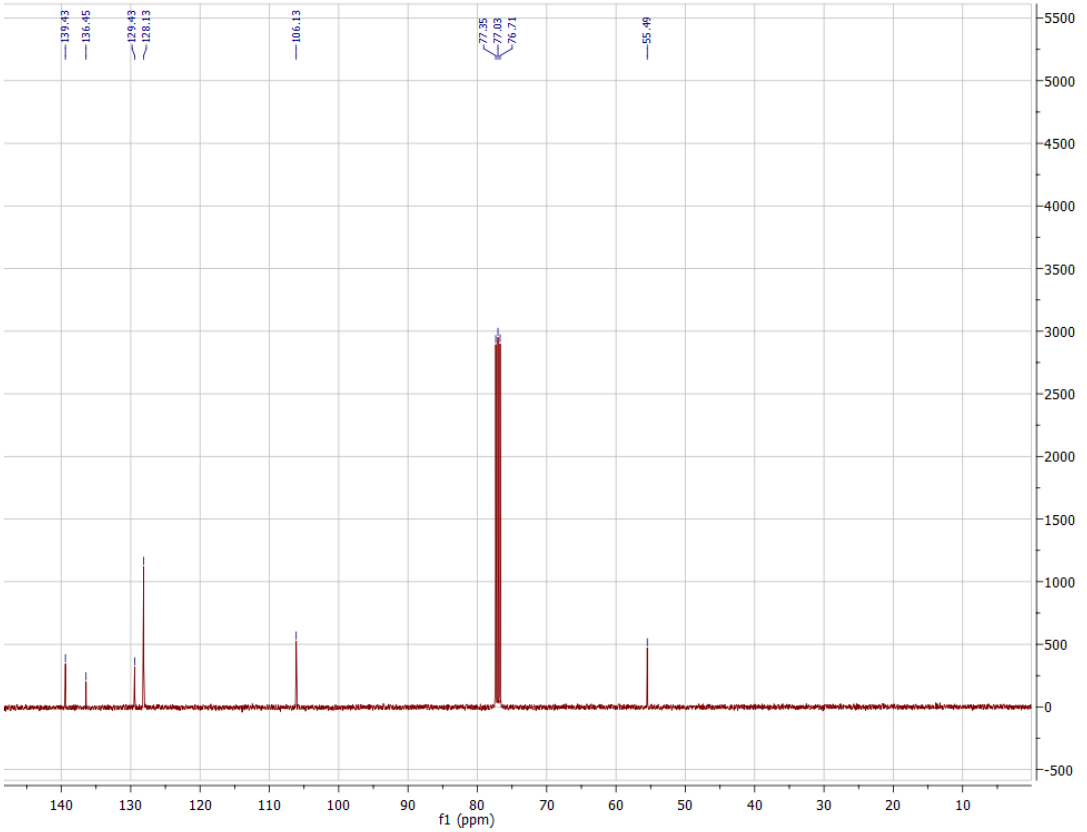

Figure 21: 13C NMR spectrum of 7

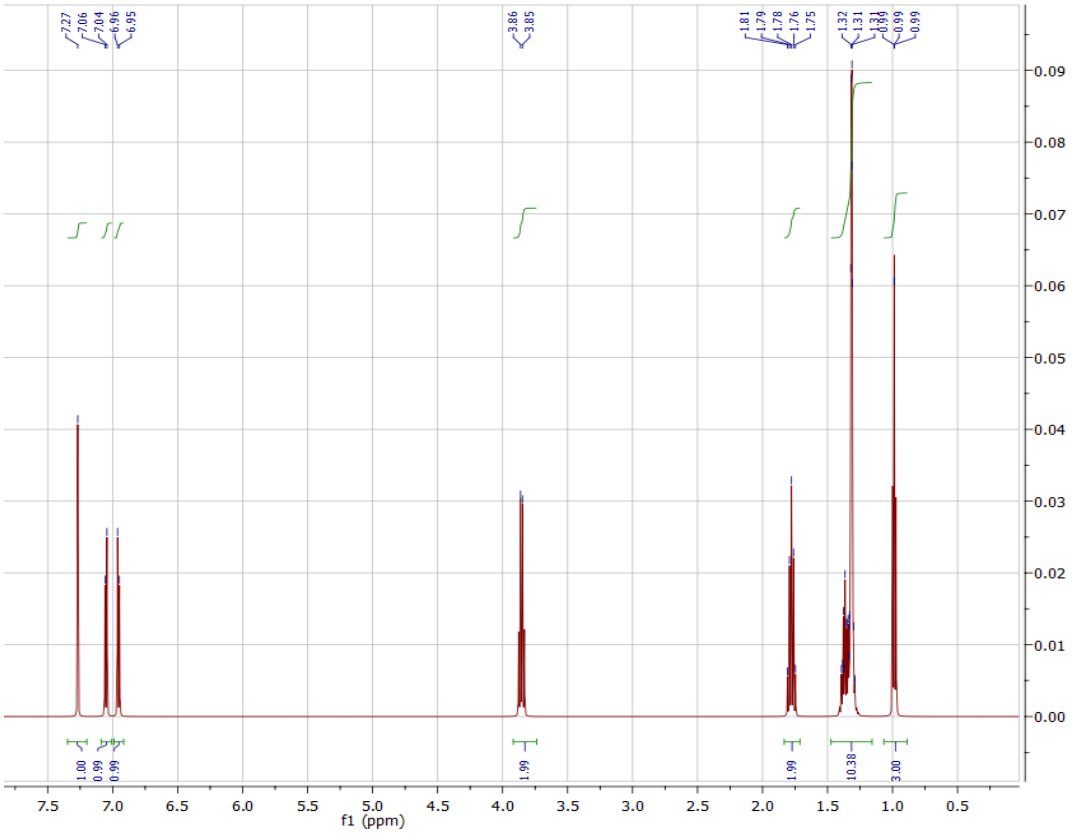

Figure 22: 1H NMR spectrum of 10

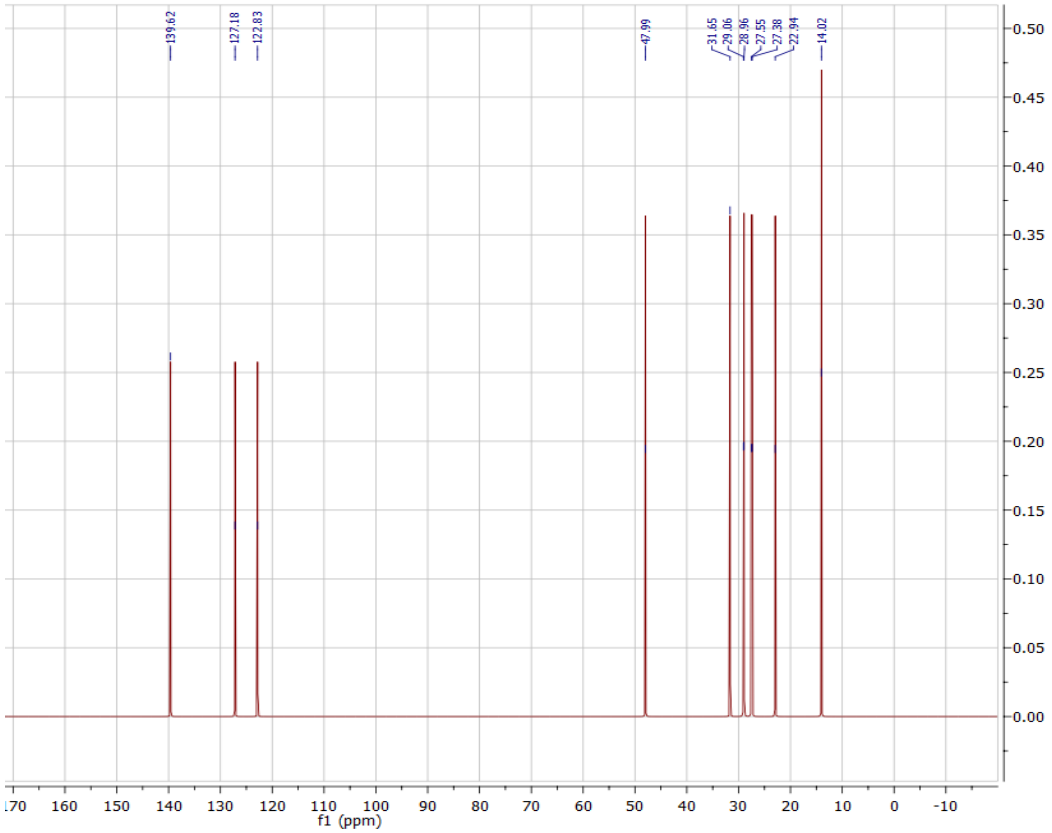

Figure 23: 13 C NMR spectrum of 10

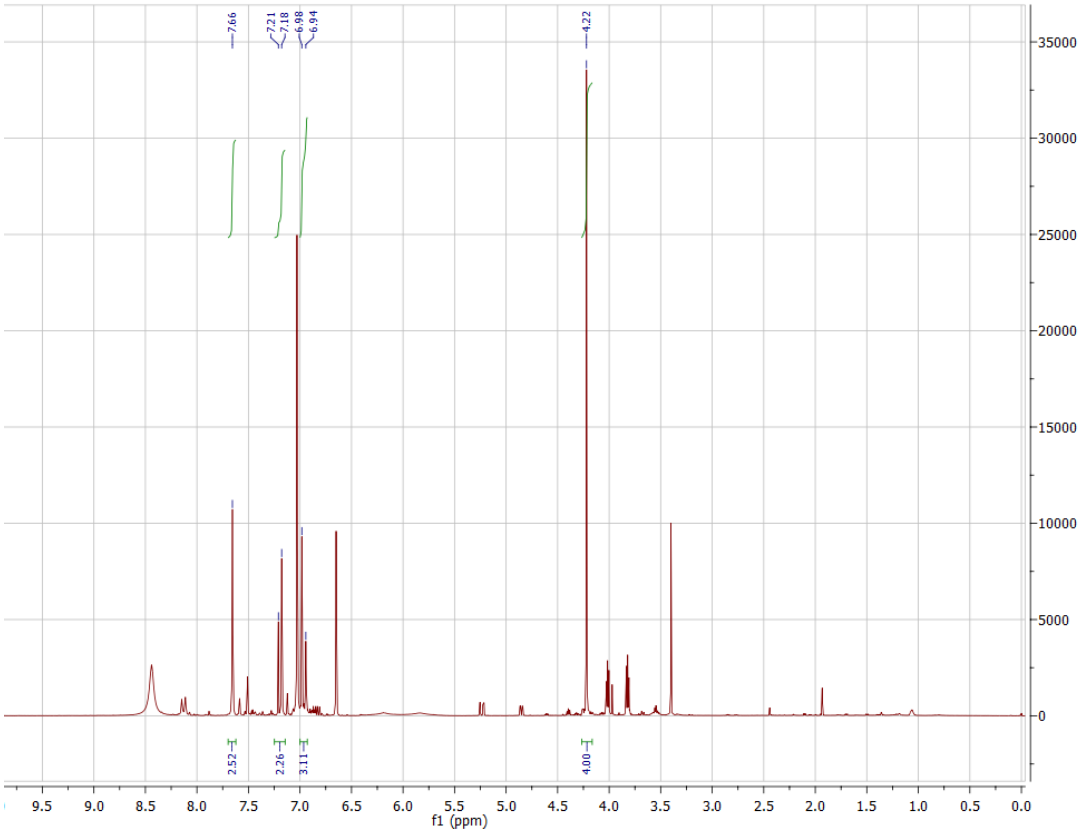

Figure 24: 1H NMR spectrum of 11

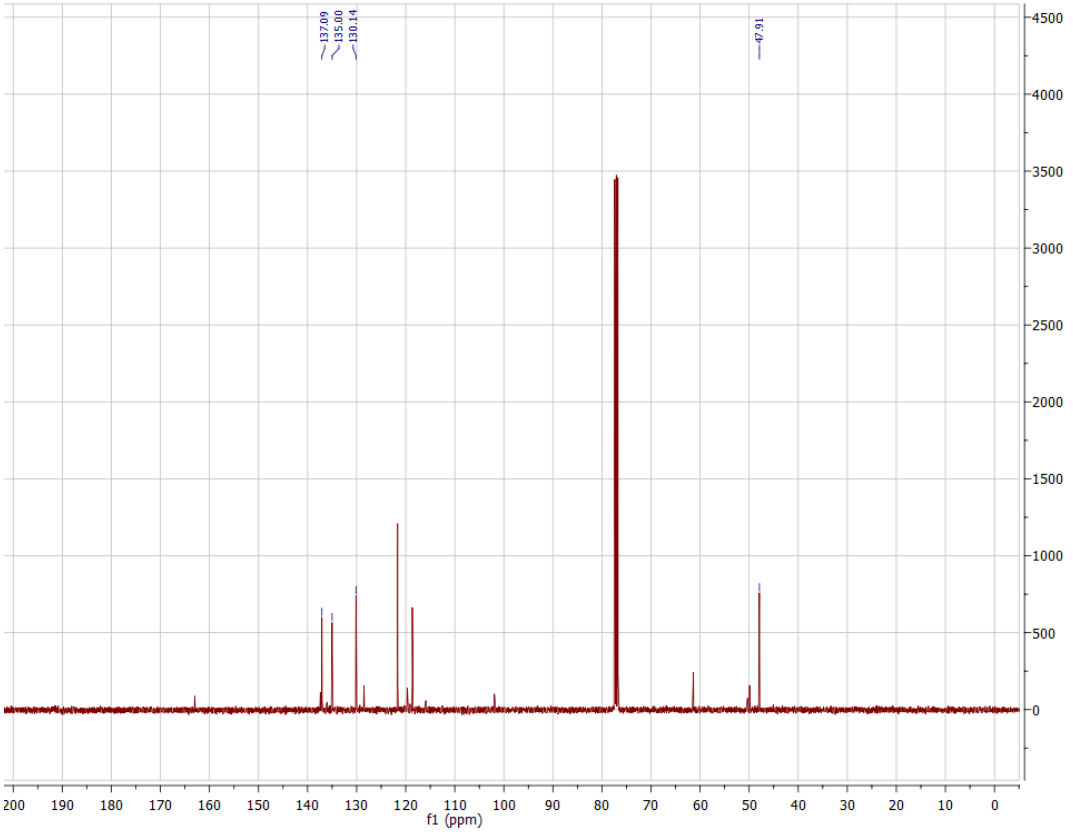

Figure 25: 13C NMR spectrum of 11

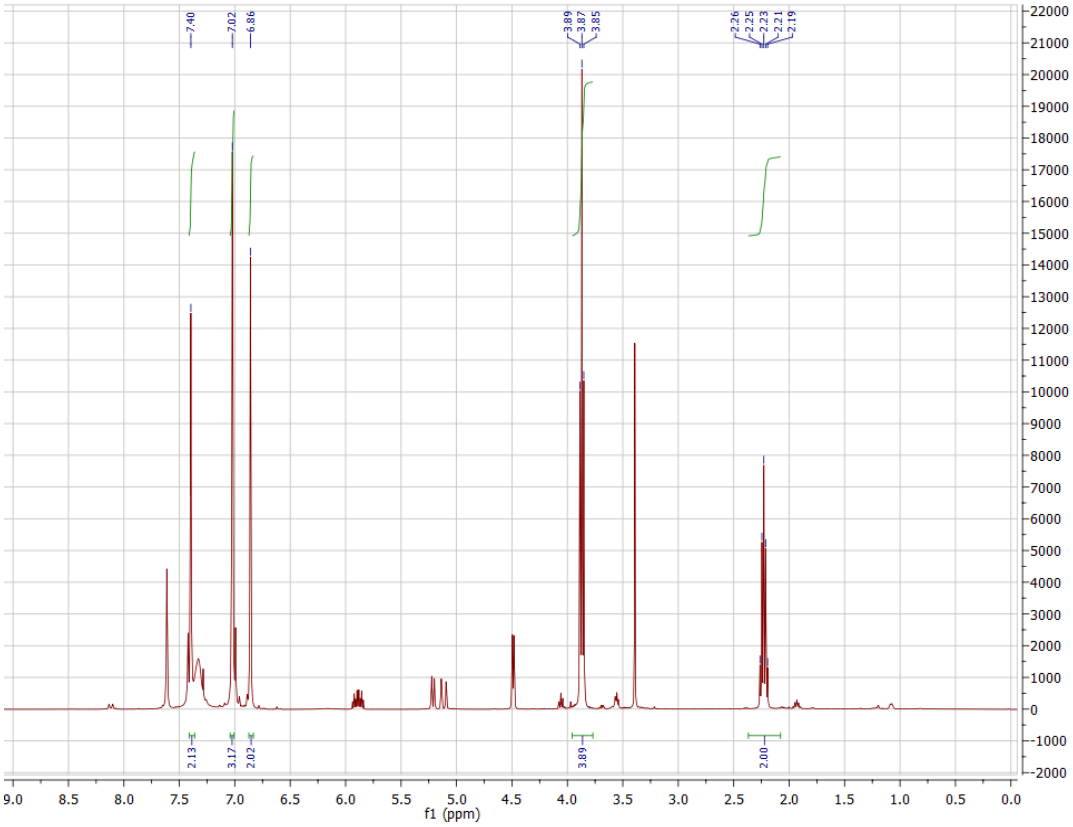

Figure 26: 1H NMR spectrum of 12

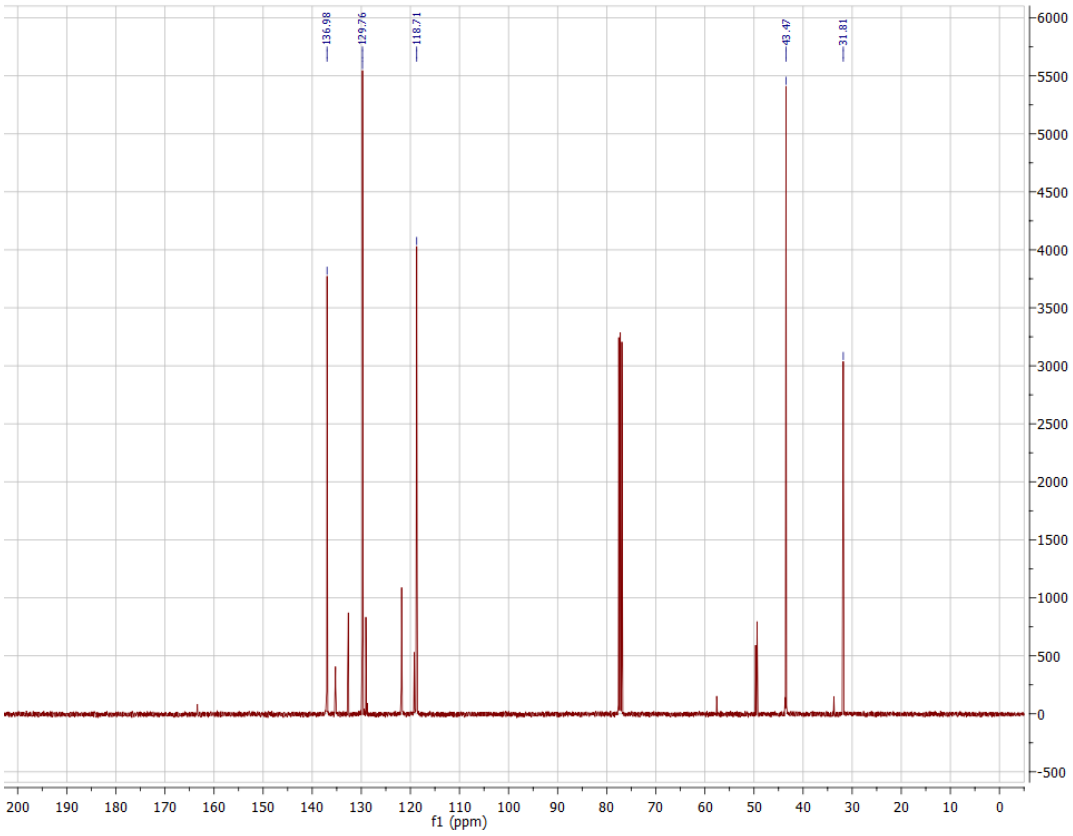

Figure 27: 13C NMR spectrum of 12

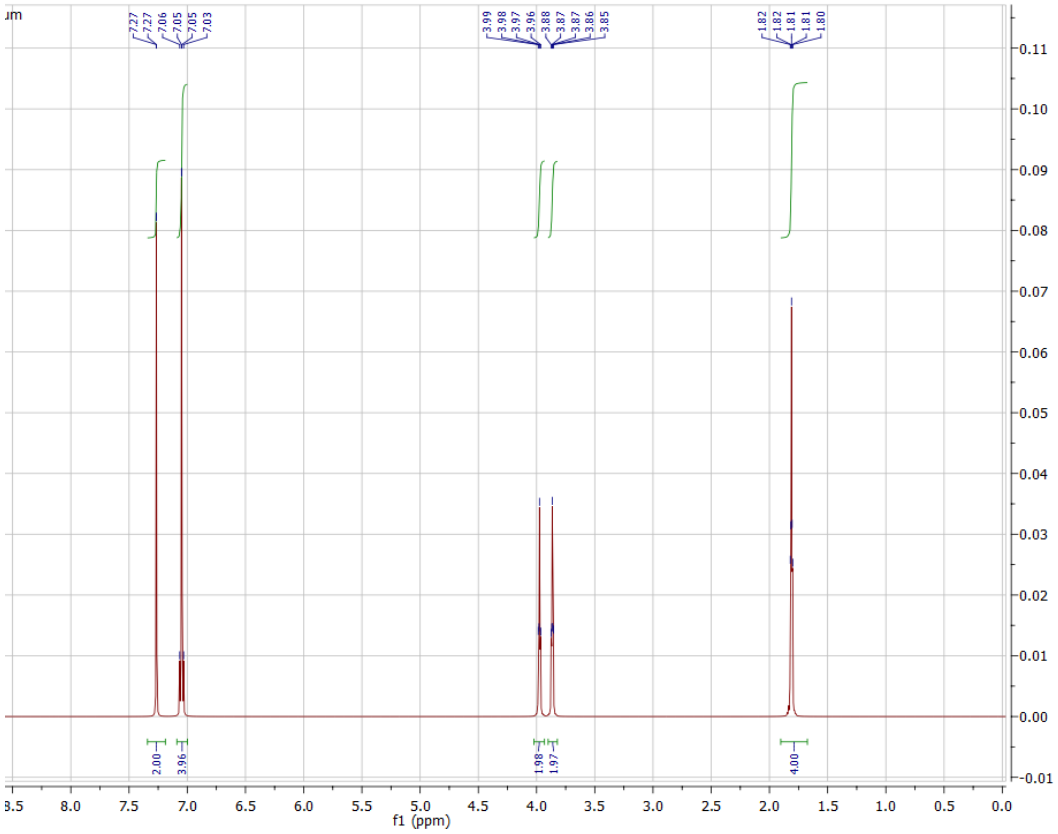

Figure 28: 1H NMR spectrum of 13

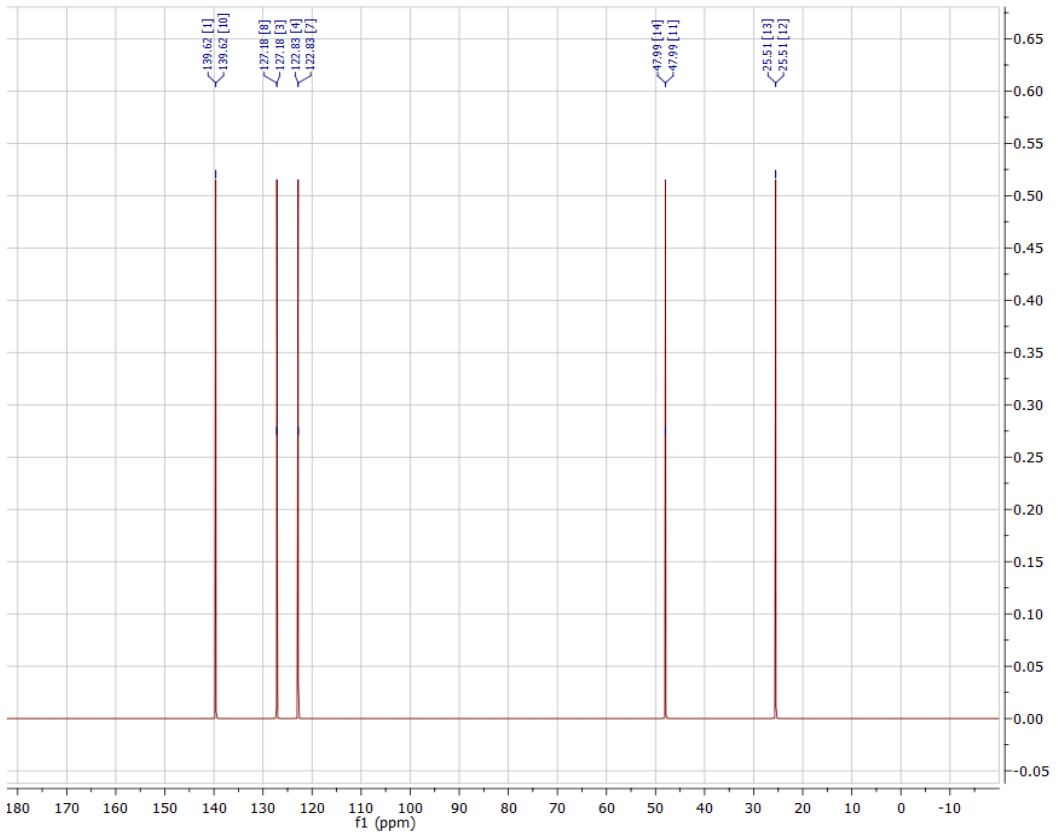

Figure 29: 13C NMR spectrum of 13

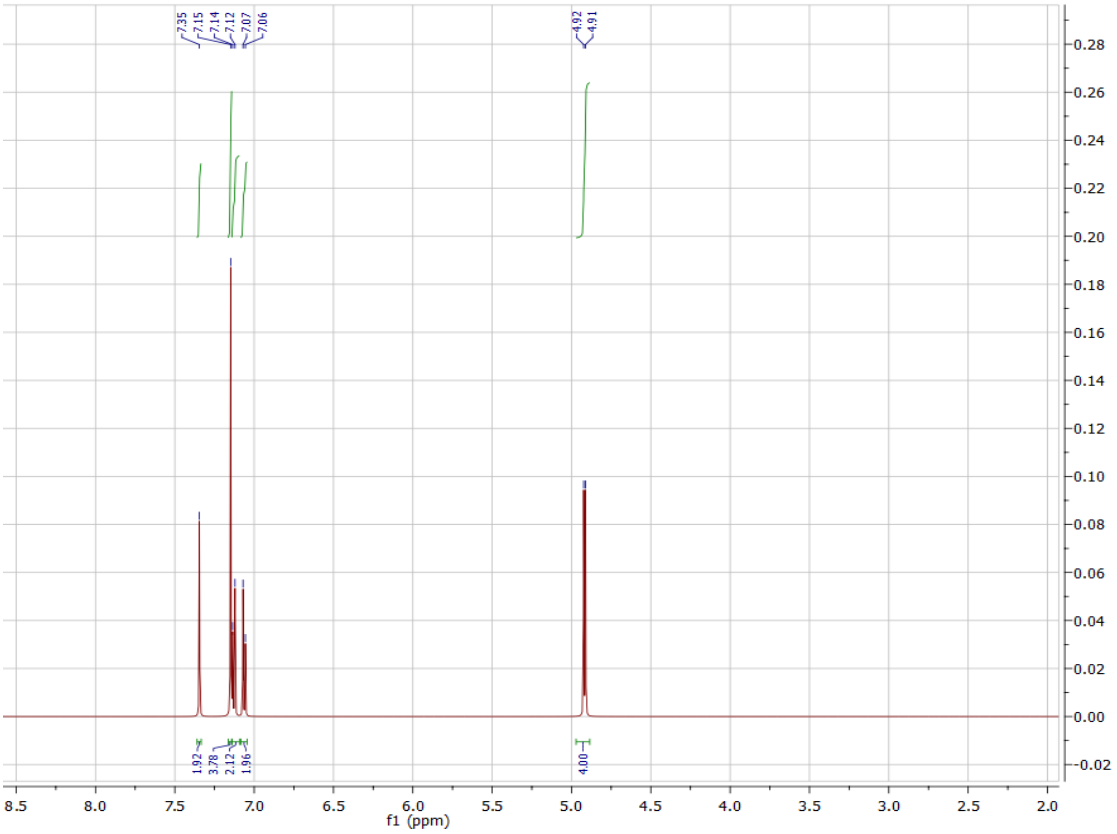

Figure 30: 1H NMR spectrum of 14

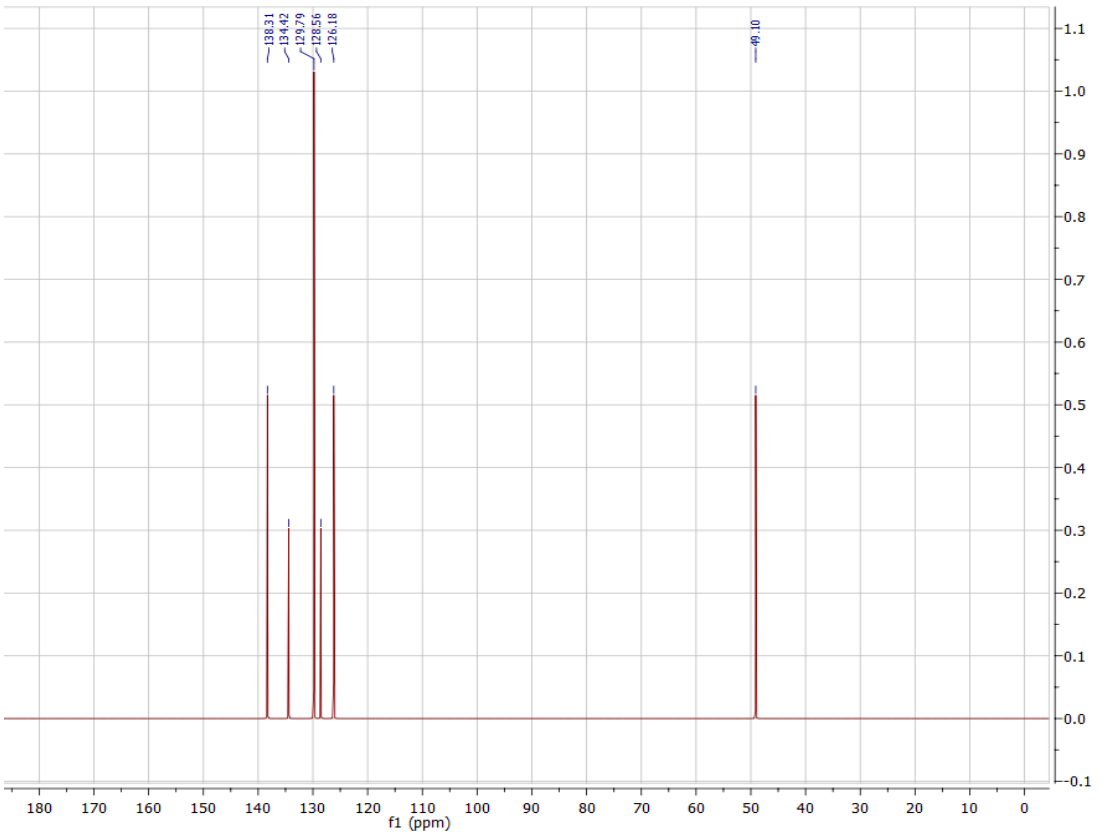

Figure 31: 13C NMR spectrum of 14

4.2 MIR SPECTRA OF DISCUSSED SUBSTANCE

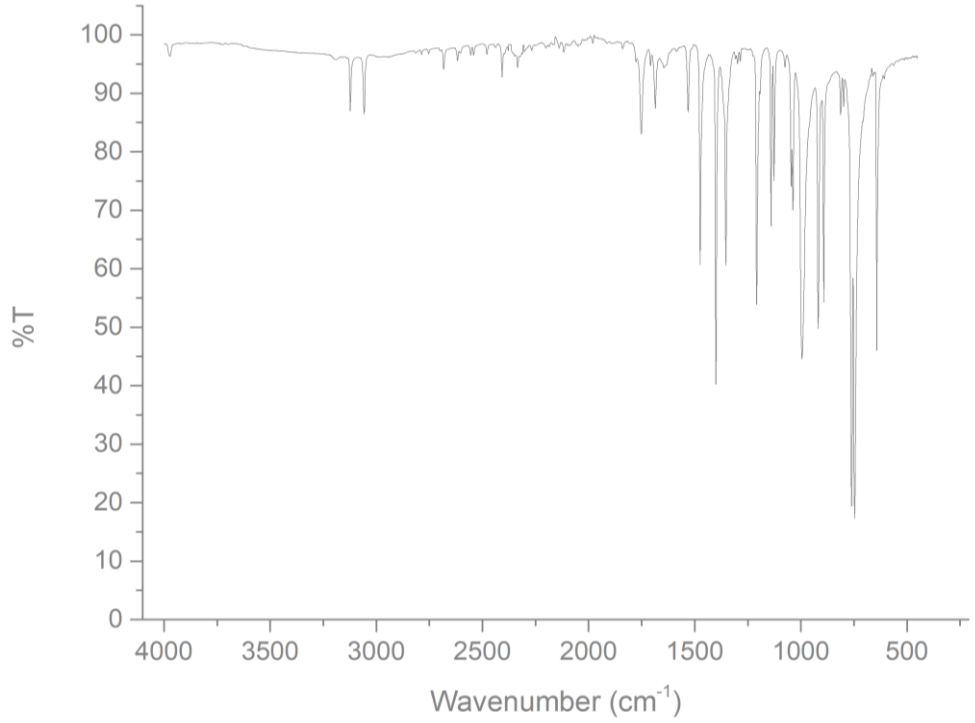

Figure 16: MIR spectrum of 1

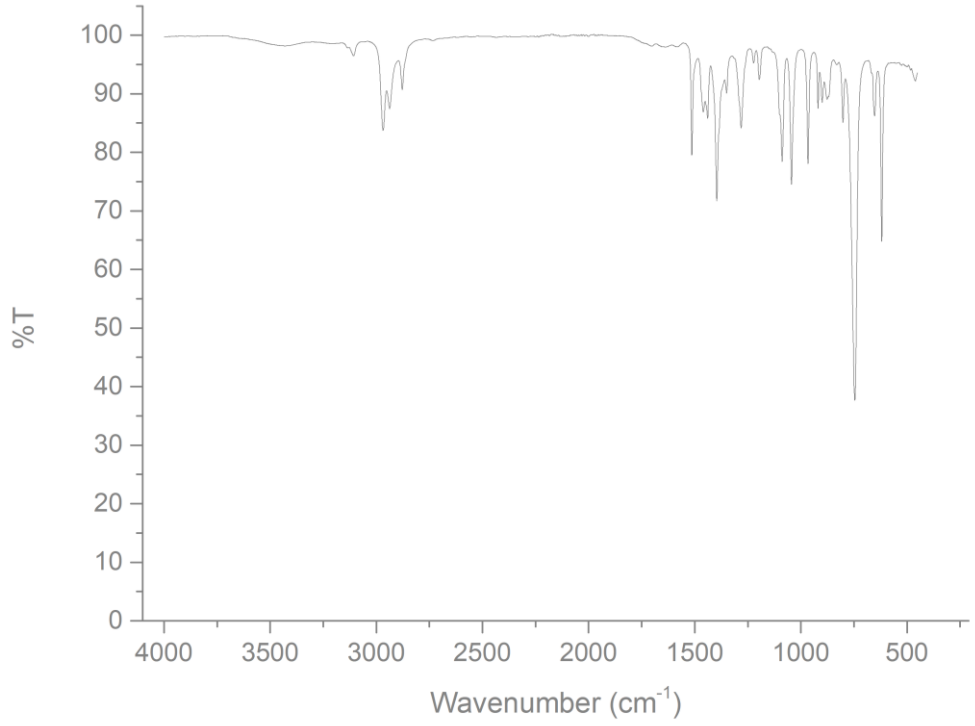

Figure 17: MIR spectrum of 2

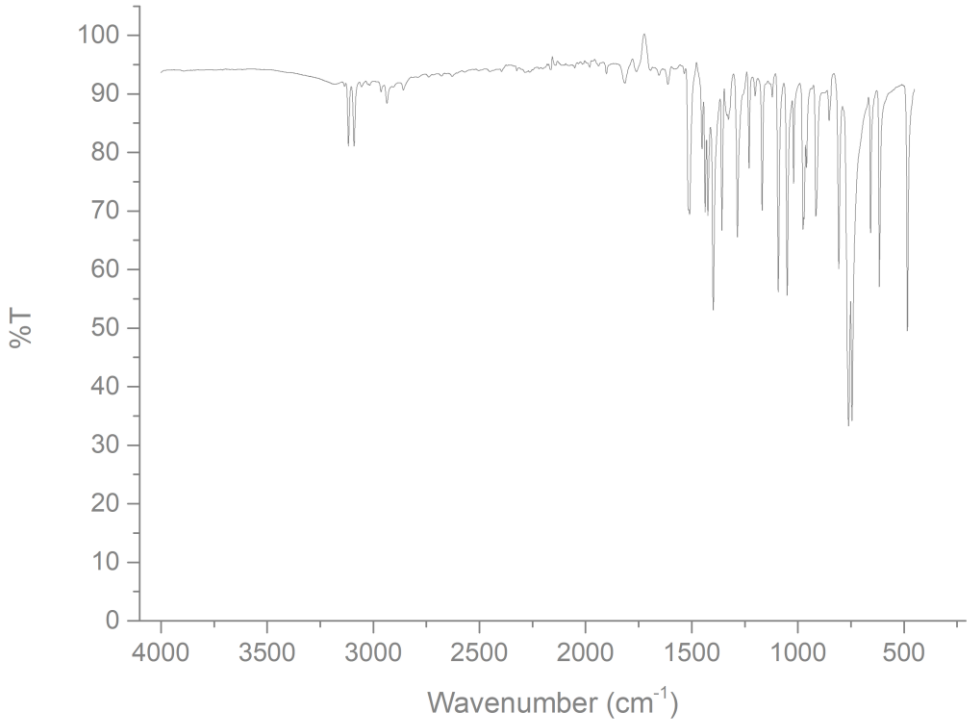

Figure 18: MIR spectrum of 3

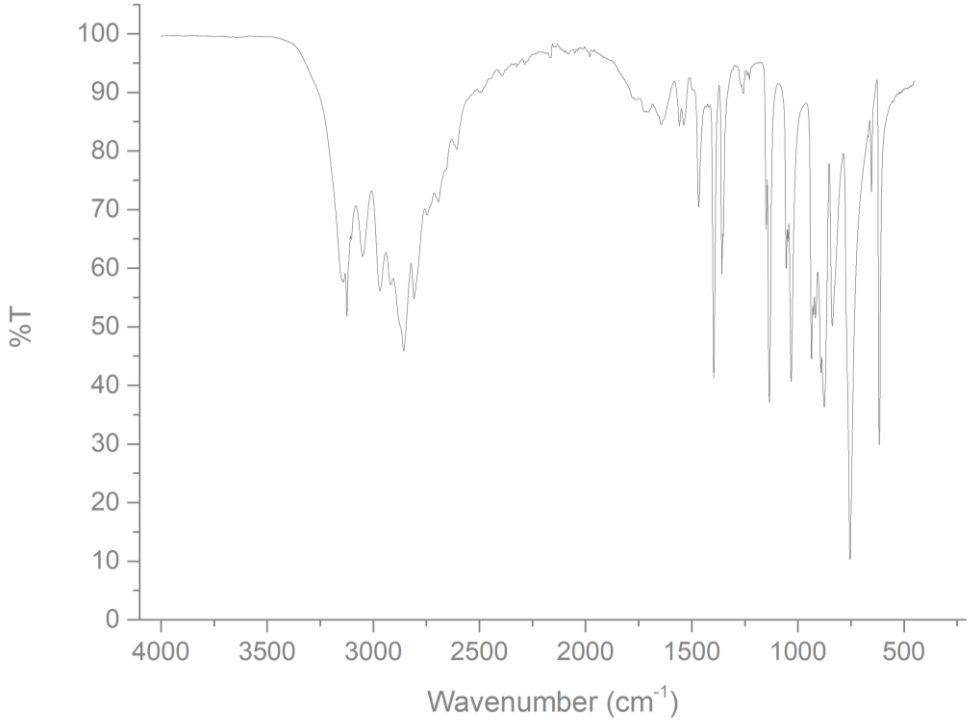

Figure 19: MIR spectrum of 4

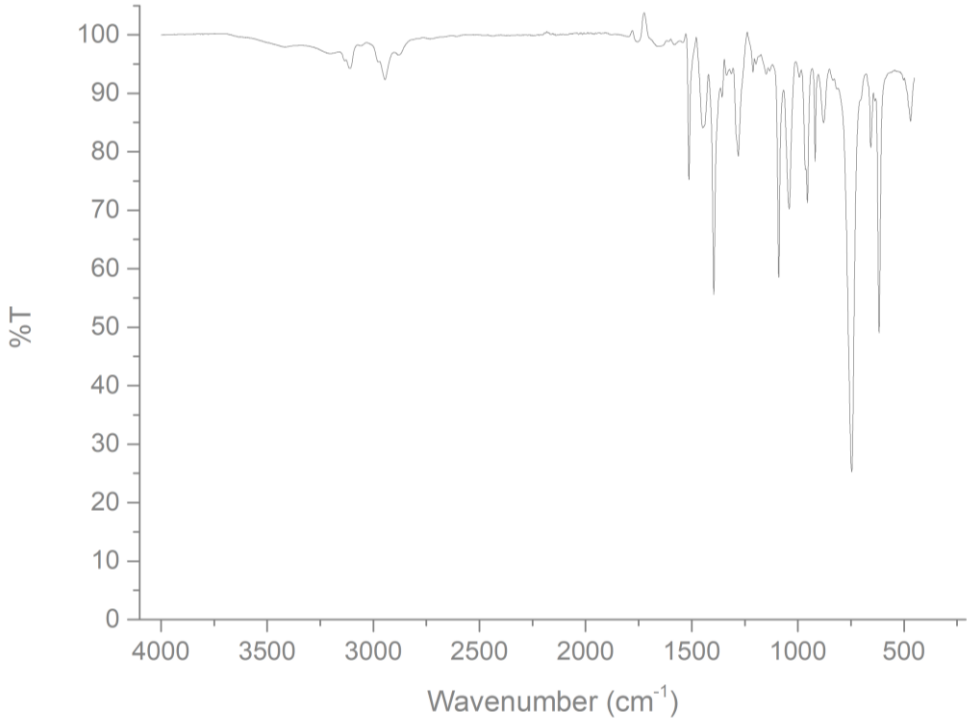

Figure 20: MIR spectrum of 5

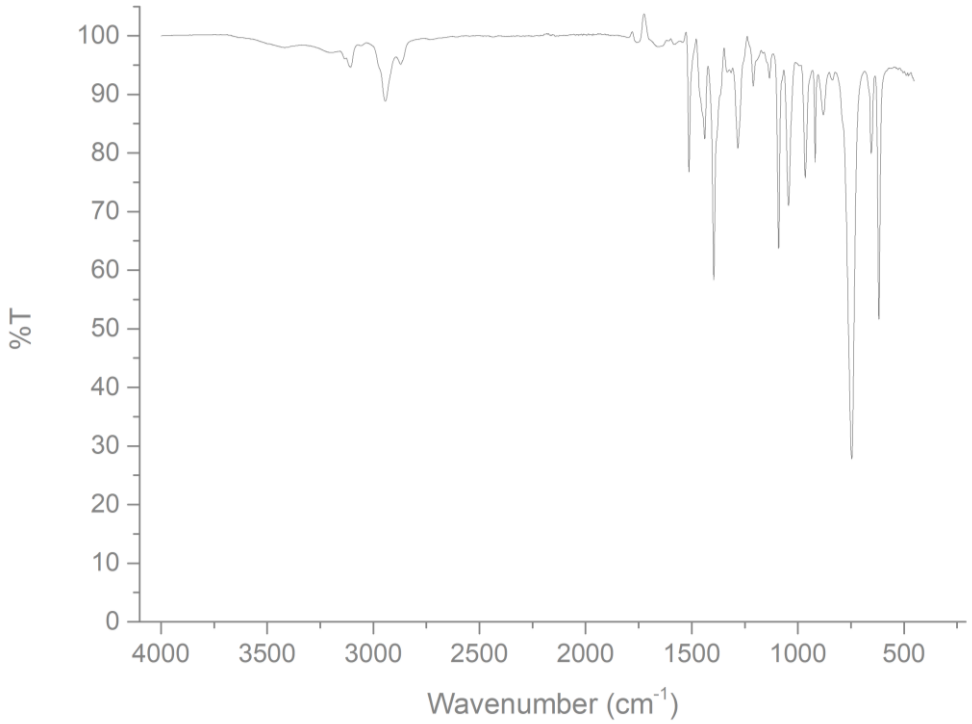

Figure 21: MIR spectrum of 6

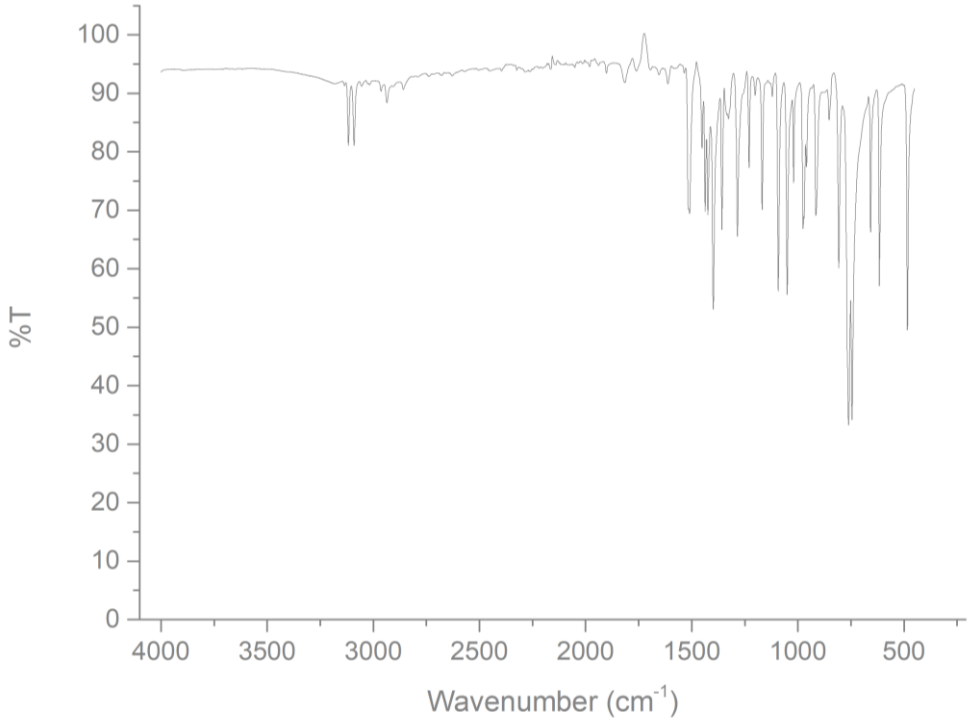

Figure 22: MIR spectrum of 7

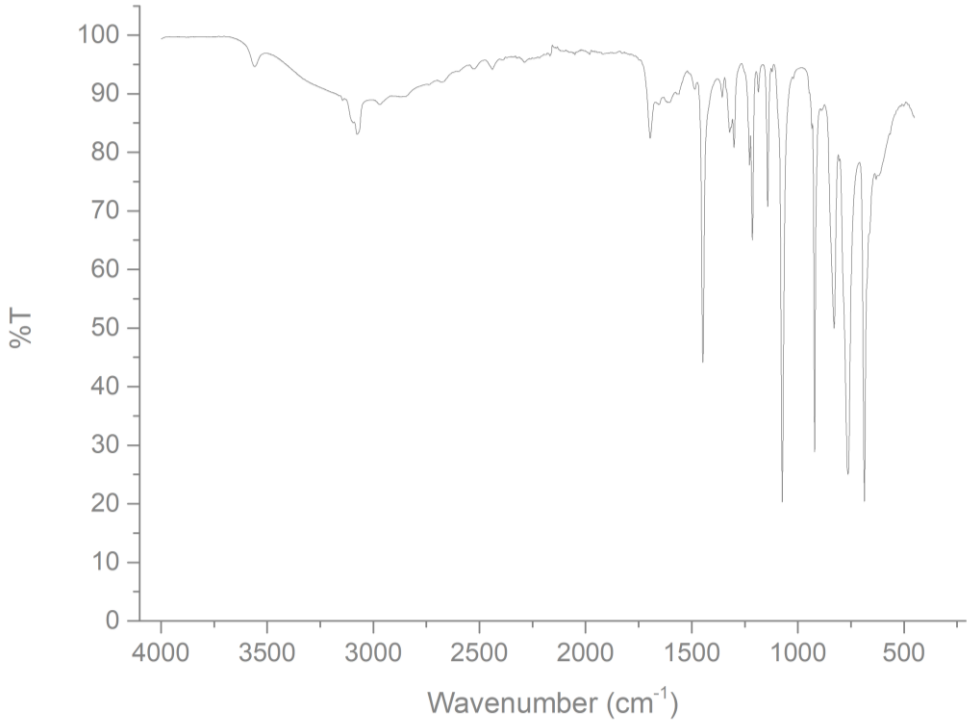

Figure 23: MIR spectrum of 8

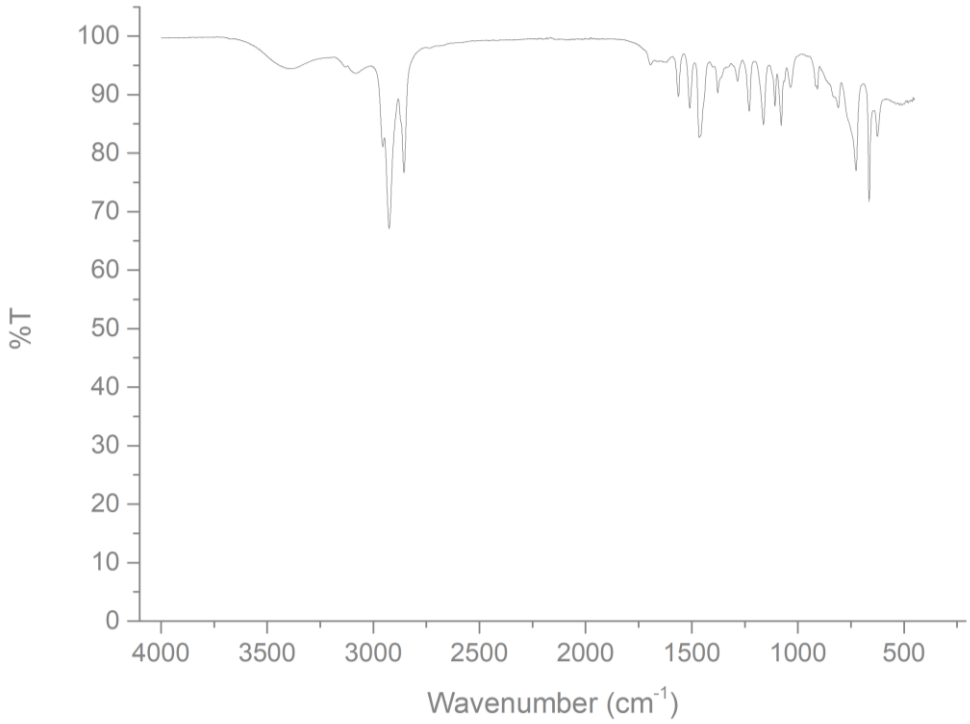

Figure 24: MIR spectrum of 9

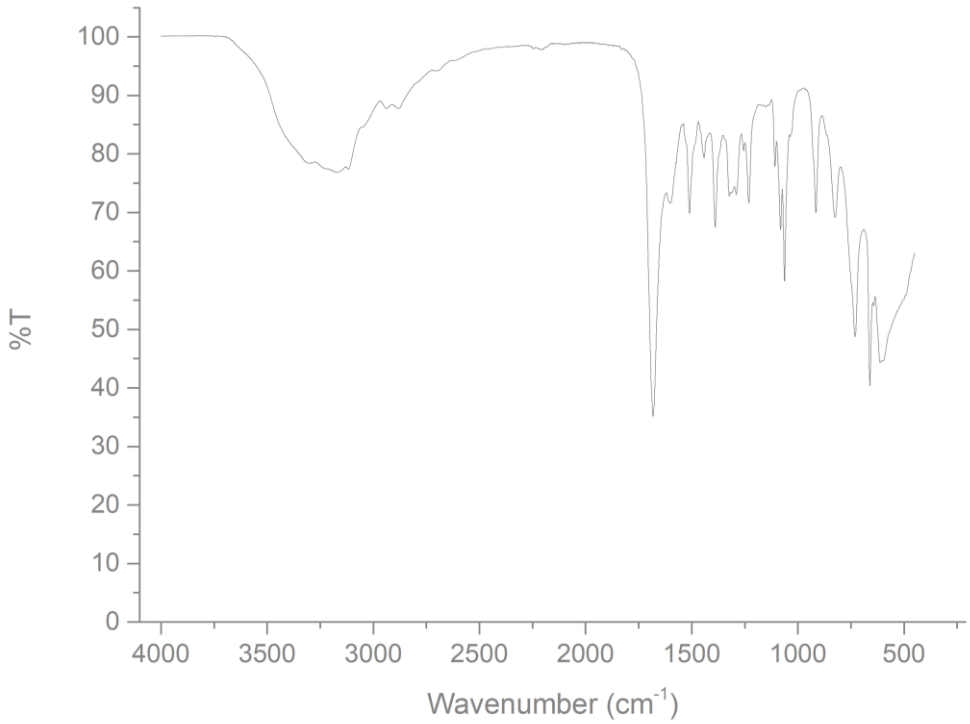

Figure 25: MIR spectrum of 10

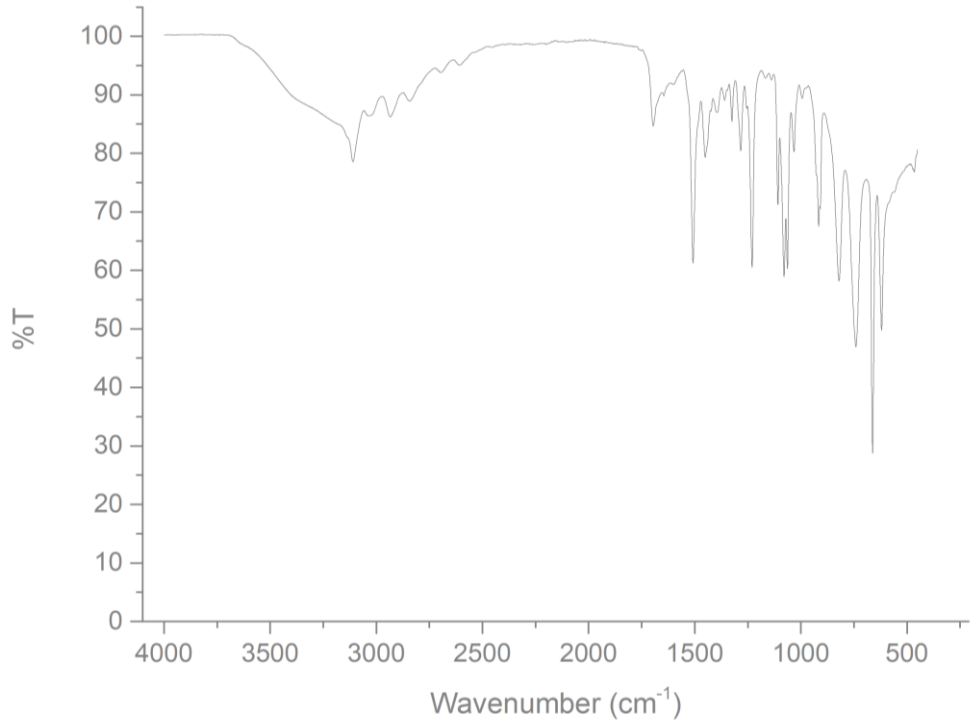

Figure 26: MIR spectrum of 11

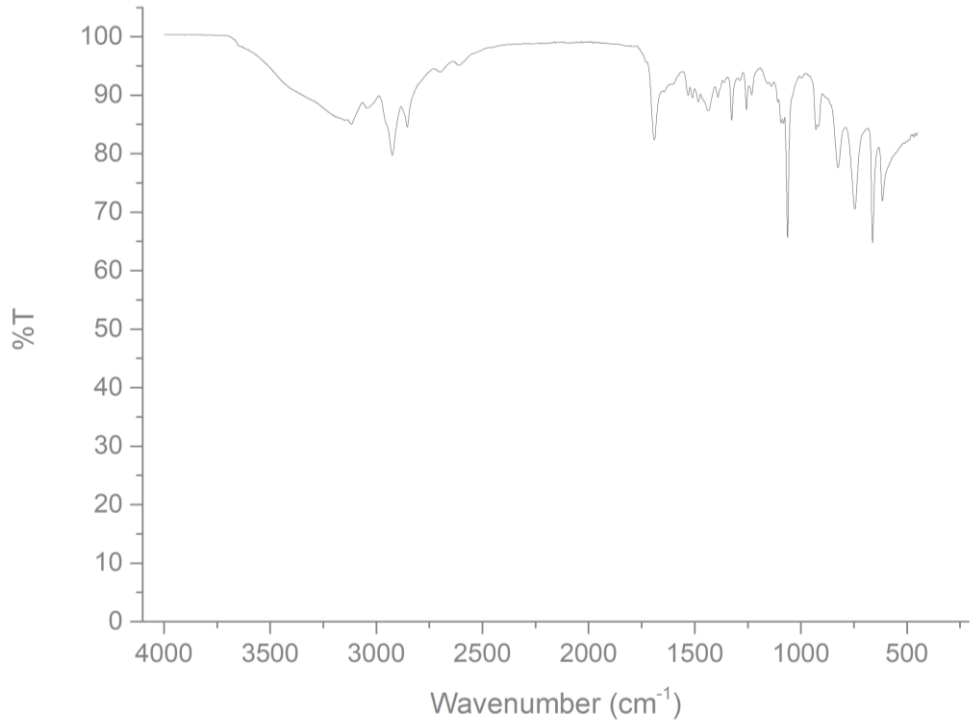

Figure 27: MIR spectrum of 12

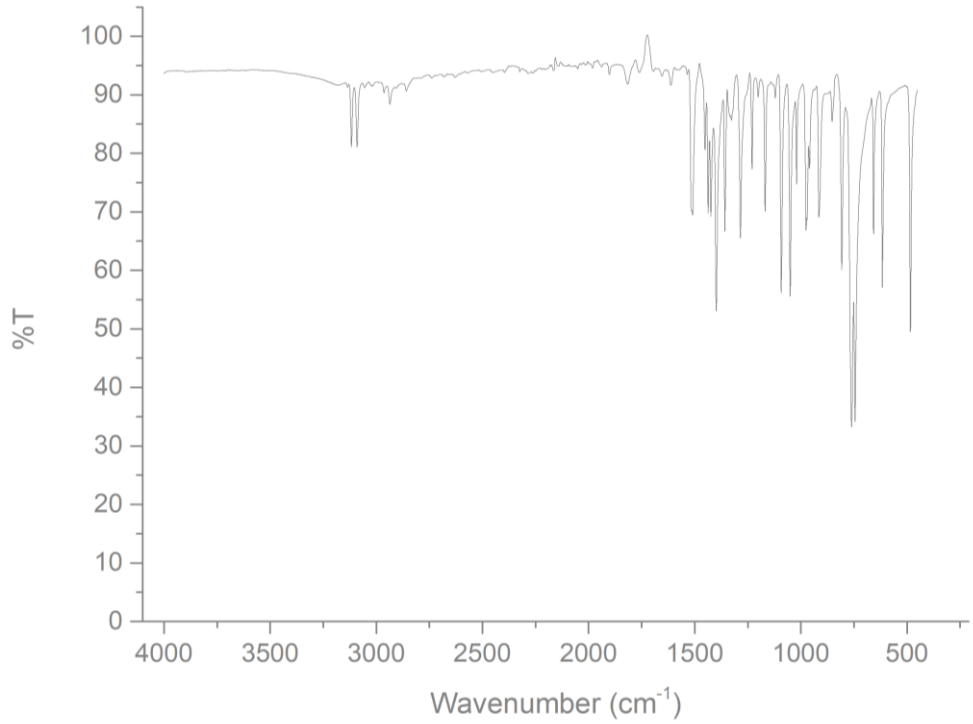

Figure 28: MIR spectrum of 13

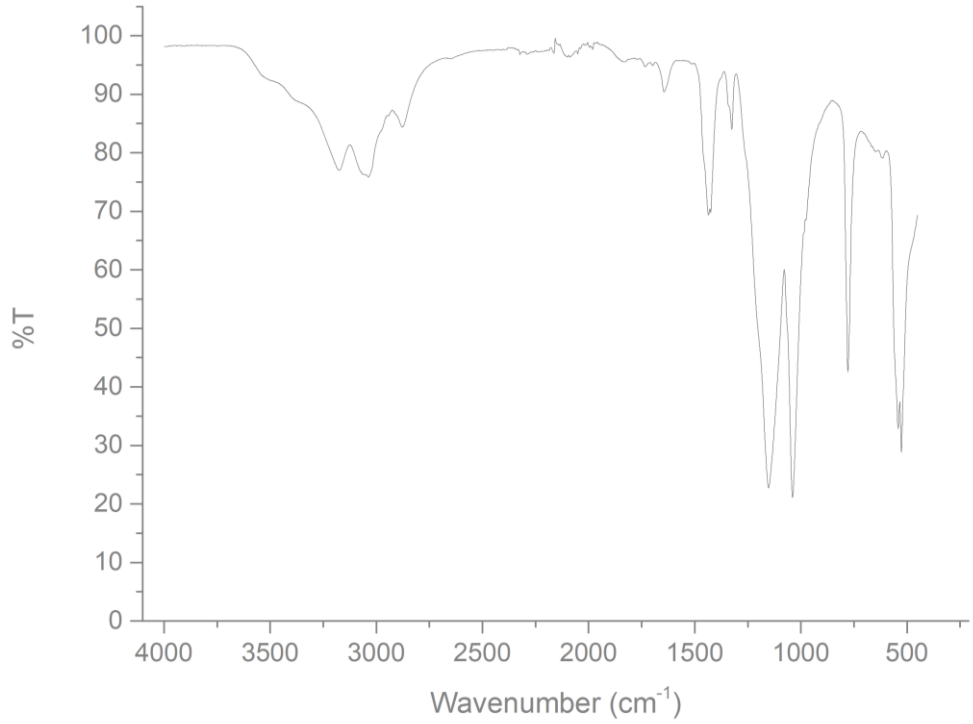

Figure 29: MIR spectrum of 14

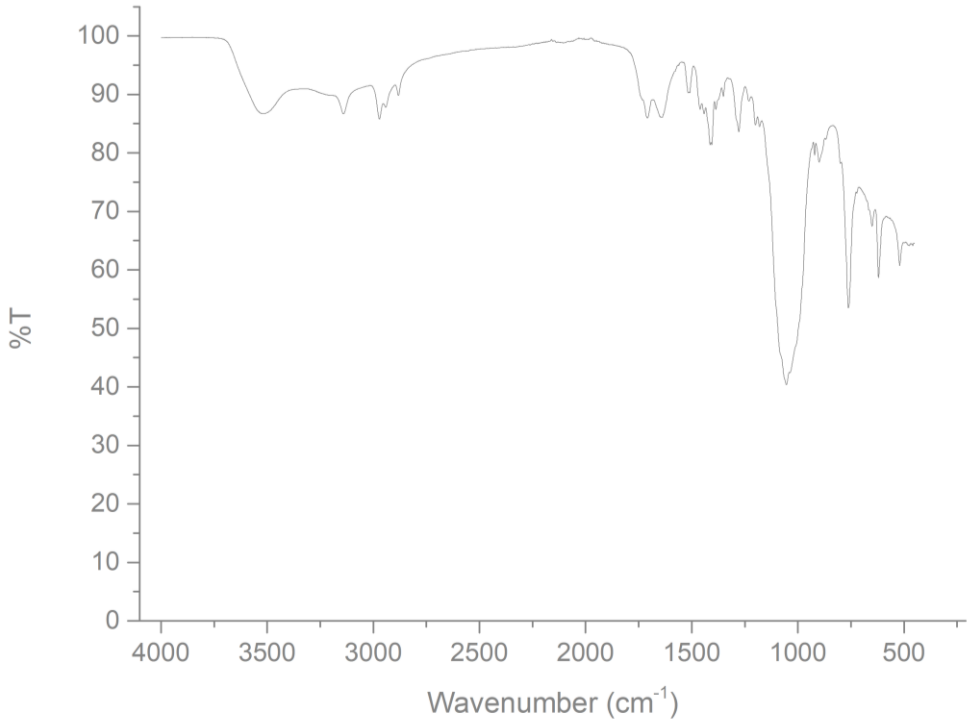

Figure 30: MIR spectrum of [Fe(1-Pr-Pz)6](BF4)2

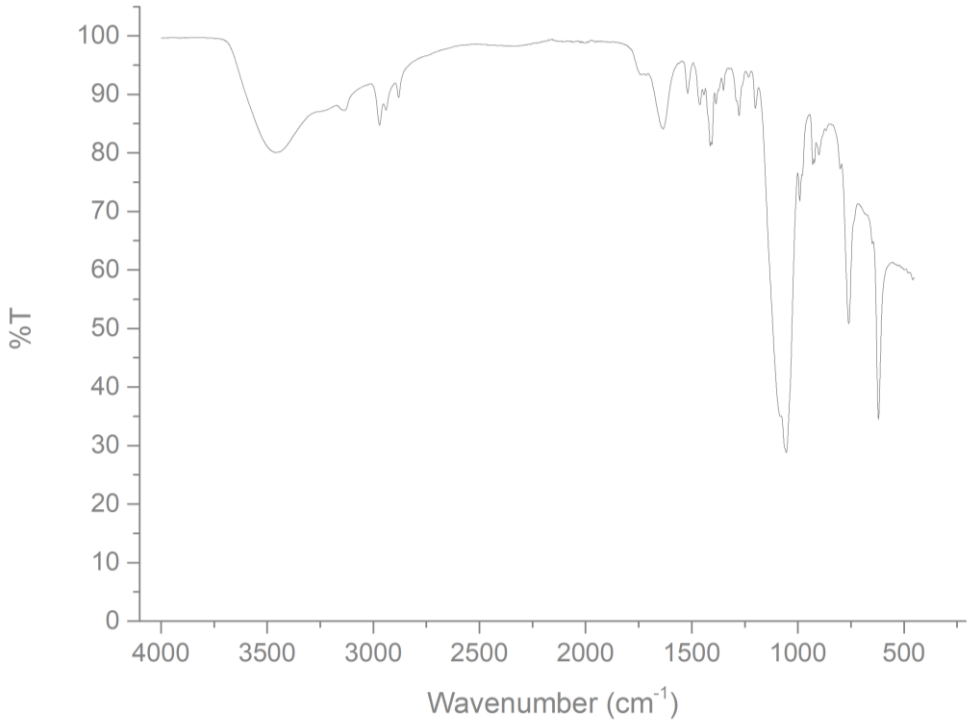

Figure 31: MIR spectrum of [Ni(1-Pr-Pz)6](BF4)2

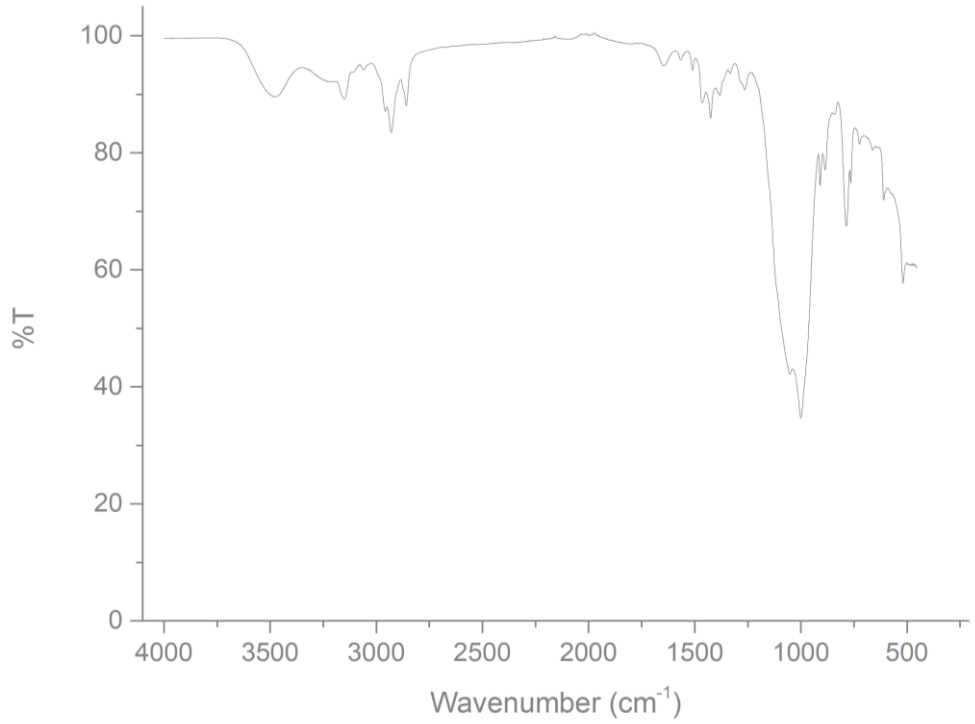

Figure 32: MIR spectrum of [Ni(1-Pr-Pz)6](ClO4)2

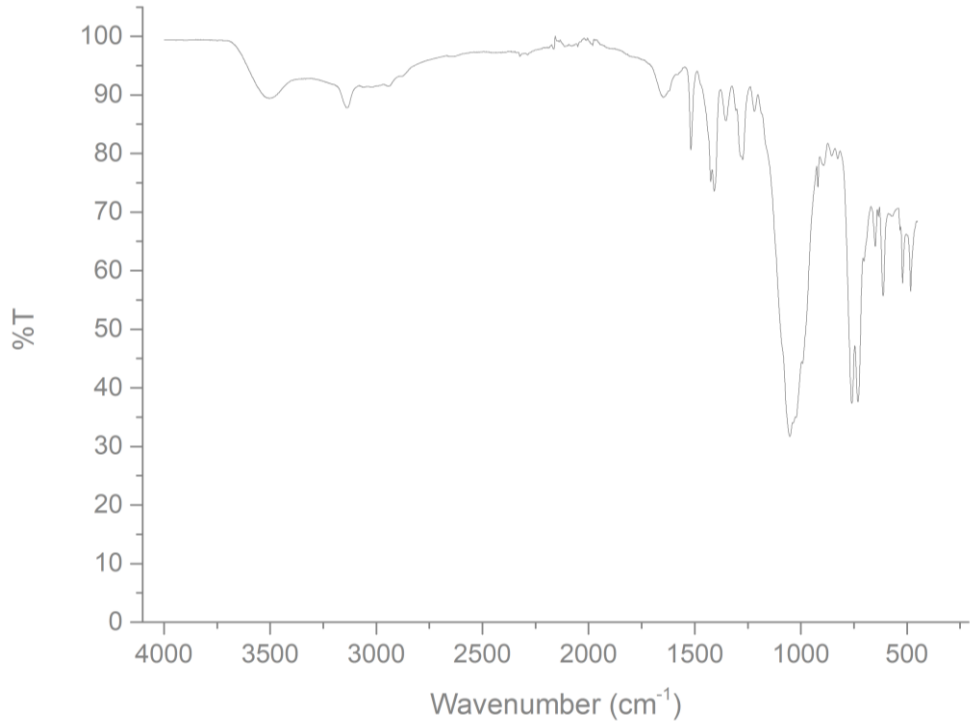

Figure 33: MIR spectrum of [Fe(1-Oct-Pz)6](BF4)2

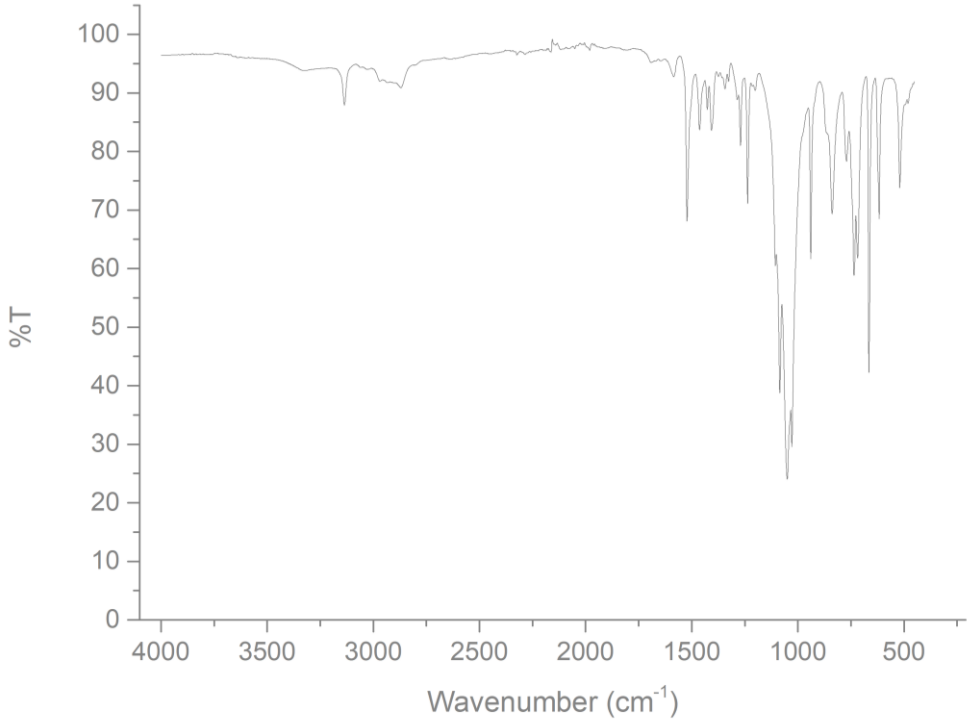

Figure 34: MIR spectrum of [Fe(1-Oct-Pz)6](ClO4)2

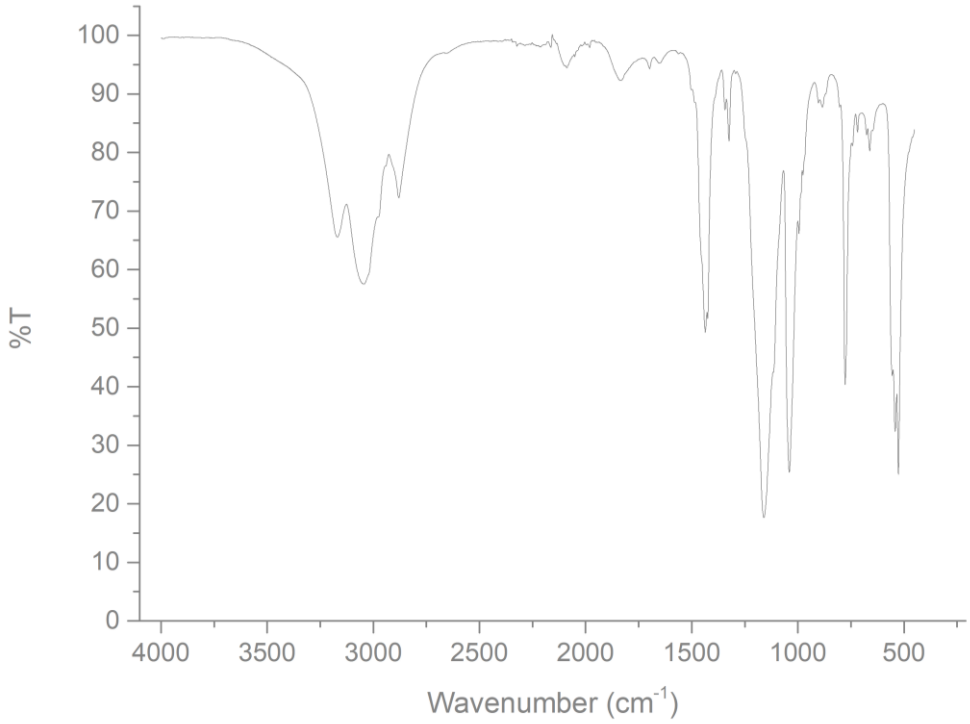

Figure 35: MIR spectrum of [Ni(1-Oct-Pz)6](BF4)2

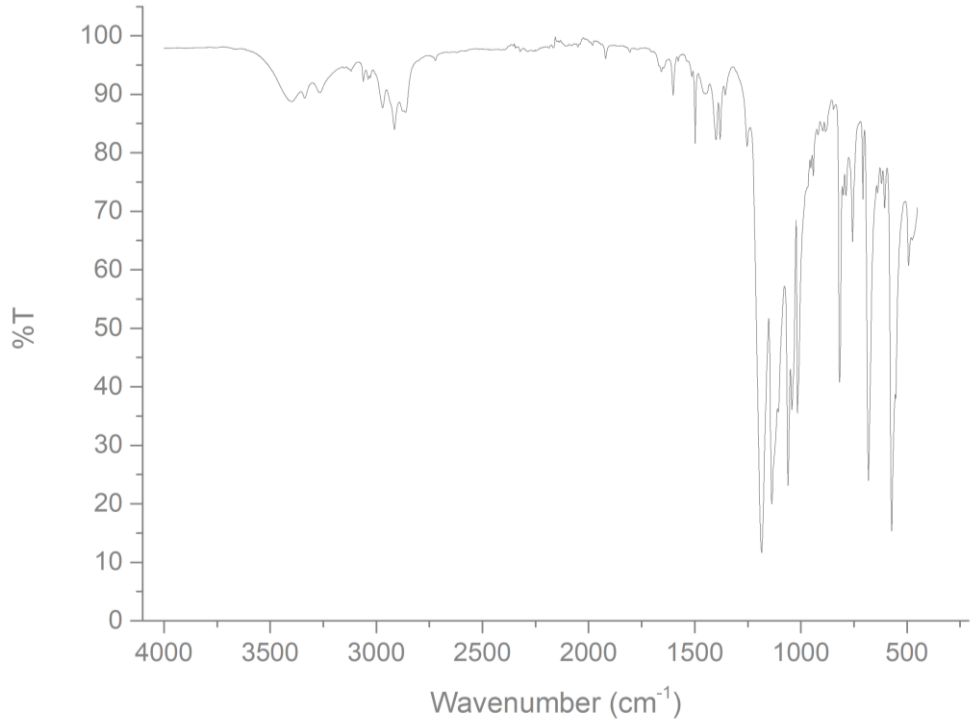

Figure 36: MIR spectrum of [Fe(Pz-Et-Pz)3](BF4)2

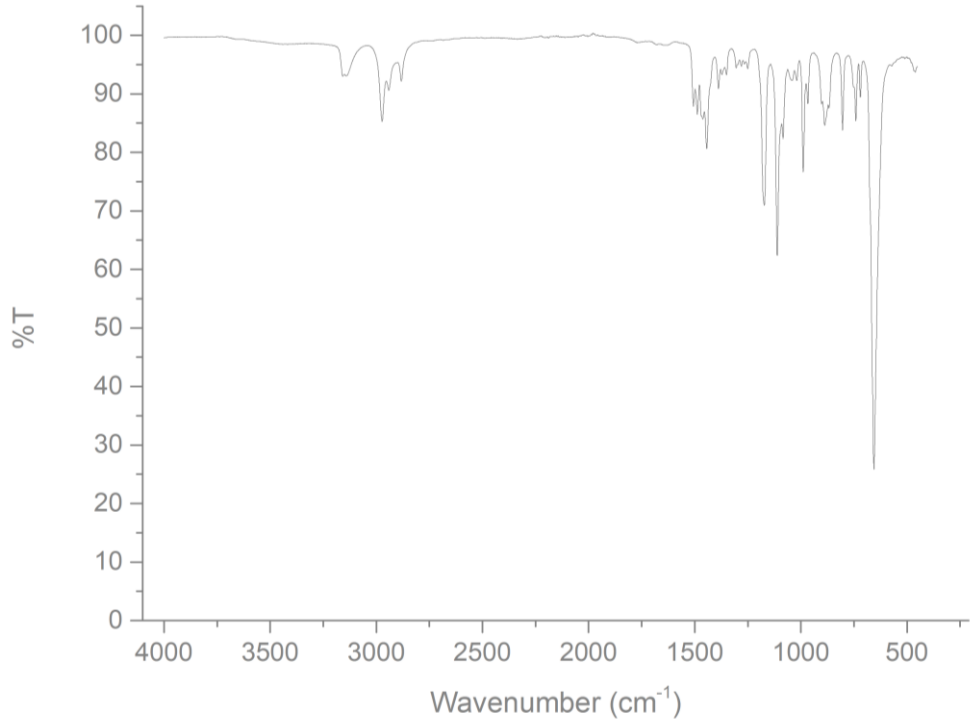

Figure 37: MIR spectrum of [Fe(Pz-Et-Pz)3](ClO4)2

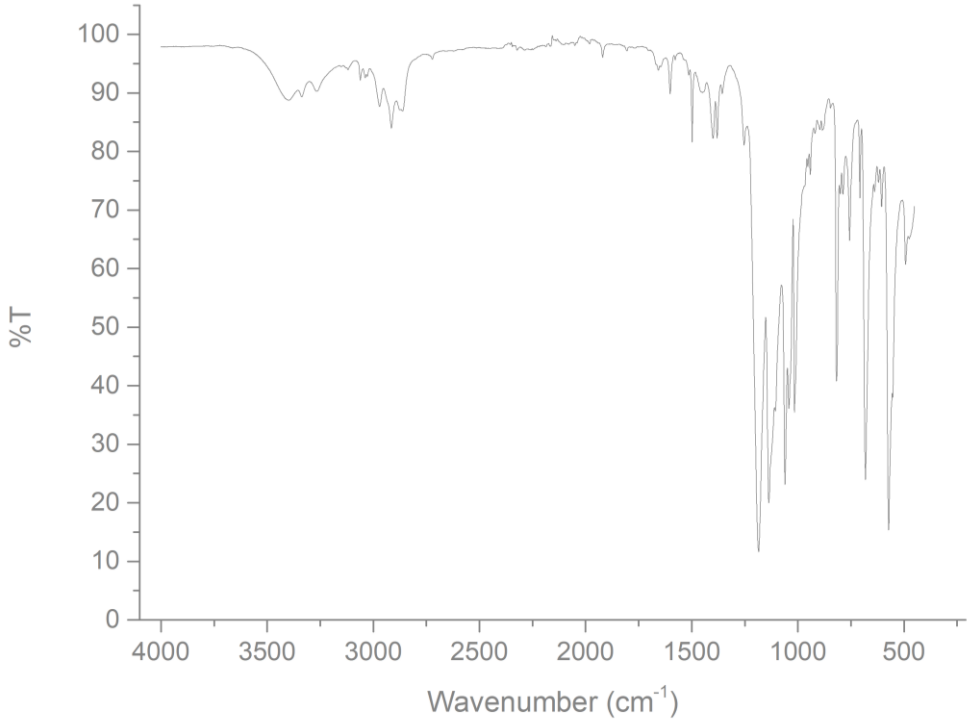

Figure 38: MIR spectrum of [Ni(Pz-Et-Pz)3](BF4)2

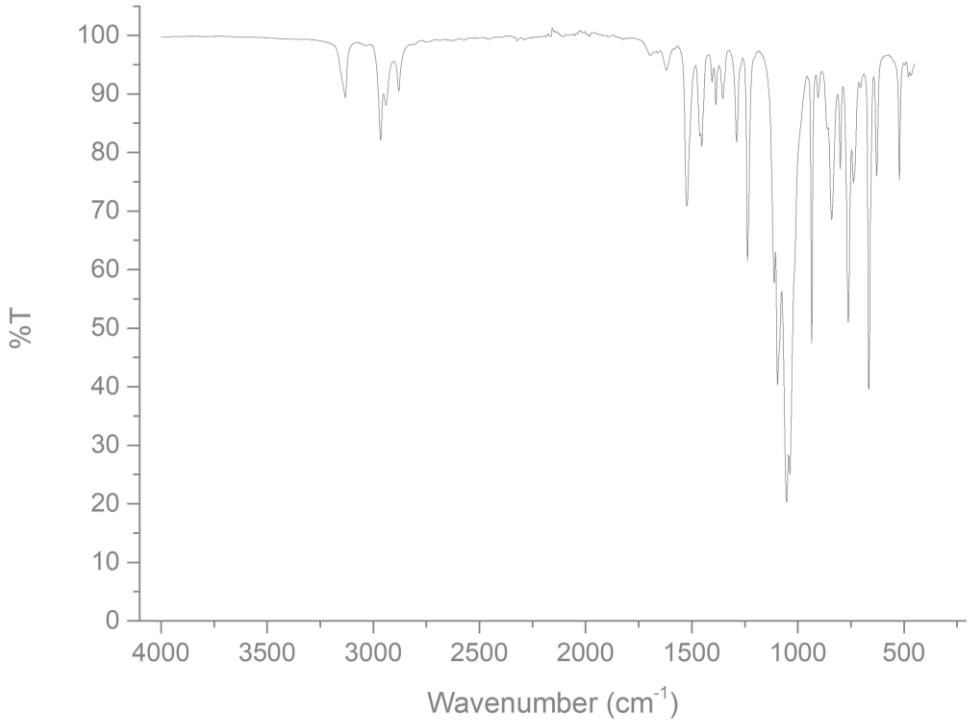

Figure 39: MIR spectrum of [Fe(Pz-Pr-Pz)3](BF4)2

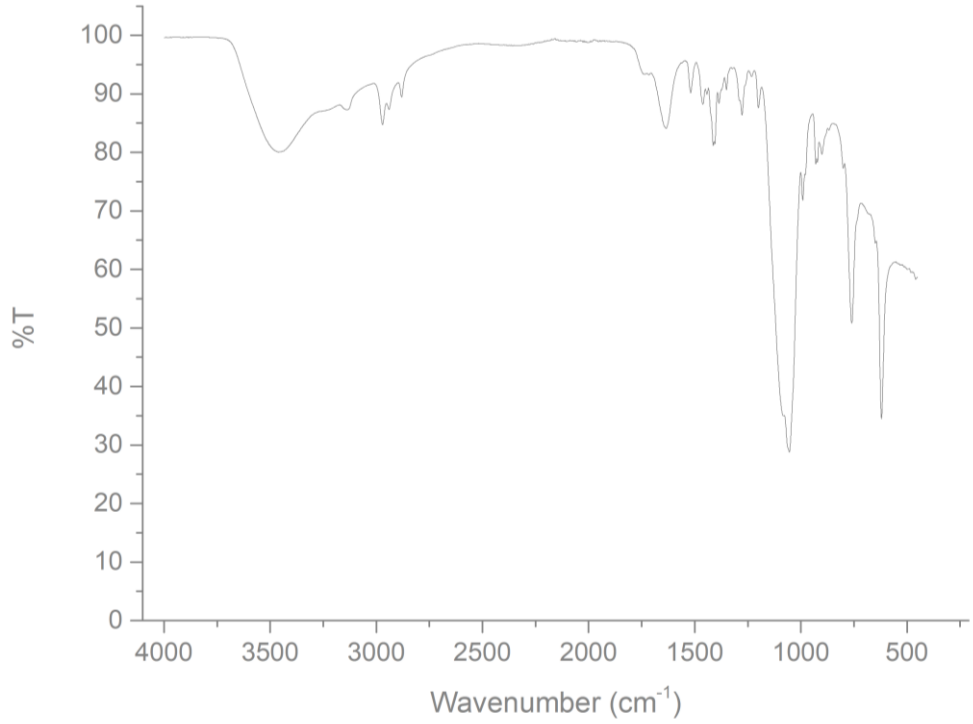

Figure 40: MIR spectrum of [Ni(Pz-Pr-Pz)3](BF4)2

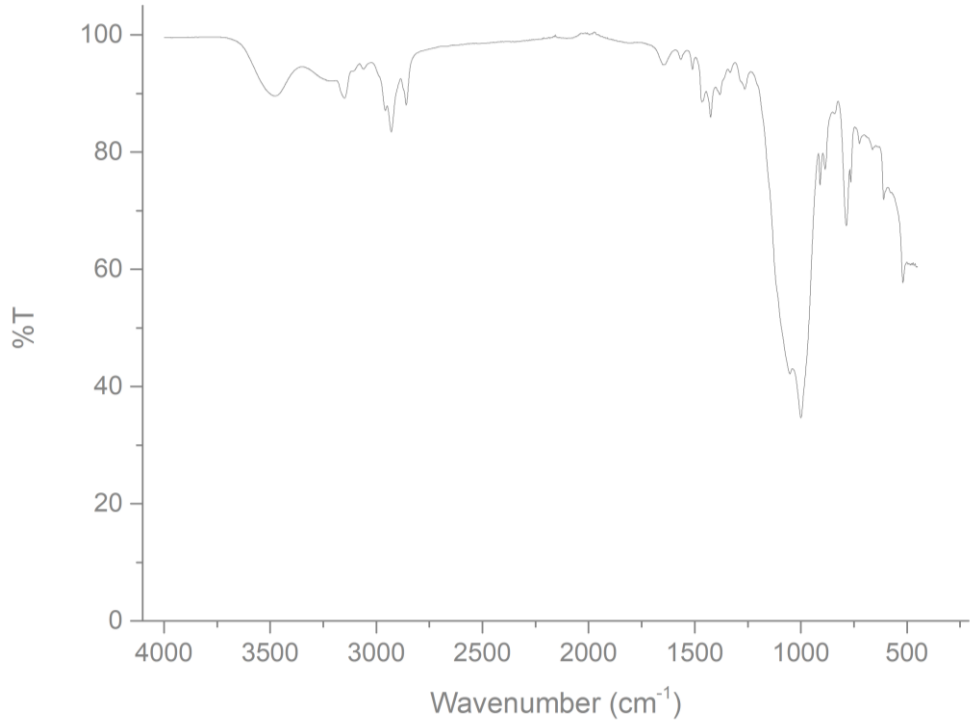

Figure 41: MIR spectra of [Fe(Pz-Bu-Pz)3](BF4)2

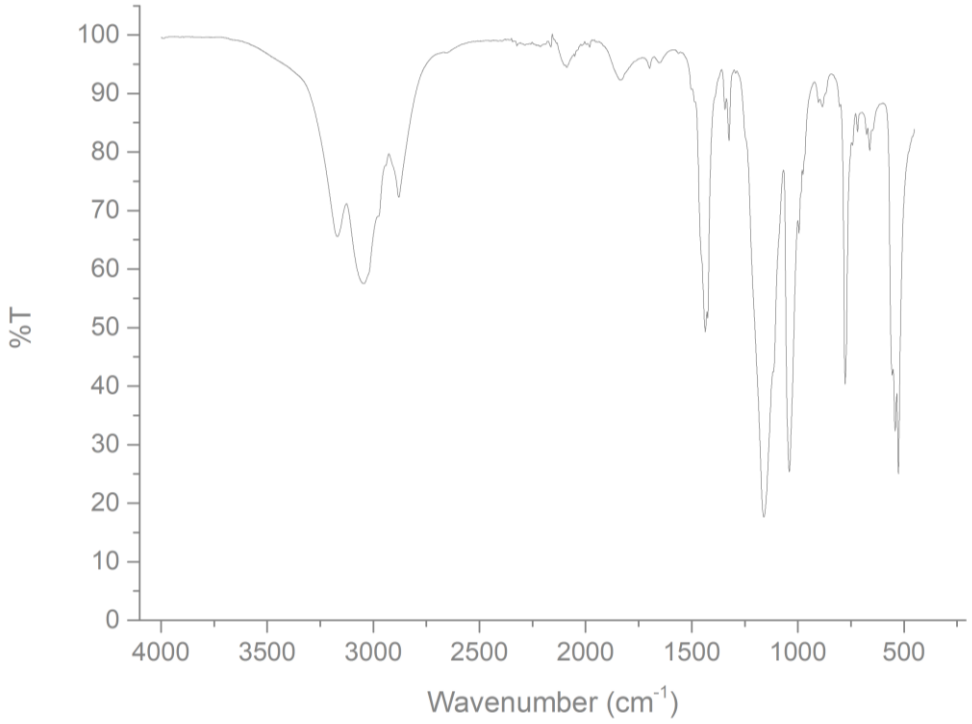

Figure 42: MIR spectrum of [Fe(Pz-Bu-Pz)3](ClO4)2

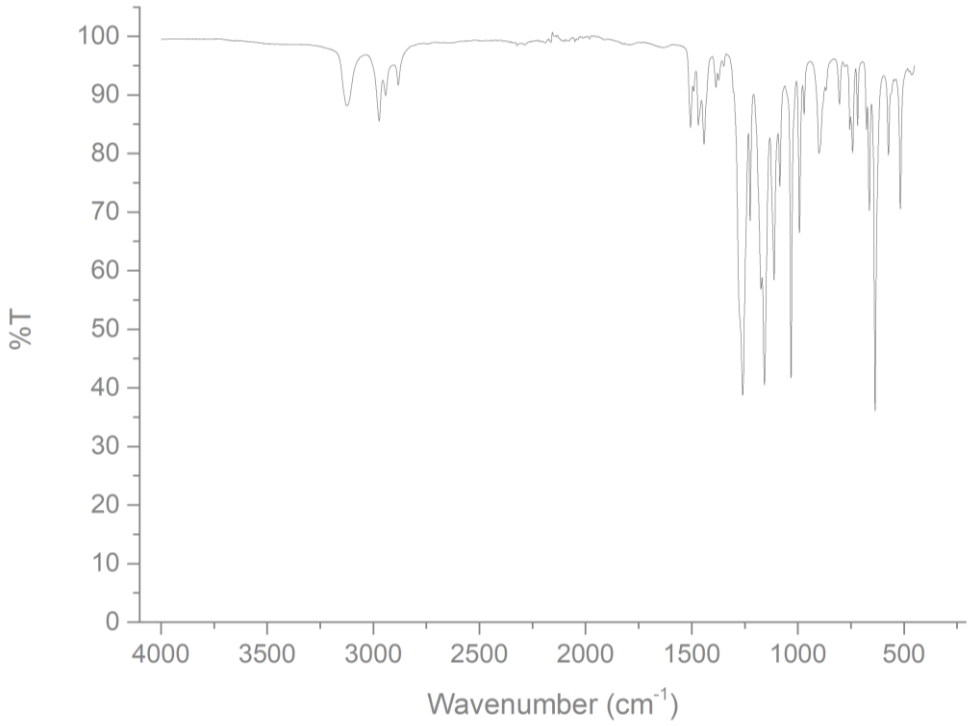

Figure 43: MIR spectrum of [Fe(Pz-PX-Pz)3](BF4)2

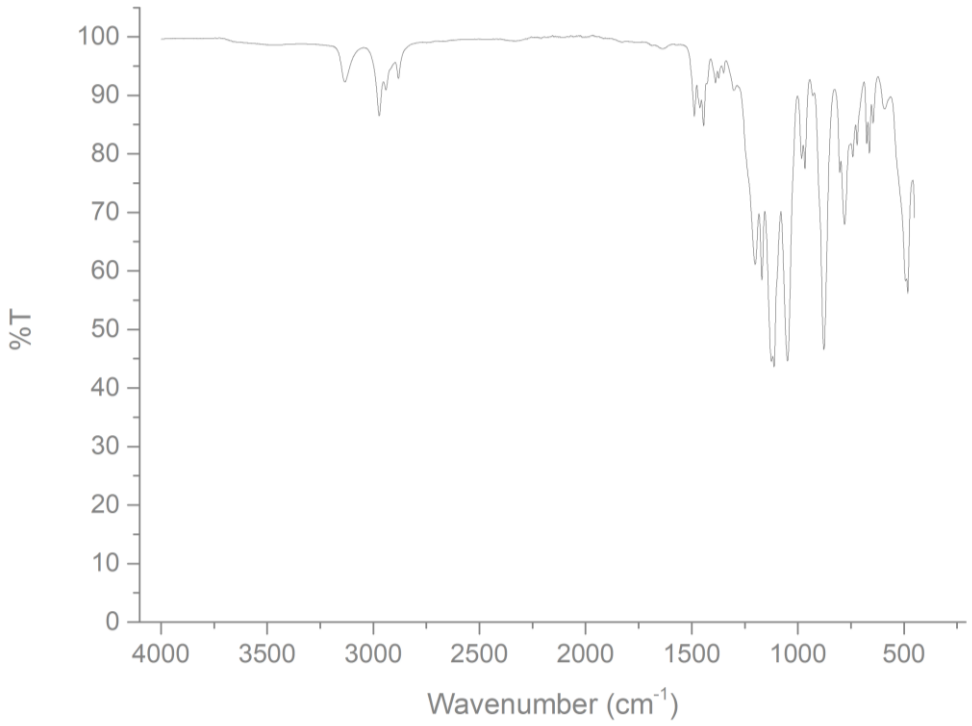

Figure 44: MIR spectrum of [Ni(Pz-PX-Pz)3](BF4)2

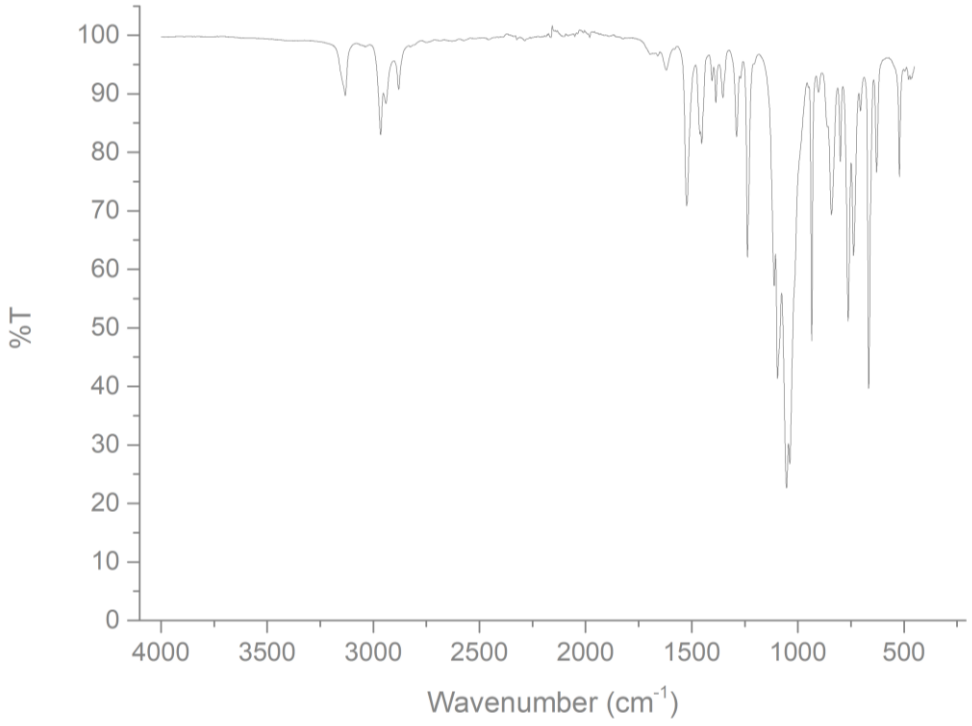

Figure 45: MIR spectrum of [Fe(1Pr-Im)6](BF4)2

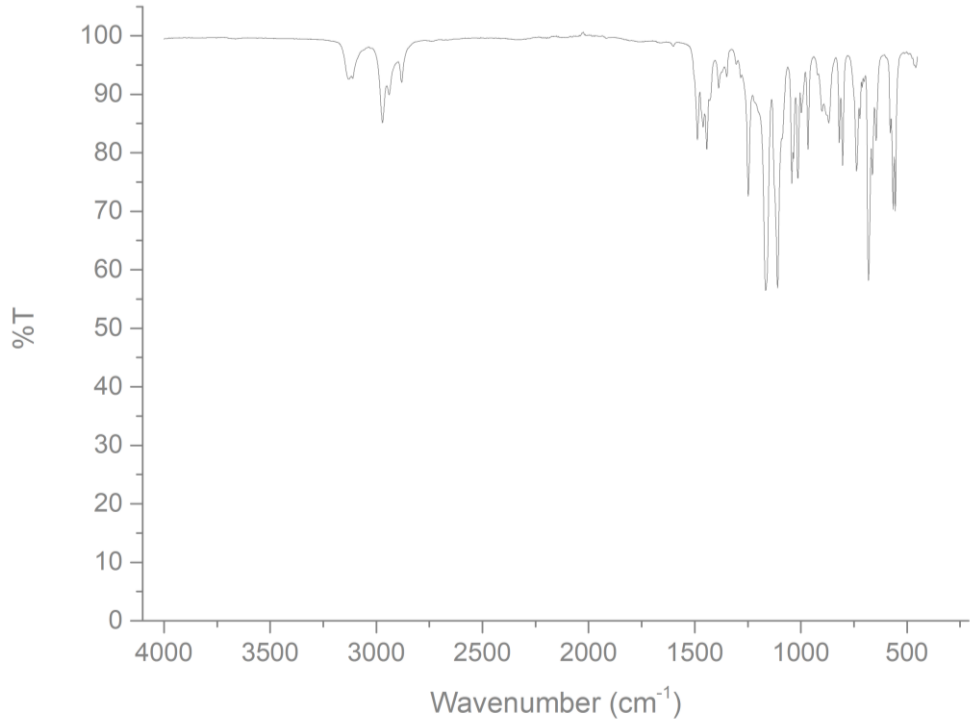

Figure 46: MIR spectrum of [Ni(1-Pr-Im)6](BF4)2

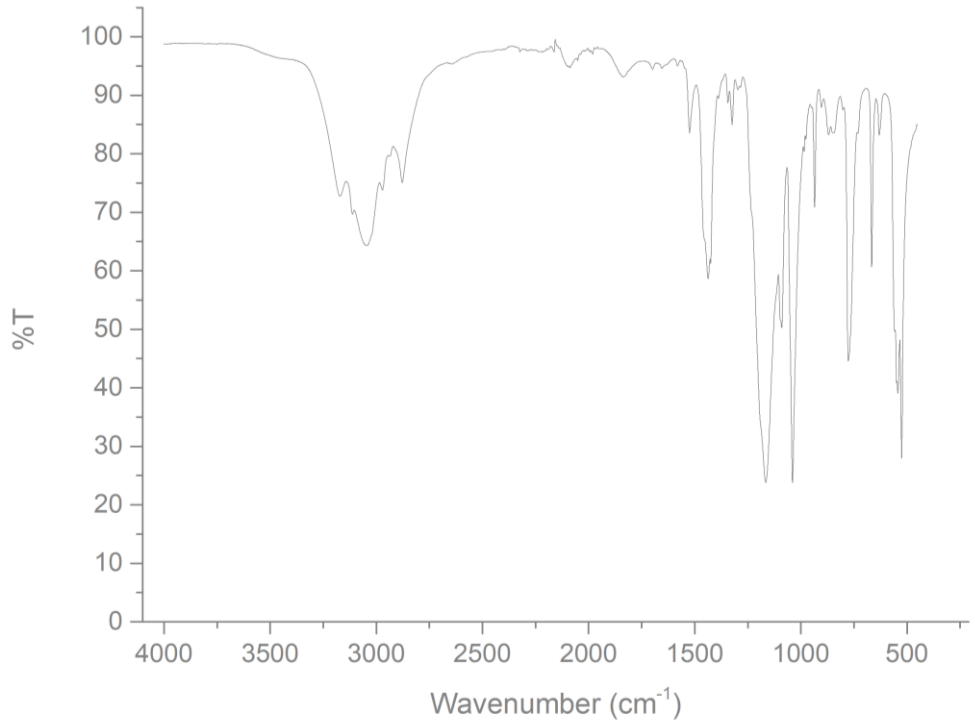

Figure 47: MIR spectrum of [Fe(1-Oct-Im)6](BF4)2

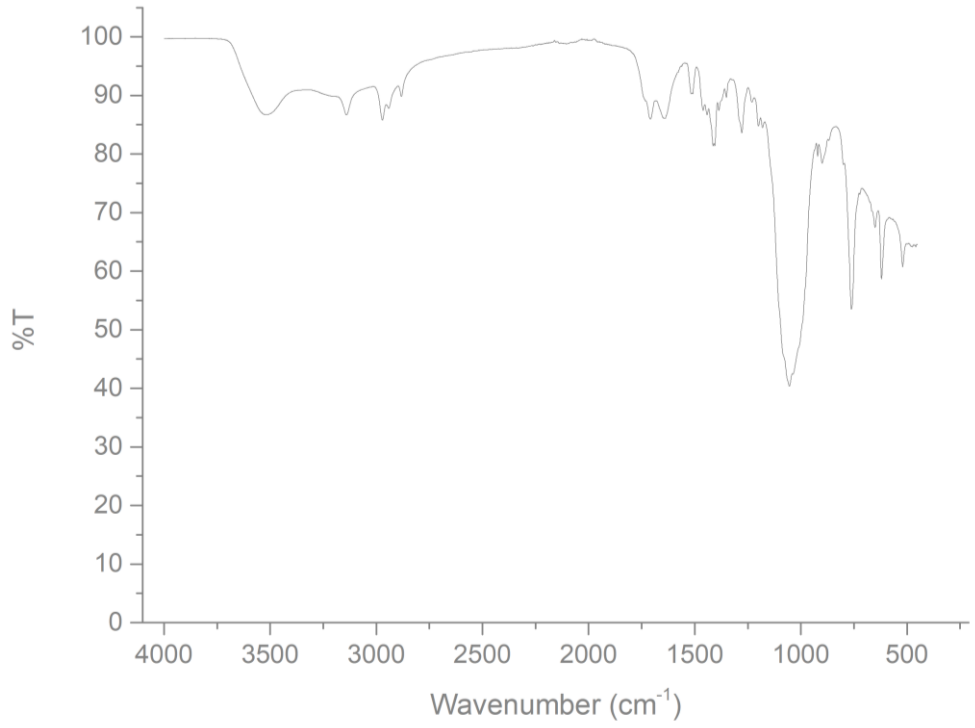

Figure 48: MIR spectrum of [Ni(1-Oct-Im)6](BF4)2

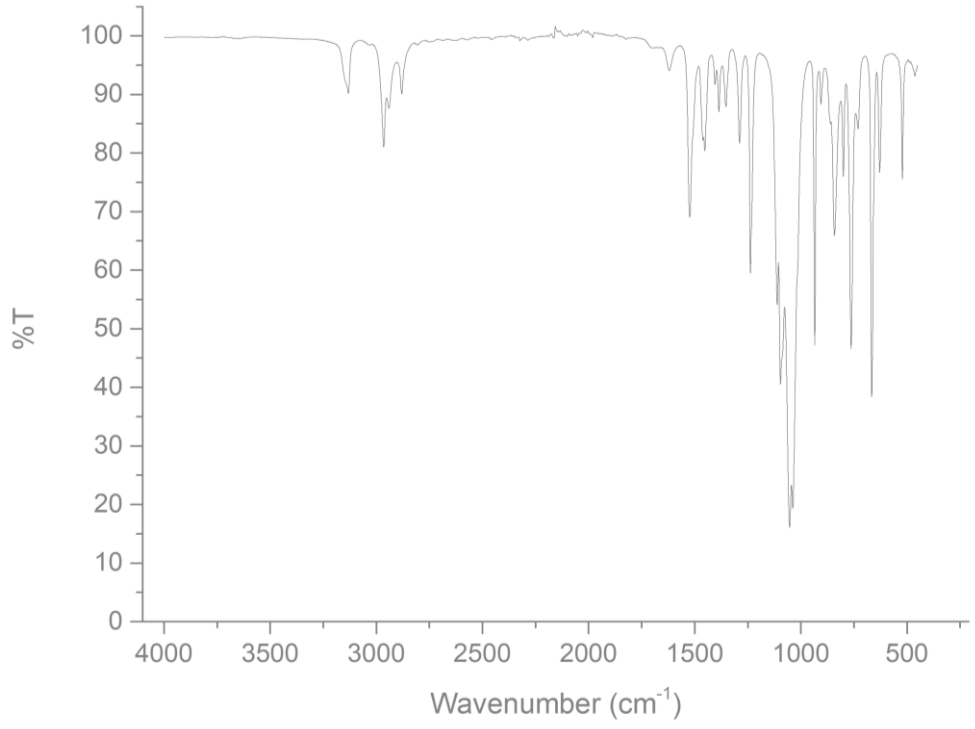

Figure 49: MIR spectrum of [Fe(Im-Et-Im)3](BF4)2

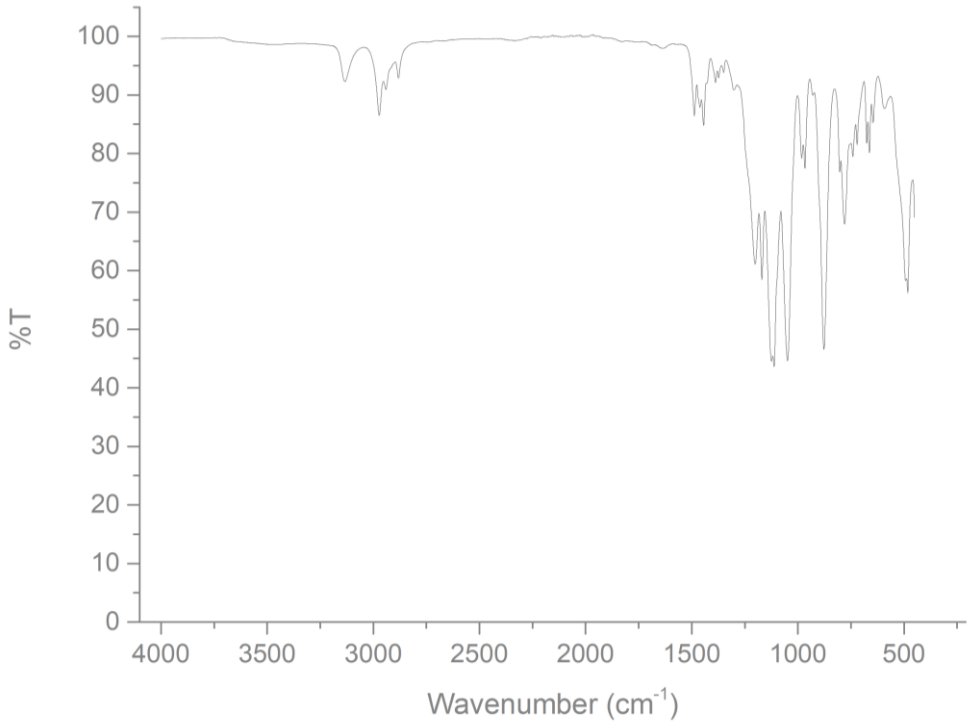

Figure 50: MIR spectrum of [Fe(Im-Et-Im)3](ClO4)2

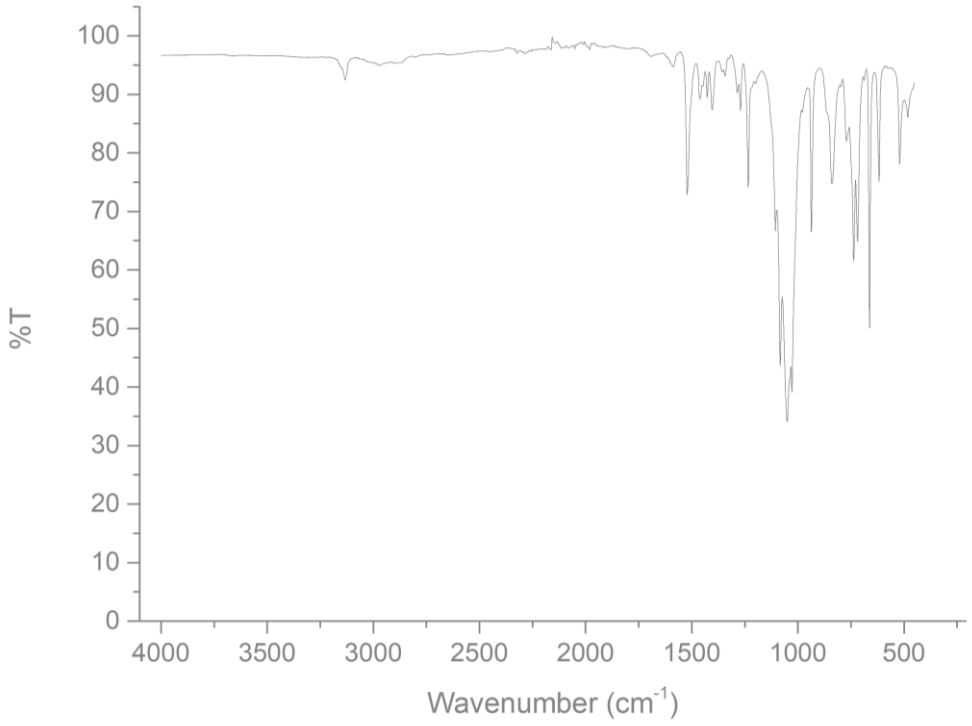

Figure 51: MIR spectrum of [Fe(Im-Pr-Im)3](BF4)2

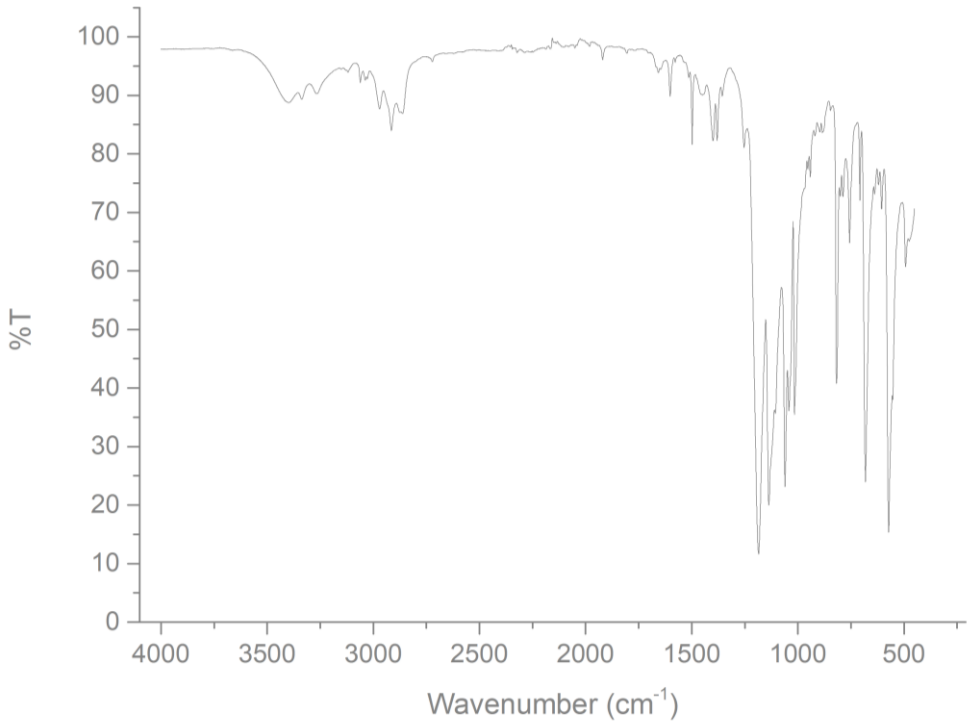

Figure 52: MIR spectrum of [Fe(Im-Pr-Im)3](ClO4)2

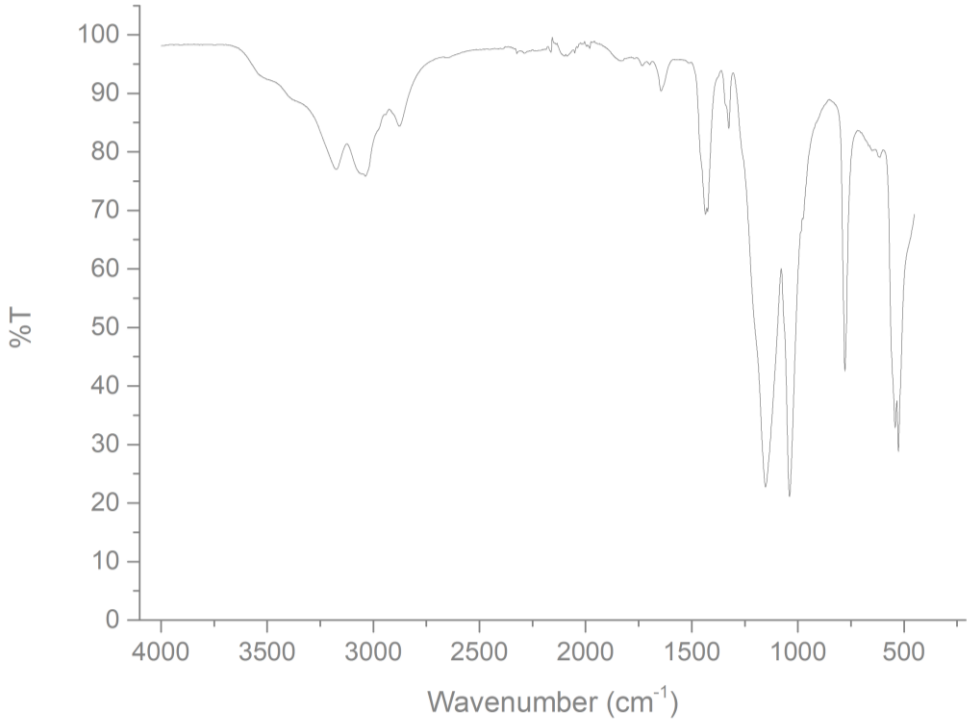

Figure 53: MIR spectrum of [Fe(Im-Bu-Im)3](BF4)2

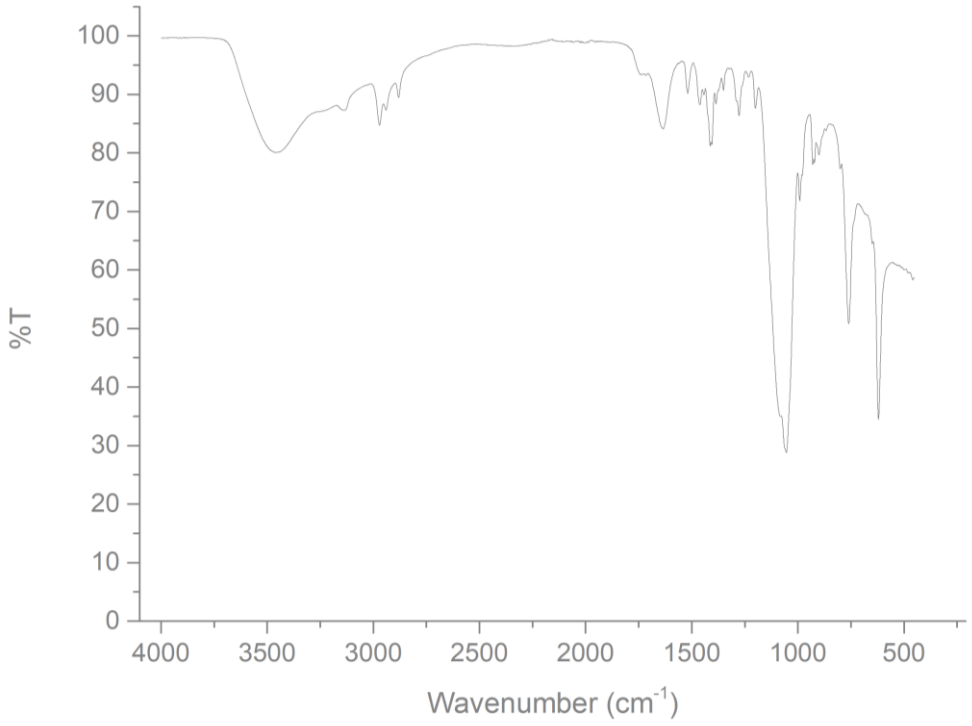

Figure 54: MIR spectrum of [Fe(Im-Bu-Im)3](ClO4)2

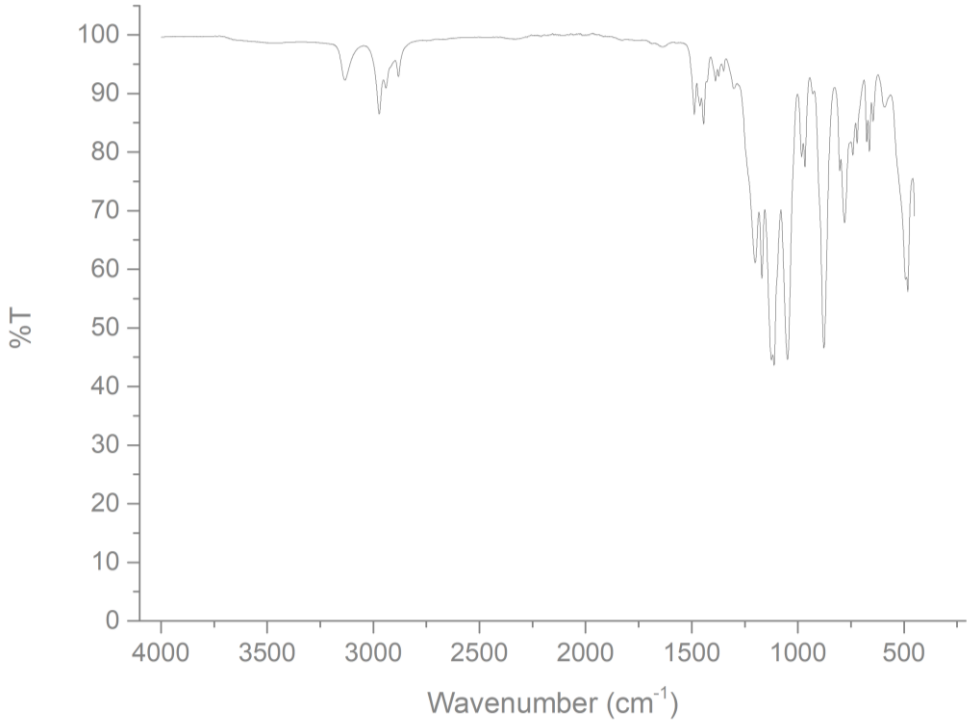

Figure 55: MIR spectrum of [Fe(Im-PX-Im)3](BF4)2

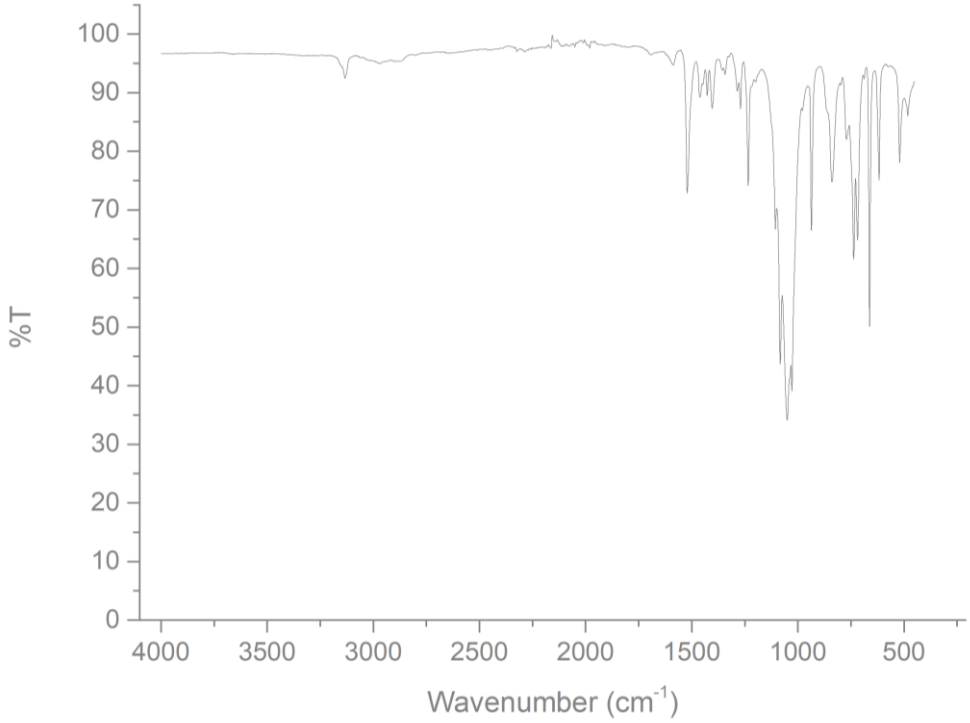

Figure 56: MIR spectrum of [Ni(Im-PX-Im)3](BF4)2

5 REFERENCES

[1] Gütlich, P. and H.A. Goodwin, *Spin Crossover in Transition Metal Compounds I*, in *Topics in Current Chemistry,*. 2004, Springer Berlin Heidelberg,: Berlin, Heidelberg. p. 1 online resource (xiii, 341 pages).

[2] Cotton, F.A., G. Wilkinson, and P.L. Gaus, *Basic inorganic chemistry*. 3rd ed. 1995, New York: J. Wiley (xii, 838 p.).

[3] Cambi, L. and L. Szego, *The magnetic susceptibility of complex compounds.* Berichte Der Deutschen Chemischen Gesellschaft, 1931. **64**: p. 2591-2598.

[4] Figgis, B.N. and G.E. Toogood, *Magnetic Properties of Some Dithiocarbamate Compounds of Chromium(III), Manganese(III), and Iron(III) at Very Low-Temperatures.* Journal of the Chemical Society-Dalton Transactions, 1972(19): p. 2177.

[5] Haddad, M.S., et al., *Spin-Crossover Ferric Complexes - Curiosities Observed for Unperturbed Solids.* Inorganic Chemistry, 1981. **20**(1): p. 123-131.

[6] Haddad, M.S., et al., *Spin-Crossover Ferric Complexes - Unusual Effects of Grinding and Doping Solids.* Inorganic Chemistry, 1981. **20**(1): p. 131-139.

[7] Franke, P.L., J.G. Haasnoot, and A.P. Zuur, *Tetrazoles as Ligands .4. Iron(II) Complexes of Monofunctional Tetrazole Ligands, Showing High-Spin Reversible Low-Spin Transitions.* Inorganica Chimica Acta-Articles, 1982. **59**(1): p. 5-9.

[8] Gaponik, P.N., S.V. Voitekhovich, and O.A. Ivashkevich, *Metal derivatives of tetrazoles.* Uspekhi Khimii, 2006. **75**(6): p. 569-603.

[9] Gütlich, P., *Spin Crossover in Iron(II)-Complexes.* Structure and Bonding, 1981. **44**: p. 83-195.

[10] Gandolfi, C., G.G. Morgan, and M. Albrecht, *A magnetic iron(III) switch with controlled and adjustable thermal response for solution processing.* Dalton Transactions, 2012. **41**(13): p. 3726-3730.

[11] Dirtu, M.M., et al., *Prediction of the Spin Transition Temperature in Fe-II One-Dimensional Coordination Polymers: an Anion Based Database.* Inorganic Chemistry, 2009. **48**(16): p. 7838-7852.

[12] Bruker Analytical X-ray Instruments, I., 2012.

[13] Palatinus, L. and G. Chapuis, *SUPERFLIP - a computer program for the solution of crystal structures by charge flipping in arbitrary dimensions.* Journal of Applied Crystallography, 2007. **40**: p. 786-790.

[14] Petricek, V., M. Dusek, and L. Palatinus, *Crystallographic Computing System JANA2006: General features.* Zeitschrift Fur Kristallographie, 2014. **229**(5): p. 345-352.